



**Calhoun: The NPS Institutional Archive**  
**DSpace Repository**

---

Theses and Dissertations

Thesis and Dissertation Collection

---

1988

# Synoptic patterns related to tropical cyclone recurvature/

Sherman, Brett T.

Monterey, California. Naval Postgraduate School

---

<http://hdl.handle.net/10945/23131>

*Downloaded from NPS Archive: Calhoun*



Calhoun is a project of the Dudley Knox Library at NPS, furthering the precepts and goals of open government and government transparency. All information contained herein has been approved for release by the NPS Public Affairs Officer.

**Dudley Knox Library / Naval Postgraduate School**  
**411 Dyer Road / 1 University Circle**  
**Monterey, California USA 93943**

<http://www.nps.edu/library>



# NAVAL POSTGRADUATE SCHOOL

## Monterey, California



# THESIS

S44827

SYNOPTIC PATTERNS RELATED TO  
TROPICAL CYCLONE RECURVATURE

by

Brett T. Sherman

March 1988

Thesis Advisor

Russell L. Elsberry

Approved for public release; distribution is unlimited.

T239238

**REPORT DOCUMENTATION PAGE**

1 REPORT SECURITY CLASSIFICATION classified		1b RESTRICTIVE MARKINGS	
2 SECURITY CLASSIFICATION AUTHORITY		3 DISTRIBUTION/AVAILABILITY OF REPORT	
4 CLASSIFICATION/DOWNGRADING SCHEDULE		Approved for public release, distribution is unlimited	
5 PERFORMING ORGANIZATION REPORT NUMBER(S)		6 MONITORING ORGANIZATION REPORT NUMBER(S)	
7a NAME OF PERFORMING ORGANIZATION	8a OFFICE SYMBOL (if applicable)	7b NAME OF MONITORING ORGANIZATION	
Naval Postgraduate School	63	Naval Postgraduate School	
8b ADDRESS (City, State, and ZIP Code)		7c ADDRESS (City, State, and ZIP Code)	
Monterey, California 93943-5000		Monterey, California 93943-5000	
9a NAME OF FUNDING/SPONSORING ORGANIZATION	8b OFFICE SYMBOL (if applicable)	9 PROCUREMENT INSTRUMENT IDENTIFICATION NUMBER	
10 ADDRESS (City, State, and ZIP Code)		11 SOURCE OF FUNDING NUMBERS	
		PROGRAM ELEMENT NO	PROJECT NO
		TASK NO	WORK UNIT ACCESSION NO
12 TITLE (include Security Classification)			
Synoptic Patterns Related to Tropical Cyclone Recurvature			
13 PERSONAL AUTHOR(S) Sherman, Brett T.			
14a TYPE OF REPORT	13b TIME COVERED FROM _____ TO _____	14 DATE OF REPORT (Year Month Day)	15 PAGE COUNT
Master's Thesis		1988 March	135
16 SUPPLEMENTARY NOTATION			
Continuation page			
17 COSATI CODES		18 SUBJECT TERMS (Continue on reverse if necessary and identify by block number)	
GROUP	SUB-GROUP	Tropical cyclone, typhoon motion, recurvature, track forecasting, vorticity	
19 ABSTRACT (Continue on reverse if necessary and identify by block number)			
Relative vorticity fields calculated from the U. S. Navy operational Global Band Analysis are used to relate synoptic and storm parameters to the track of tropical cyclones in the western North Pacific Ocean. In this preliminary study, synoptic patterns are developed, described and discussed from the perspective of a pattern recognition technique to assist forecasters at the Joint Typhoon Warning Center, Guam. The focus is on track turning motions to the left and right of the persistence track on trying to accurately predict the point of the turn or recurvature in relation to the time evolution of the vorticity patterns. The developmental sample of storms indicates that there is potential in the Global Band Analysis to guide the selection of the appropriate track aid in the 48-60 hour time range.			
20 DISTRIBUTION/AVAILABILITY OF ABSTRACT CLASSIFIED UNLIMITED <input type="checkbox"/> SAME AS RPT <input type="checkbox"/> DTIC USERS <input type="checkbox"/>		21 ABSTRACT SECURITY CLASSIFICATION Unclassified	
22a NAME OF RESPONSIBLE INDIVIDUAL L. Elsberry		22b TELEPHONE (Include Area Code) 408-646-2373	22c OFFICE SYMBOL 63Es

Item 16:

The views expressed in this article are those of the author and do not reflect the official policy of the Department of Defense or the U. S. Government.

Approved for public release; distribution is unlimited.

Synoptic Patterns Related to  
Tropical Cyclone Recurvature

by

Brett T. Sherman  
Lieutenant Commander, United States Navy  
B.S., State University of New York, Stony Brook, 1972

Submitted in partial fulfillment of the  
requirements for the degree of

MASTER OF SCIENCE IN METEOROLOGY AND OCEANOGRAPHY

from the

NAVAL POSTGRADUATE SCHOOL  
March 1988

## ABSTRACT

Relative vorticity fields calculated from the U. S. Navy operational Global Band Analysis are used to relate synoptic and storm parameters to the track of tropical cyclones in the western North Pacific Ocean. In this preliminary study, synoptic patterns are developed, described and discussed from the perspective of a pattern recognition technique to assist the forecasters at the Joint Typhoon Warning Center, Guam. The focus is on track turning motions to the left and right of the persistence track and on trying to accurately predict the point of the turn or recurvature in relation to the time evolution of the vorticity patterns. The developmental sample of storms indicates that there is potential for using synoptic patterns in the Global Band Analysis to guide the selection of the appropriate track aid in the 48-60 hour time range.

## TABLE OF CONTENTS

I.	INTRODUCTION .....	1
A.	BACKGROUND .....	1
B.	RECENT STUDIES IN SUPPORT OF THE JOINT TYPHOON WARNING CENTER .....	2
C.	OBJECTIVES .....	4
II.	DATA BASE DEVELOPMENT AND DISPLAY .....	5
A.	GLOBAL BAND ANALYSIS AND STORM DATA .....	5
B.	STORM SELECTION .....	6
C.	DATA RETRIEVAL .....	11
D.	GEMPAK AND GEMPLT PROGRAMS .....	12
III.	DATA ANALYSIS .....	14
A.	ANALYSIS PARAMETERS .....	14
B.	STREAMLINE FIELD ANALYSIS .....	15
C.	VORTICITY FIELD ANALYSIS .....	15
1.	Vorticity Field Presentations .....	15
2.	Proposed Synoptic Analysis Technique .....	20
3.	Summary of the Relative Vorticity Analysis of STY Marge's Track .....	77
D.	APPLICATION OF THE ANALYSIS TECHNIQUE TO OTHER STORMS .....	79
1.	Dominant Vorticity Patterns .....	79
2.	Cyclone-Cyclone Interaction .....	80
3.	Forecast Performance .....	88
IV.	CONCLUSIONS AND RECOMMENDATIONS .....	92
APPENDIX A:	PROGRAM--GLOBAL BAND FILE IDENTIFICATION .....	95

APPENDIX B: PROGRAM--GET GLOBAL BAND ANALYSIS .....	99
APPENDIX C: PROGRAM--GLOBAL BAND TAPE TO DISK .....	110
APPENDIX D: PROGRAM--FILE CONVERTER .....	112
LIST OF REFERENCES .....	117
INITIAL DISTRIBUTION LIST .....	120

## LIST OF TABLES

1. TRACK FORECAST ERRORS (N MI) IN SUPER TYPHOON MARGE COMPARED TO 1983 OVERALL ERRORS .....	6
2. STORM PARAMETERS .....	14
3. SYNOPTIC PARAMETERS .....	16
4. STORM CHART LEGEND .....	24
5. BEST TRACK - RELATIVE VORTICITY PATTERN ANGULAR CORRELATION EVALUATION CRITERIA .....	25
6. RATING VALUES FOR SUPER TYPHOON MARGE .....	78
7. RELATIVE VORTICITY CONTOUR PATTERNS OBSERVED .....	79
8. AVERAGE RATING VALUES BY STORM, PRESSURE LEVEL AND VORTICITY CONTOUR .....	89
9. RELATIVE VORTICITY CONTOUR PERFORMANCE BY LEVEL .....	90
10. TURN PREDICTION PERFORMANCE OF THE RELATIVE VORTICITY PATTERN TECHNIQUE .....	90

## LIST OF FIGURES

1.1	Forecast track aids for Tropical Storm Dom at 12 UTC 19 Aug 1983 . . . . .	3
2.1a	Super Typhoon Marge best track (dots) and forecast tracks (stars) during the first step. Labels indicate date and hour (02 00 means 00 UTC 02 Nov) . . . . .	7
2.1b	Super Typhoon Marge best track and forecast tracks during the second step . . . . .	8
2.1c	Super Typhoon Marge best track and forecast tracks during the recurvature . . . . .	9
3.1a	Streamline chart at 400 mb at 12 UTC 31 Oct 1983 . . . . .	18
3.1b	Relative vorticity ( $\times 10^5 \text{s}^{-1}$ ) chart at 400 mb at 12 UTC 31 Oct 1983 . . . . .	19
3.2a	Relative vorticity contour - channel pattern . . . . .	21
3.2b	Relative vorticity contour - node pattern . . . . .	21
3.2c	Closed relative vorticity contour pattern . . . . .	22
3.2d	Pinched or broken ridge contour pattern . . . . .	22
3.2e	Storm - storm interaction contour pattern . . . . .	23
3.2f	Dual node-derived resultant vector pattern . . . . .	23
3.3a	Relative vorticity ( $\times 10^5 \text{s}^{-1}$ ) at 400 mb at 12 UTC 30 Oct 1983 . . . . .	26
3.3b	Relative vorticity ( $\times 10^5 \text{s}^{-1}$ ) at 700 mb at 12 UTC 30 Oct 1983 . . . . .	27
3.3c	Relative vorticity ( $\times 10^5 \text{s}^{-1}$ ) in LAV at 12 UTC 30 Oct 1983 . . . . .	28
3.4a	Relative vorticity ( $\times 10^5 \text{s}^{-1}$ ) at 400 mb at 00 UTC 31 Oct 1983 . . . . .	30
3.4b	Relative vorticity ( $\times 10^5 \text{s}^{-1}$ ) at 700 mb at 00 UTC 31 Oct 1983 . . . . .	31
3.4c	Relative vorticity ( $\times 10^5 \text{s}^{-1}$ ) in LAV at 00 UTC 31 Oct 1983 . . . . .	32
3.5a	Relative vorticity ( $\times 10^5 \text{s}^{-1}$ ) at 400 mb at 12 UTC 31 Oct 1983 . . . . .	33
3.5b	Relative vorticity ( $\times 10^5 \text{s}^{-1}$ ) at 700 mb at 12 UTC 31 Oct 1983 . . . . .	34
3.5c	Relative vorticity ( $\times 10^5 \text{s}^{-1}$ ) in LAV at 12 UTC 31 Oct 1983 . . . . .	35
3.6a	Relative vorticity ( $\times 10^5 \text{s}^{-1}$ ) at 400 mb at 00 UTC 01 Nov 1983 . . . . .	37
3.6b	Relative vorticity ( $\times 10^5 \text{s}^{-1}$ ) at 700 mb at 00 UTC 01 Nov 1983 . . . . .	38
3.6c	Relative vorticity ( $\times 10^5 \text{s}^{-1}$ ) in LAV at 00 UTC 01 Nov 1983 . . . . .	39
3.7a	Relative vorticity ( $\times 10^5 \text{s}^{-1}$ ) at 400 mb at 12 UTC 01 Nov 1983 . . . . .	40

3.7b	Relative vorticity ( $\times 10^5 \text{s}^{-1}$ ) at 700 mb at 12 UTC 01 Nov 1983 .....	41
3.7c	Relative vorticity ( $\times 10^5 \text{s}^{-1}$ ) in LAV at 12 UTC 01 Nov 1983 .....	42
3.8a	Relative vorticity ( $\times 10^5 \text{s}^{-1}$ ) at 400 mb at 00 UTC 02 Nov 1983 .....	44
3.8b	Relative vorticity ( $\times 10^5 \text{s}^{-1}$ ) at 700 mb at 00 UTC 02 Nov 1983 .....	45
3.8c	Relative vorticity ( $\times 10^5 \text{s}^{-1}$ ) in LAV at 00 UTC 02 Nov 1983 .....	46
3.9a	Relative vorticity ( $\times 10^5 \text{s}^{-1}$ ) at 400 mb at 12 UTC 02 Nov 1983 .....	47
3.9b	Relative vorticity ( $\times 10^5 \text{s}^{-1}$ ) at 700 mb at 12 UTC 02 Nov 1983 .....	48
3.9c	Relative vorticity ( $\times 10^5 \text{s}^{-1}$ ) in LAV at 12 UTC 02 Nov 1983 .....	49
3.10a	Relative vorticity ( $\times 10^5 \text{s}^{-1}$ ) at 400 mb at 00 UTC 03 Nov 1983 .....	51
3.10b	Relative vorticity ( $\times 10^5 \text{s}^{-1}$ ) at 700 mb at 00 UTC 03 Nov 1983 .....	52
3.10c	Relative vorticity ( $\times 10^5 \text{s}^{-1}$ ) in LAV at 00 UTC 03 Nov 1983 .....	53
3.11a	Relative vorticity ( $\times 10^5 \text{s}^{-1}$ ) at 400 mb at 12 UTC 03 Nov 1983 .....	54
3.11b	Relative vorticity ( $\times 10^5 \text{s}^{-1}$ ) at 700 mb at 12 UTC 03 Nov 1983 .....	55
3.11c	Relative vorticity ( $\times 10^5 \text{s}^{-1}$ ) in LAV at 12 UTC 03 Nov 1983 .....	56
3.12a	Relative vorticity ( $\times 10^5 \text{s}^{-1}$ ) at 400 mb at 00 UTC 04 Nov 1983 .....	58
3.12b	Relative vorticity ( $\times 10^5 \text{s}^{-1}$ ) at 700 mb at 00 UTC 04 Nov 1983 .....	59
3.12c	Relative vorticity ( $\times 10^5 \text{s}^{-1}$ ) in LAV at 00 UTC 04 Nov 1983 .....	60
3.13a	Relative vorticity ( $\times 10^5 \text{s}^{-1}$ ) at 400 mb at 12 UTC 04 Nov 1983 .....	61
3.13b	Relative vorticity ( $\times 10^5 \text{s}^{-1}$ ) at 700 mb at 12 UTC 04 Nov 1983 .....	62
3.13c	Relative vorticity ( $\times 10^5 \text{s}^{-1}$ ) in LAV at 12 UTC 04 Nov 1983 .....	63
3.14a	Relative vorticity ( $\times 10^5 \text{s}^{-1}$ ) at 400 mb at 00 UTC 05 Nov 1983 .....	64
3.14b	Relative vorticity ( $\times 10^5 \text{s}^{-1}$ ) at 700 mb at 00 UTC 05 Nov 1983 .....	65
3.14c	Relative vorticity ( $\times 10^5 \text{s}^{-1}$ ) in LAV at 00 UTC 05 Nov 1983 .....	65
3.15a	Relative vorticity ( $\times 10^5 \text{s}^{-1}$ ) at 400 mb at 00 UTC 06 Nov 1983 .....	68
3.15b	Relative vorticity ( $\times 10^5 \text{s}^{-1}$ ) at 700 mb at 00 UTC 06 Nov 1983 .....	69
3.15c	Relative vorticity ( $\times 10^5 \text{s}^{-1}$ ) in LAV at 00 UTC 06 Nov 1983 .....	70
3.16a	Relative vorticity ( $\times 10^5 \text{s}^{-1}$ ) at 400 mb at 12 UTC 06 Nov 1983 .....	71
3.16b	Relative vorticity ( $\times 10^5 \text{s}^{-1}$ ) at 700 mb at 12 UTC 06 Nov 1983 .....	71
3.16c	Relative vorticity ( $\times 10^5 \text{s}^{-1}$ ) in LAV at 12 UTC 06 Nov 1983 .....	72
3.17a	Relative vorticity ( $\times 10^5 \text{s}^{-1}$ ) at 400 mb at 00 UTC 07 Nov 1983 .....	73
3.17b	Relative vorticity ( $\times 10^5 \text{s}^{-1}$ ) at 700 mb at 00 UTC 07 Nov 1983 .....	75
3.17c	Relative vorticity ( $\times 10^5 \text{s}^{-1}$ ) in LAV at 00 UTC 07 Nov 1983 .....	75
3.18	Relative vorticity ( $\times 10^5 \text{s}^{-1}$ ) in LAV at 12 UTC 18 Oct 1984 for Typhoon Thad. Forecast tracks are dashed with stars .....	81

3.19	Relative vorticity ( $\times 10^5 \text{s}^{-1}$ ) in LAV at 12 UTC 30 Aug 1984 for Typhoon Ike .....	82
3.20	Streamline analysis at 925 mb at 12 UTC 18 Nov 1984 illustrating Typhoon Bill and Typhoon Clara interaction (Joint Typhoon Warning Center, 1984) .....	83
3.21	Relative vorticity ( $\times 10^5 \text{s}^{-1}$ ) in LAV at 00 UTC 30 Aug 1982 illustrating Typhoon Gordon and Typhoon Faye interaction .....	84
3.22a	Relative vorticity ( $\times 10^5 \text{s}^{-1}$ ) in LAV at 00 UTC 11 Aug 1983 illustrating Super Typhoon Abby - Typhoon Ben - Typhoon Carmen interaction .....	85
3.22b	Relative vorticity ( $\times 10^5 \text{s}^{-1}$ ) in LAV at 12 UTC 11 Aug 1983 illustrating Super Typhoon Abby - Typhoon Ben - Typhoon Carmen interaction .....	85
3.22c	Relative vorticity ( $\times 10^5 \text{s}^{-1}$ ) in LAV at 00 UTC 12 Aug 1983 illustrating Super Typhoon Abby - Typhoon Ben - Typhoon Carmen interaction .....	86

## ACKNOWLEDGEMENTS

I would like to thank the individuals who made this study possible. First I thank Dr. Russell Elsberry for his patience, guidance, support and instruction through the course of the study. I appreciate the critical review of the study and manuscript by Dr. Greg Holland. I also thank the people who helped in the area of data management and display. Mr. Dennis Mar and Ms. June Favorite were most helpful in modification of the programs for the preparation of data tapes in the W. C. Church Computer Center. Mr. Russell Schwanz provided guidance on the operating system of the IDEA Lab. I especially thank Mr. James Cowie. Without Jim's help, co-authoring programs for use in the IDEA Lab and his efforts toward making the installed software work in the western North Pacific Ocean, the generation of the more than 1500 maps used in the study would have been impossible. Also, appreciation goes to Drs. Ted Tsui and Michael Fiorino for their encouragement and advice throughout the course of the study.

Another group deserving thanks includes Colonel David McClawhorn, USAF, Commander Scott Sandgathe, USN and Major Frank Wells, USAF (ret). They taught me to look at everything available in the development of the tropical cyclone forecast at JTWC, how to recognize patterns and question the information that fails to fit the picture. Their patience, support and instruction are most appreciated. This study is a direct result of the desire to improve the state of tropical cyclone forecasting they developed in the team that served under them.

Finally I would like to express the deep appreciation I feel for my wife, Beverly, and my daughters, Kimberley and Emily. Many times during the past year they have been most understanding when "The Thesis" took priority over other things that they would have rather done as a family. This study could not have reached completion without their ever present support and understanding, I dedicate this work to the three ladies in my life.



# I. INTRODUCTION

## A. BACKGROUND

The successful forecasting of tropical cyclone motion is one of the most difficult problems in tropical meteorology. The training process for the operational forecaster includes a process of integrating knowledge contained in the literature and learning from experienced forecasters. One aspect of the training is the development of an ability to recognize significant patterns in the synoptic analyses, satellite imagery and forecast fields. The better forecasters are able to recognize the synoptic patterns that indicate that significant changes will occur (or not occur) in the track of the storm during the forecast period, or are able to recognize the synoptic patterns earlier and more often than the less successful forecasters.

A significant problem at the Joint Typhoon Warning Center (JTWC), Guam, is the short tour length for Air Force and Naval officers assigned as forecasters. Nearly half of the forecaster's tour at JTWC is spent learning the job. The actual time required to complete the basic training phase depends on the ability and experience of the forecaster trainee and the number and type of storms that occur during the training period (McLawnhorn, 1984). The short tour length at JTWC is not the only obstacle to meeting the COMSEVENTHFLT requirement to reduce forecast errors to 50, 100 and 150 n mi for the 24, 48 and 72 h forecast periods respectively. The National Hurricane Center (NHC), Miami experiences forecast errors of magnitudes similar to those at JTWC without having to deal with the problem of forecasters subject to 15 to 24 month rotation periods as in the military. JTWC and NHC each have several forecasting aids available for the development of the operational forecasts. Both centers are continually testing new methods developed by the research community, as well as making improvements to current operational models.

It is sometimes stated that the forecaster does not need more forecast aids. Rather, the need is to develop the ability to better utilize the schemes that are available in the forecast centers (Neumann and Pelissier, 1981; Tsui, 1984; Elsberry and Peak, 1986). Each of the forecast aids has strengths and weaknesses that depend on a complex combination of the storm size, speed, intensity, location and the synoptic features in the basin. The features of importance in the western North Pacific Ocean

region include the subtropical ridge, long-wave troughs, short-wave troughs, the Northeast and Southwest monsoons, the upper-level flow patterns and features, and other tropical systems. Each of these features is displayed to some extent in the analysis and prognostic fields that are used by the forecaster, who must decide which of the forecast aids is the best at depicting the interaction of the environmental fields and the storm. In many cases, the more subtle features that are undetected by the forecaster under pressure to issue the forecast are later "discovered" in the post-storm analysis. Successful forecasts both incorporate a maximum of information into a warning track and help the operational customer to make prudent and timely decisions to save life and property at a minimal monetary cost.

Consider the set of forecast aids available for the 12 UTC 19 August 1983 warning on Tropical Storm Dom (Fig. 1.1). This is not an atypical pattern and makes the selection of an accurate forecast track very difficult. What is required is a method that will incorporate the storm and synoptic parameters into a pattern or set of patterns that are easily recognizable under the pressures of getting the forecast out. This will assist in the selection of the primary forecast aid and simplify the track forecasting dilemma for the operational forecaster. This feasibility study will seek the synoptic pattern relationships involved in the recurvature or nonrecurvature forecast.

## **B. RECENT STUDIES IN SUPPORT OF THE JOINT TYPHOON WARNING CENTER**

One attempt at developing a technique that assists in the interpretation of the environmental fields is the CYCLOPS Objective Steering Model Output Statistics (COSMOS) forecast aid (Allen, 1984), which uses the output from the CYCLOPS Prediction System (CYCLOPS). The success of this technique in predicting the unusual track of Tropical Storm Dom is shown in Fig. 1.1. COSMOS is a model output statistics technique applied to the CYCLOPS geostrophic steering flow aid, which is the most recent version of the HATRACK/MOHATT steering flow model (Renard, 1968; Renard and Levings, 1969; Renard *et al.*, 1970; Renard *et al.*, 1972; Renard *et al.*, 1973). The COSMOS program compares the current flow pattern to a set of seven typical patterns and calculates a forecast track that incorporates the 850, 700 and 500 mb steering flow outputs from the CYCLOPS model. The output of a single track (versus separate tracks at each level) simplifies the forecaster's decision problem, incorporates past pattern information and allows the display of the CYCLOPS components that are used in the technique.

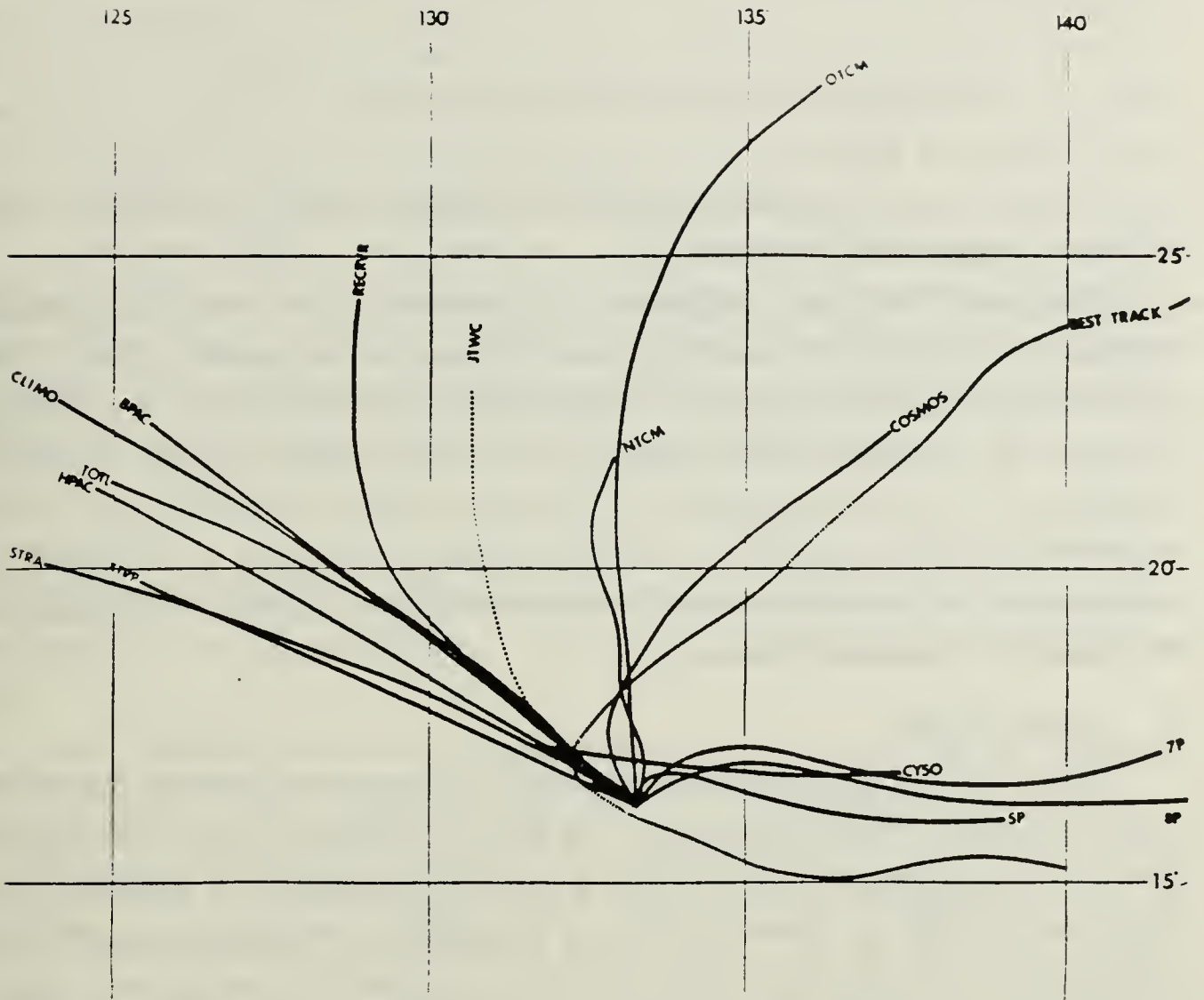


Fig. 1.1 Forecast track aids for Tropical Storm Dom at 12 UTC 19 Aug 1983.

Another recent attempt to incorporate the environmental circulation pattern into a forecast aid is the Colorado State University Model (CSUM) developed by Matsumoto (1984). This statistical technique categorizes the track forecast problem into one of three classes depending on the storm center location relative to the subtropical ridge at 500 mb. The three classes are defined as under the ridge, on the ridge and above the ridge. The predicted track is divided into three 24-hour periods and uses the prognostic fields as if they are analyses at the valid time.

A series of investigations at the Naval Postgraduate School over the past three years has attempted to improve the use of forecast guidance at JTWC. Curry (1985) developed an objective technique to improve the initial location of the storm center

that is used for the forecast aids. Wilson (1984), Schott (1985), Williams (1986), Jones (1986), Meanor (1987) and Weniger (1987) have studied various combinations of storm and synoptic parameters to develop information for possible inclusion in a decision-tree scheme for selecting the optimum track forecast guidance for a particular forecast scenario (Peak and Elsberry, 1987). These studies have increased the knowledge base for the forecaster and researcher, but have not produced a straight-forward pattern that is easily recognizable by the forecaster.

Sandgathe (1987) has categorized and described the various storm-synoptic relationships that appear to have the greatest influence on the tropical cyclone tracks in the western North Pacific Ocean. He has also reviewed the 1982-1985 storm seasons and listed the interactions that affected the tracks of selected storms. A detailed description of the interactions and the forecast problems that arise due to the occurrence of the interaction, or a multiple interaction, are given in the report. A description of the interactions studied in this investigation are given in the section on the data set development in Chapter II.

### **C. OBJECTIVES**

This study is a preliminary investigation of the storm and synoptic parameters related to tropical cyclone recurvature. The goal is to develop a way to display and analyze the parameters in a manner that is useful to the operational forecaster. The recurvature problem is chosen because of the difficulty experienced in accurately forecasting the recurvature location and time. An inconsistent performance of this critical forecast task often results in 72 h position errors in excess of 1000 n mi. These errors far exceed the COMSEVENTHFLT requirements and create major problems for operational commanders tasked with making decisions to implement typhoon evasion and preparation plans. Reduction of these track errors to levels comparable to the current performance for straight-moving storms would provide a credible and useful product to the operational decision makers.

Several approaches to the problem have been used to discover a more optimal method of identifying and displaying the storm and synoptic parameters that determine the track of the tropical cyclone. The data fields, data retrieval and display are described in Chapter II, analysis techniques and results are presented in Chapter III. Chapter IV discusses the conclusions and possible avenues for further development and study.

## II. DATA BASE DEVELOPMENT AND DISPLAY

### A. GLOBAL BAND ANALYSIS AND STORM DATA

The wind fields in this study are taken from the United States Navy Fleet Numerical Oceanography Center (FNOC) Global Band Analysis (GBA). The GBA is the analysis used to initialize the Navy's two dynamic tropical cyclone track forecast models, the Nested Tropical Cyclone Model (NTCM) and the One-way Influence Tropical Cyclone Model (OTCM). The GBA are produced at 00 and 12 UTC each day on a 49 x 144 grid with grid spacing of 2.5 degrees of longitude on a Mercator projection. The grid extends from 40.956°S to 59.745°N and has 360 degrees longitudinal coverage. The grid spacing decreases toward the poles as the meridians converge. At the standard latitude of the grid (22.5°N or S), the grid distance is 257 km.

A complete description of the GBA can be found in the Numerical Environmental Products Manual (United States Naval Weather Service, 1975) and a review of recent developments in the Navy's tropical analysis is given in Elsberry and Fiorino (1985). The analysis is done at the surface, 700 mb, 400 mb, 250 mb and 200 mb. Thermal analyses at intermediate levels provide data for the vertical coupling using the thermal wind relationship. The operational centers receive intermediate level fields calculated from analyzed levels, but these fields are not archived. When a tropical cyclone is present, the storm is depicted by eight wind vectors bogussed into the surface field around the position of the center at chart time. Data used in the GBA are from the surface observation network, rawinsondes, pibals, aireps and cloud motion vectors. If no observations are available for the current analysis, a blend of the 12 hour old analysis with a 5% reversion to climatology is used.

Data for tropical cyclones in the western North Pacific basin are available on an annual basis from the JTWC's Annual Tropical Cyclone Report (ATCR). The report provides a narrative description of each storm with the storm best track, satellite pictures, significant synoptic patterns and occasionally storm damage photographs. The data annex of the report gives six-hourly best track, warning and forecast positions; forecast error statistics; satellite, aircraft and radar fixes; best track intensity, aircraft wind reports and satellite intensity estimates. In this study, ATCR's for 1982, 1983 and 1984 were used for case selection and analysis.

## B. STORM SELECTION

Super Typhoon Marge (18W) 1983 was chosen as the first storm to be studied due to the difficulty experienced by JTWC in accurately forecasting the storm track throughout the life of the system (Fig. 2.1). Marge was categorized by Sandgathe (1987, p.19) as a step-recurver that later underwent extratropical transition. A step-recurver is a system that is influenced by the passage of mid-latitude troughs to the north of the storm. The step phase of the track takes place as the storm slows and moves northward under the influence of a passing trough, but does not recurve. As the trough passes or weakens, the subtropical ridge builds westward and the storm turns to the left and tracks to the northwest or west under the ridge. Marge stepped twice before the eventual recurvature. Each time the step started, large forecast errors were recorded as forecasters predicted recurvature. When the storm finally did recurve, the forecasters unfortunately continued a track toward the northwest, which again added to the overall error.

TABLE 1  
TRACK FORECAST ERRORS (N MI) IN  
SUPER TYPHOON MARGE COMPARED TO 1983 OVERALL ERRORS

	Warning	24 h	48 h	72 h
Marge	19	191	484	755
1983	16	117	259	405
Marge/1983	1.18	1.63	1.87	1.86

Inconsistent forecast tracks as found in the Marge case can be responsible for premature evacuations of aircraft and ships and the early or unnecessary setting of typhoon conditions. Both actions entail major expenditures in terms of both man-hours and money. Table 1 is a summary of the average track errors for Marge compared with the overall errors for 1983. Although the errors and the ratio to the 1983 average are large, there were even larger errors on other 1983 storms in all categories except the 72 h forecast.

A set of storms was then compiled to test the preliminary results based on Marge. The goal was to develop a set of storms that would allow the study of varying

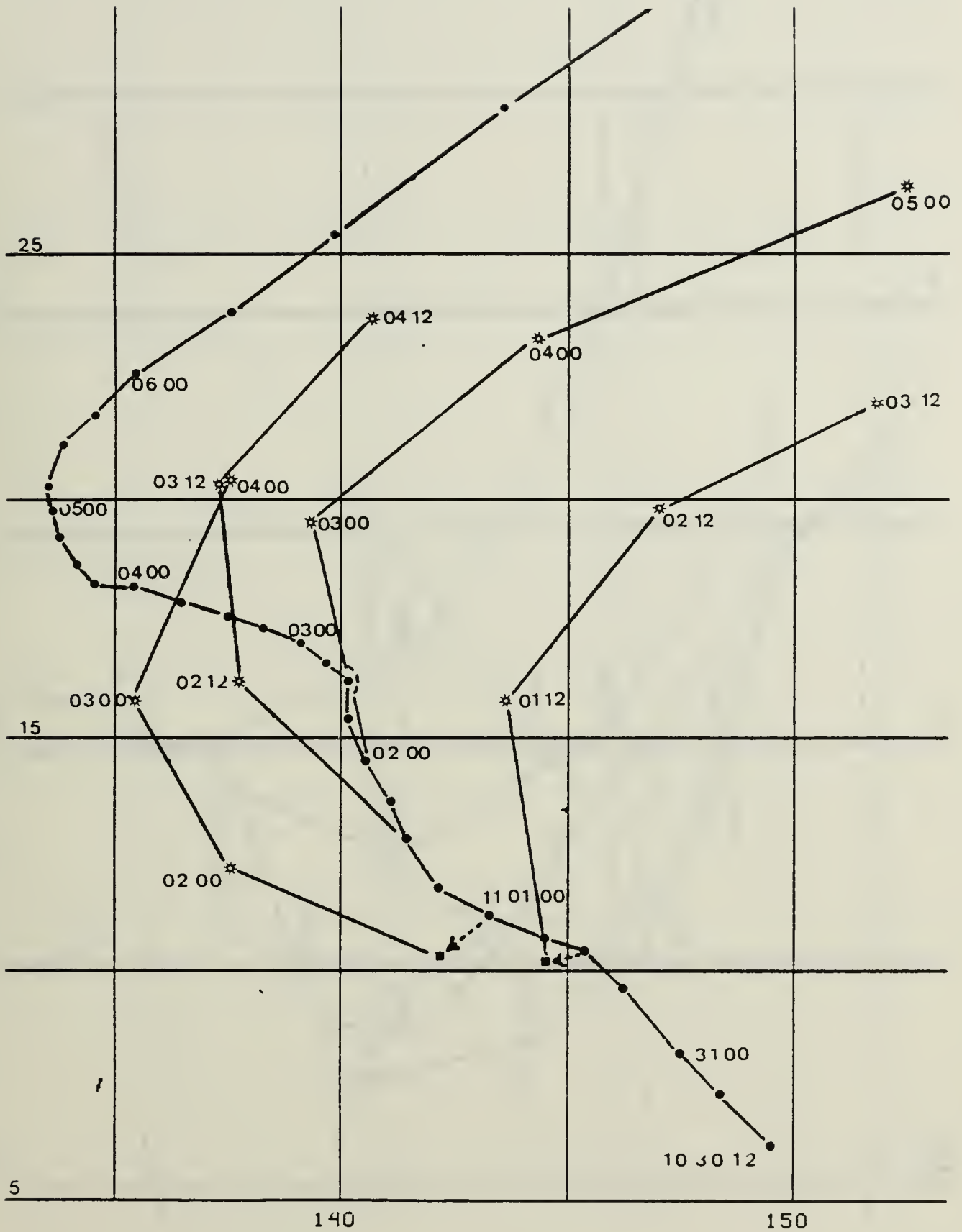


Fig. 2.1a Super Typhoon Marge best track (dots) and forecast tracks (stars) during the first step. Labels indicate date and hour (02 00 means 00 UTC 02 Nov).

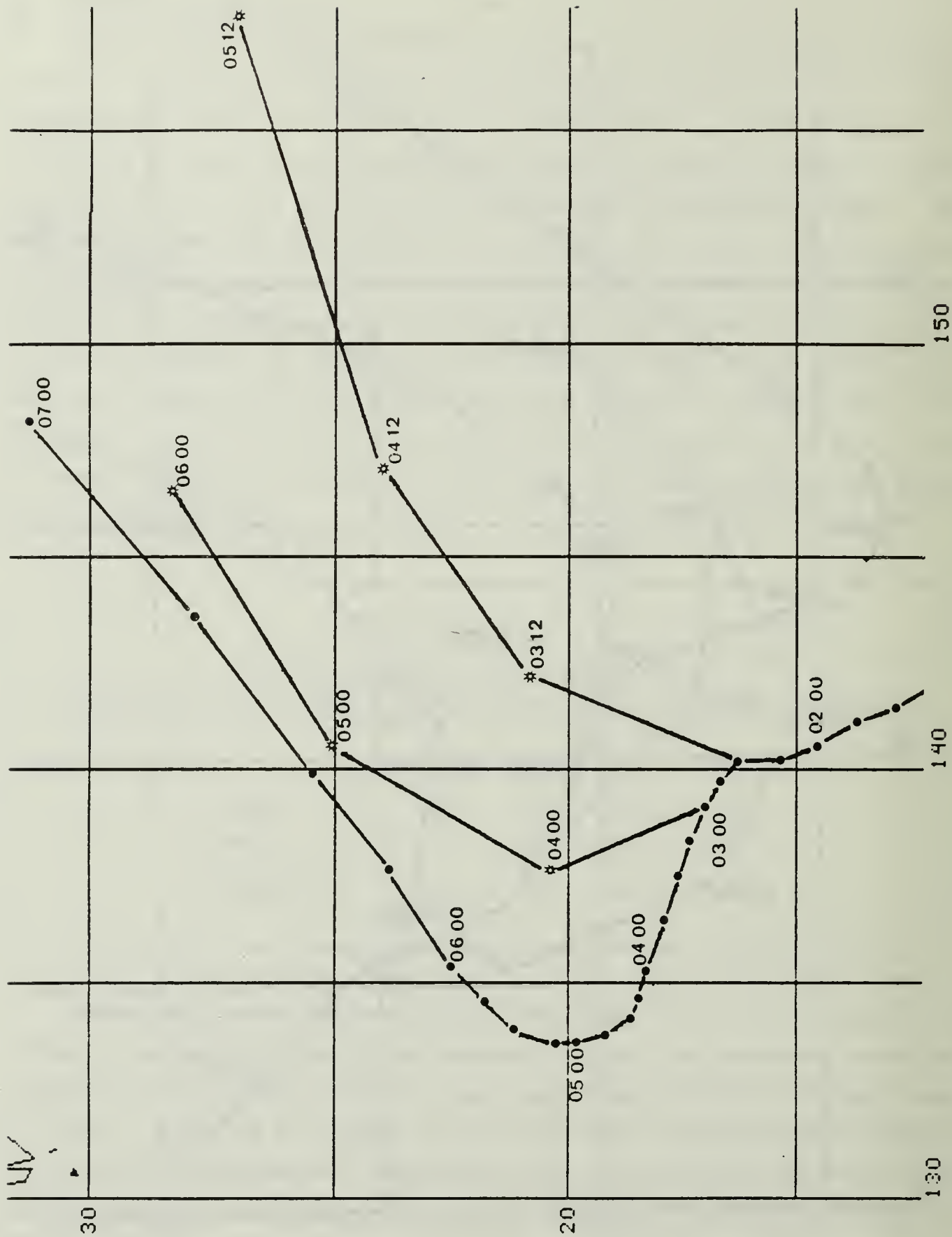


Fig. 2.1b Super Typhoon Marge best track and forecast tracks during the second step.

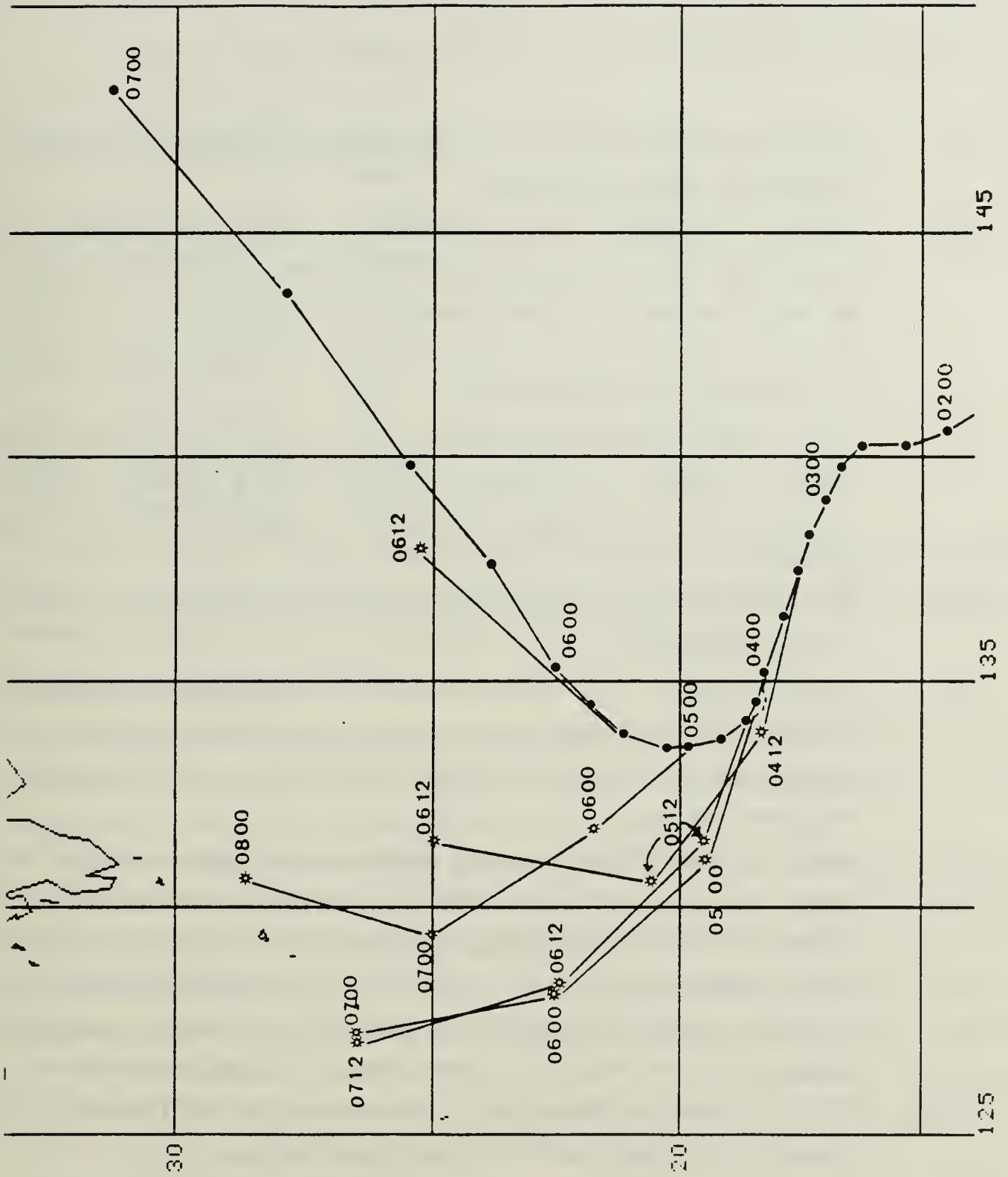


Fig. 2.1c Super Typhoon Marge best track and forecast tracks during the recurvature.

storm tracks to test the pattern relationships between the synoptic field and the storm envelope and to include as many storm-synoptic interactions as possible.

Sandgathe (1987) has described the track forecasting problem in the western North Pacific Ocean in terms of the storm-synoptic interactions. His list, which is ranked by need for improved forecaster understanding, includes:

- (i) Multiple cyclone interaction -- the flow created or modified by one cyclone influences the track of the second.
- (ii) Cyclone - midlatitude trough interaction -- the trough influences the cyclone track and causes a movement to the north and then recurvature if the trough influence is strong enough, or a step pattern if the trough influence is overcome by a strengthening of the subtropical ridge. Looping may also result from this interaction.
- (iii) Cyclone - subtropical ridge interaction -- the shape and extent of the ridge dictates the path of the cyclone to the west or in a gradual recurvature around the end of the ridge. The ridge also influences the step and loop patterns.
- (iv) Extratropical transition -- the warm core cyclone transforms into a hybrid or cold-core system.
- (v) Terrain interaction -- the track and intensity of the cyclone are influenced by interaction of the steering flow or the storm circulation with the various major islands and coastal areas in the Pacific basin that have significant orographic features.
- (vi) Monsoon surge interaction -- the tracks of some tropical storms show diurnal variations due to the diurnal fluctuations in the monsoon flow during the Southwest monsoon, which sometimes causes the storms to become quasi-stationary in the South China Sea and Philippine Sea. The Northeast monsoon also has a strong influence on the track of late season tropical storms, and may lead to erratic tracks and large forecast errors.
- (vii) TUTT or upper low interaction -- the influence of the Tropical Upper Tropospheric Trough (TUTT) lows on cyclone motion.

The 12 storms in the data set and the interaction categories according to Sandgathe are listed below (numerals following the storm name indicate the storm number and year and the Roman numerals correspond to the interaction list above):

- (1) Bess (11W/82) (ii,iii)
- (2) Gordon (16W/82) (i,ii,iii)
- (3) Wayne (04W/83) (v,vii)
- (4) Abby (05W/83) (i,ii,iii,iv,v)
- (5) Forrest (11W/83) (ii,iv,vii)
- (6) Ida (14W/83) (ii,iv,vii)
- (7) Lex (17W/83) (ii,vi)
- (8) Marge (18W/83) (ii,iv)
- (9) Ike (13W/84) (iii)
- (10) Thad (24W/84) (ii,vii)
- (11) Vanessa (25W/84) (i,ii,iv)
- (12) Clara (29W/84) (i,ii)

In addition to Super Typhoon Marge, the set includes five storms that have the step pattern, five that recurved without first stepping and two storms that had no apparent interaction with the mid-latitude troughs and had straight tracks.

### C. DATA RETRIEVAL

Wind fields are extracted from the GBA archives at 00 and 12 UTC for each of the storms studied. The fields include the zonal (u) and meridional (v) wind components at the surface, 700 mb, 400 mb and 250 mb.

The data tapes are processed in a series of steps to allow the display of the wind data and derived fields in the Interactive Digital Environmental Analysis Laboratory (IDEA Lab) at the Naval Postgraduate School. The IDEA Lab consists of a VAX8200 mini-computer and two micro-VAX computers linked to various display terminals and input/output devices. The system allows interactive display of satellite, observational and gridded data as well as a variety of data processing capabilities (Wash *et al.*, 1987). The first step in the process is to match the fields and storm tracks. A list is compiled using the ATCR best track data for each storm and is compared to the fields available on the data tape. A full listing of the fields available can be produced using the Global Band File Identification (GBFID) program found in Appendix A.

The next step is to extract the fields required for study from the Naval Environmental Display Network (NEDN) format tapes and create a tape in ASC II format for use in the IDEA Lab. This is accomplished using the program GETGBA listed in Appendix B. The data section of the program must be carefully prepared to avoid problems due to missing fields in the GBA archives. If a complete set of fields for a date and time are missing from the set, that date-time code entry must be omitted from the GETGBA data file. If only a partial set of levels or component fields is missing, the date-time code information should be entered, which allows the subroutines to extract the fields that are present. The number of records to be skipped to get to the desired fields must also be accurate (see documentation in Appendix B).

The ASC II tape is used to create the data base in the IDEA Lab. The creation of the files for display and manipulation of the data is a two part process. First, the tape data is read to storage on a disk using the program Global Band Tape To Disk (GBTOD) found in Appendix C. The conversion of the data to a format that is compatible with the graphics software is accomplished using the FILE CONVERTER program in Appendix D. This program changes the GBA grid to a 2.5 degree latitude by 2.5 degree longitude grid using an interpolation subroutine, and inverts the grid array to make it compatible with the GEneral Meteorological (GEM) software (developed at NASA's Goddard Space Flight Center) used in the IDEA Lab. Once the data are written to a GEMFILE, the fields can be displayed and manipulated using the programs GEMPAK and GEMPLT.

#### D. GEMPAK AND GEMPLT PROGRAMS

The GEMPAK and GEMPLT software are used to display the data in a variety of ways including tabular data, grid point plots of data, contour plots, vector plots, streamlines and vertical profiles. The gridded data can also be manipulated with a variety of Grid Diagnostic Programs to display numerous derived fields including:

- a) Sums (ADD)
- b) Difference (SUB)
- c) Laplacian (LAP)
- d) Layer Average (LAV)
- e) Time Derivative (DDT)
- f) Time Difference (TDF)
- g) Time Average (TAV)
- h) Divergence (DIV)
- i) Relative Vorticity (VOR)

j) Absolute Vorticity (AVOR)

k) Gradients (GRAD)

and a number of other functions found in the GEMPAK User's Guide (desJardin *et al.*, 1986) Some of the diagnostic grids can be created "on the fly" and be directly displayed or sent to a hard copy output device. More complicated functions require that intermediate grids be created before further processing. In either case, an option exists to save the diagnostic grids in the same GEM file as the original storm data in date-time order.

The display terminals give multi-color depictions of the fields including geography of various resolutions and projections. Fields can be overlaid on the screen for analysis and can be reproduced in hard copy on laser printers or full color, on the VERSATEC plotter.

### III. DATA ANALYSIS

#### A. ANALYSIS PARAMETERS

Analysis of the fields is based on significant storm and synoptic parameters and the changes with time in the synoptic fields. The storm parameters used in the study are those used by the operational forecaster to request and initialize the forecast aids generation programs at FNOC. The parameters used in the study (Table 2) differ slightly from the combined aids request (CARQ) as the storm position information is reduced from 48 to 36 h and the intensity and size data are increased to 36 h of history. The storm size information is taken from the warning messages using the wind radii for 30, 50 and 100 kt. The values relating to the outer closed isobar as required in the forecast aids request were unavailable.

TABLE 2  
STORM PARAMETERS

1. Month of year, day of month
2. Position
  - a. Latitude, longitude
  - b. Fix platform (aircraft, satellite, radar, synoptic or extrapolation)
  - c. Position and direction change - movement past 12, 24, 36 h
3. Intensity
  - a. Surface wind (kt), MSLP (mb)
  - b. 700 mb winds (kt), height (m)
  - c. Change in above parameters in the last 12, 24, 36 h
4. Storm size
  - a. Radii of 100, 50 and 30 kt winds
  - b. Change in radii in the last 12, 24, 36 h

The synoptic parameters (Table 3) include those required for the CARQ as well as features used in other forecast techniques or deemed significant through developmental research findings. The position and intensity of the subtropical ridge and mid-latitude trough are included as they are part of the CARQ values, and the history change values are extended to 36 hours. The polar and subtropical jets are considered in light of the Typhoon Acceleration Prediction Technique (TAPT) developed by Weir (1982). The positions of the short wave trough north of the tropical cyclone were added to the list after the initial analysis had begun, as small deviations in the track were often found to coincide with the short-wave trough passage. As in the storm parameters, the changes in the synoptic parameters are recorded for the past 36 h.

## B. STREAMLINE FIELD ANALYSIS

The initial analysis of the data involved a detailed study of Super Typhoon Marge using the streamline version of the GBA wind fields (as used at JTWC) and the National Meteorological Center (NMC) Tropical-Mercator surface and upper-air analyses. This approach proved difficult for several reasons. The NMC analyses were not available for all time periods, and the mid-tropospheric chart was for the 500 mb vice the 400 mb level in the GBA series. This led to problems in developing a continuous history and determining accurate height center locations corresponding to the wind field features. The GBA streamline output presented inconsistencies in the depiction of some small centers, and often showed cyclones and anticyclones with reverse flow patterns. While the bearings from the storm center to the synoptic features could be determined in a consistent manner, the range determinations were often suspect due to scale changes across the Mercator grid. After completing the analysis of Marge using this approach, several conclusions were made:

- a. The process requires too much time to be useful in a forecast situation;
- b. The results are not clear due to the large number of variables involved; and
- c. Inconsistencies from chart to chart reduce the value of the information.

## C. VORTICITY FIELD ANALYSIS

### 1. Vorticity Field Presentations

The storm and synoptic parameters are important and require a presentation format that will incorporate the variations in the parameters into a more easily interpreted form. This idea led to the use of the vorticity fields (Fig. 3.1), which are

TABLE 3  
SYNOPTIC PARAMETERS

1. Subtropical ridge (Surface, 700 and 400 mb)
  - a. range and bearing to the maximum height of the ridge
  - b. range and bearing to the lowest height or break
  - c. height magnitude range and extent of the ridge
2. Long-wave trough (Surface, 700 and 400 mb)
  - a. range and bearing to the trough axis at 35 deg N to the west
  - b. height of the trough
  - c. closing rate of trough to the storm center
3. Short-wave trough
  - a. range and bearing to trough to the NW-NE of the storm center
  - b. closing or opening rate
4. Upper-level trough
  - a. TUTT location
  - b. closed cell locations and intensity
5. Subtropical and polar jets
  - a. range and bearing to the jet max NW-NE of the storm center
  - b. TAPT pattern type (Weir, 1982)
6. Second, third or fourth storm in the basin
  - a. bearing and range to each storm
  - b. closing rates
  - c. pressure and wind speed differentials
7. Topographic influence
  - a. range and bearing to the nearest influential land feature
  - b. flow direction and speed over the feature
  - c. closing or opening rate between the storm and feature

presently not available to the JTWC forecaster. The bogussed storm and the analyzed features in the GBA wind field are displayed well in the relative and absolute vorticity

fields using the diagnostic capabilities of the GEMPAK software in the IDEA Lab. The conversion to vorticity eliminated the reverse flow around small features that appeared in the streamlines and allowed better analysis of the details in the major features. The subtropical ridge in the vorticity fields gives details of the relative strength of different areas of the ridge that are not represented well in the streamline chart. The intensity of the synoptic troughs is also better shown in the contoured vorticity chart. The packing of the contours around the low centers shows the relative strengths of the centers as well as the changes in intensity when viewed in a time sequence. Thus, the vorticity presentation conveys important information to the forecaster at a glance without requiring lengthy data tabulation. The smaller scale storm and synoptic features appear to be integrated into the vorticity fields and presented through the variations found in the contour patterns between the major ridge and trough depictions.

It is hypothesized that the presence and location of a weakness in the ridge is very important when trying to predict the longitude of a turning or recurvature event. Perhaps an improvement in the prediction of the recurvature point could result from using the vorticity charts in conjunction with the objective track forecast aids.

DeMaria (1985) suggests that the storm motion can be related to the absolute vorticity gradient of the steering current with motion components in the direction of the gradient and cross-gradient. Thus the analysis of the vorticity fields was done initially using the gradients of relative and absolute vorticity. The model results of DeMaria were not evident in the operational fields, perhaps because of errors and inconsistencies in the operationally-analyzed fields that are then magnified by taking gradients. Since the error characteristics of these vorticity fields are not well known, the forecaster must determine whether a vorticity feature represents a real circulation or is caused by data inconsistencies.

The relative and absolute vorticity fields contain several dominant patterns that are found to vary gradually in time as the interactions among the tropical storm and the adjacent synoptic features strengthen and weaken with time. The relationship of the cyclone track to the synoptic patterns revealed in this study (Fig. 3.2) are:

- (i) CHANNEL -- linear pattern with relatively straight relative vorticity contours on each side of the storm that results in a "cork in a stream" type pattern (Fig. 3.2a). That is, the past and future storm positions tend to lie within the same "channel" of relative vorticity.

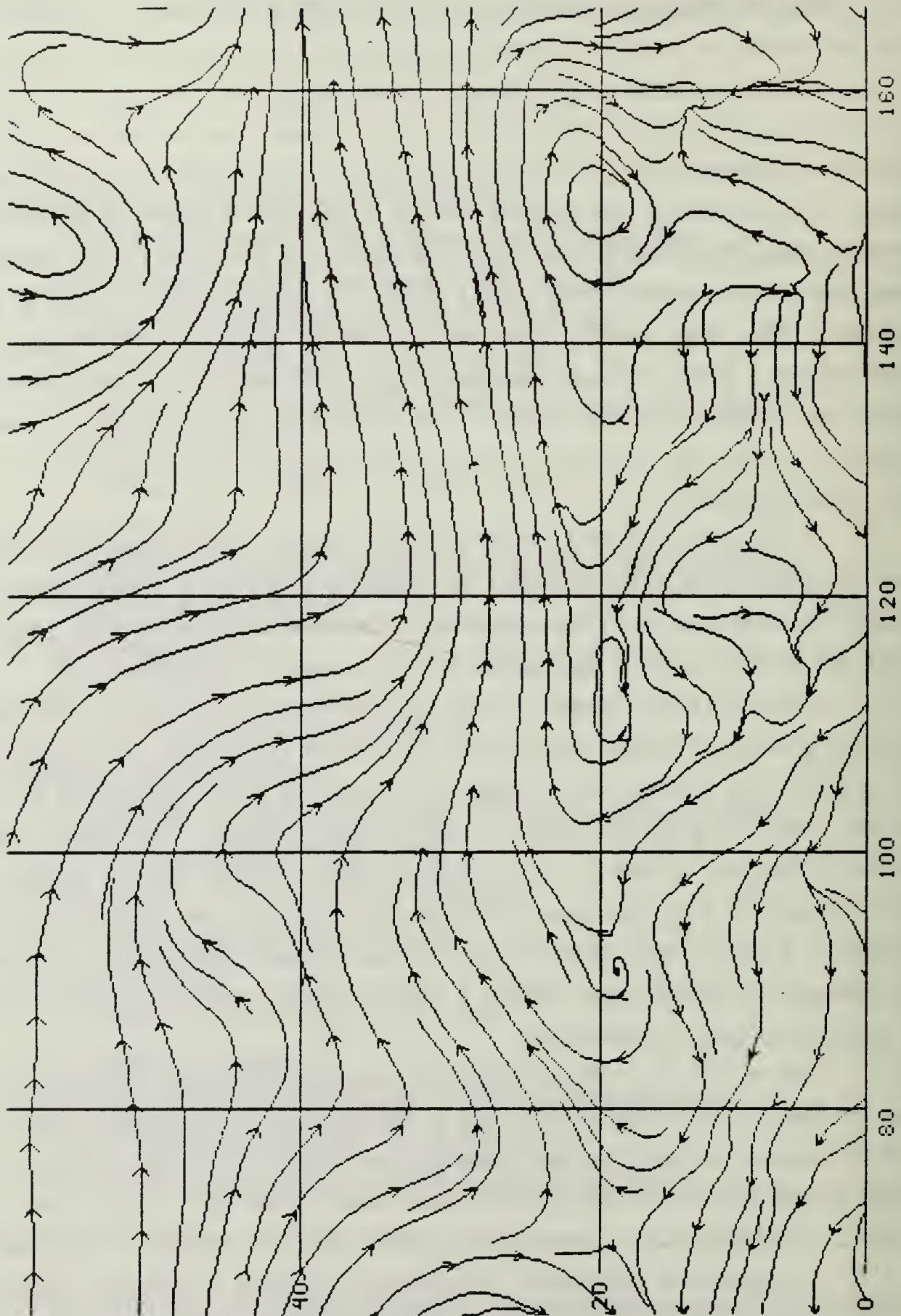


Fig. 3.1a Streamline chart at 400 mb at 12 UTC 31 Oct 1983.



Fig. 3.1b Relative vorticity ( $\times 10^5 \text{ s}^{-1}$ ) chart at 400 mb at 12 UTC 31 Oct 1983.

- (ii) **NODE** -- bulges in the contour(s) around the storm center that extend outward from the average circumference of the contour around the center, or extend northward from the average latitude of a zonally-oriented contour to the north of the center (Fig. 3.2b). Primary nodes are defined to be along the major axis of an elliptical vorticity contour that encloses the storm, or along the persistence track. That is, the tropical cyclone appears to track toward a primary node. However, secondary nodes are also monitored because they may become the major axis of the elliptical center, and thus be related to the subsequent storm direction changes with time.
- (iii) **CLOSED CONTOURS** -- vorticity (positive and negative) centers adjacent to the storm center that potentially may influence the long-term track (Fig. 3.2c).
- (iv) **PINCHED or BROKEN RIDGE** -- areas of contour deformation in the ridge north of the center that indicate weaknesses in the ridge (Fig. 3.2d).
- (v) **STORM-STORM INTERACTION** -- pattern transition from independent closed contours enclosing separate storm systems to a continuous vorticity contour enclosing two or more storm centers (Fig. 3.2e).
- (vi) **RESULTANT VECTOR PATTERN** -- a closed vorticity contour with a primary and a secondary node with axes approximately 80-120 deg apart (Fig. 3.2f). In some cases, a resultant vector from these two nodes can be constructed that appears to have very good correlation with the track at 60-72 h.

## 2. Proposed Synoptic Analysis Technique

The proposed analysis technique involves a recognition of the dominant synoptic pattern from the above list. Changes in the synoptic pattern with time are then recorded and are related to expected changes in the storm track. The orientation and deformations in the zero contour of relative vorticity is the key to the analysis, as it is common to all plots and usually encloses the storm center. Based on George (1975), Chan and Gray (1982), Chan (1984) and Chan (1985), vorticity fields at 700 mb, 400 mb and the layer average from 700-400 mb are examined to define synoptic pattern relationships to the track of the storm. The layer average is more consistent in time than the 700 and 400 mb fields alone. The layer average gives a smoother contour field that seems to change more conservatively through time than either of the individual levels, as suggested by Chan and Gray (1982). The relative vorticity fields

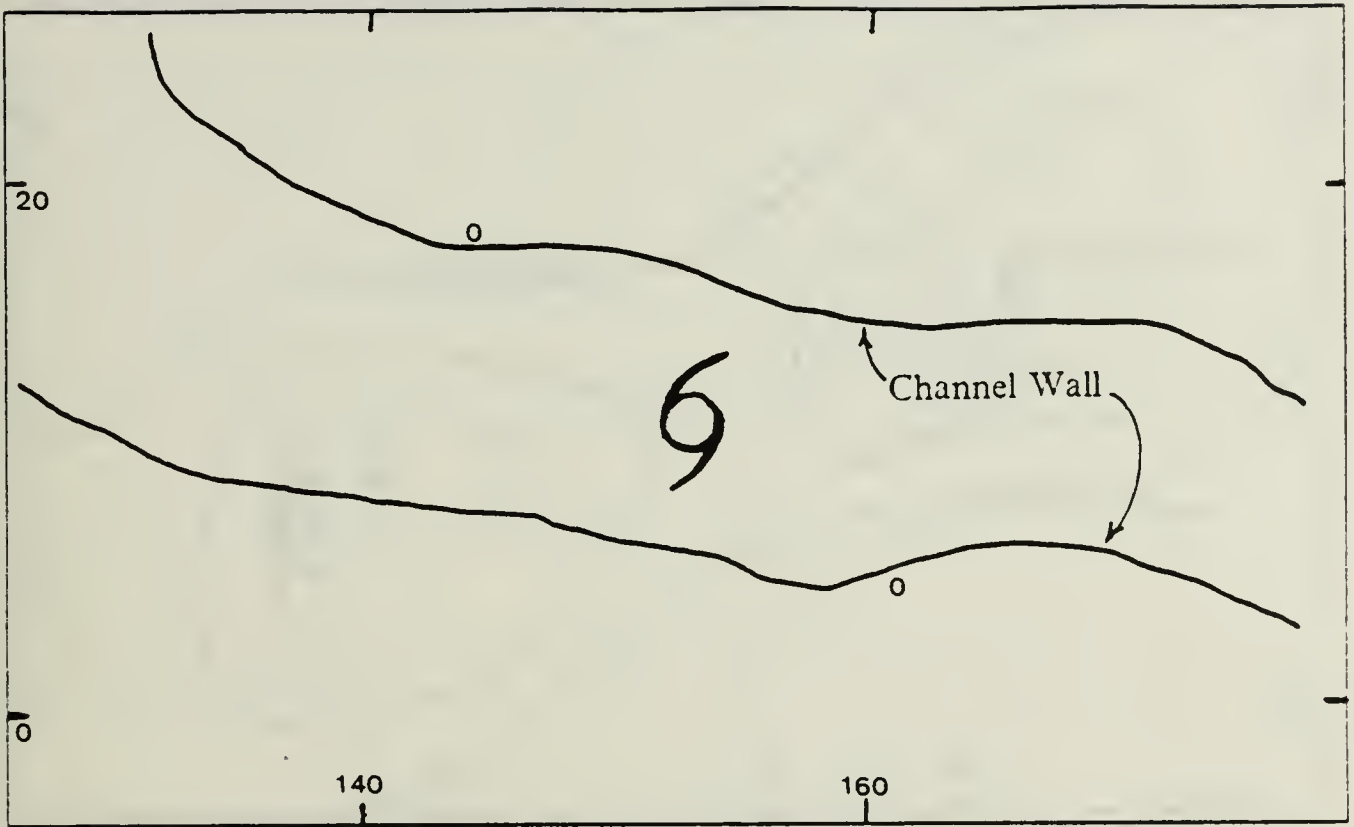


Fig. 3.2a Relative vorticity contour - channel pattern.

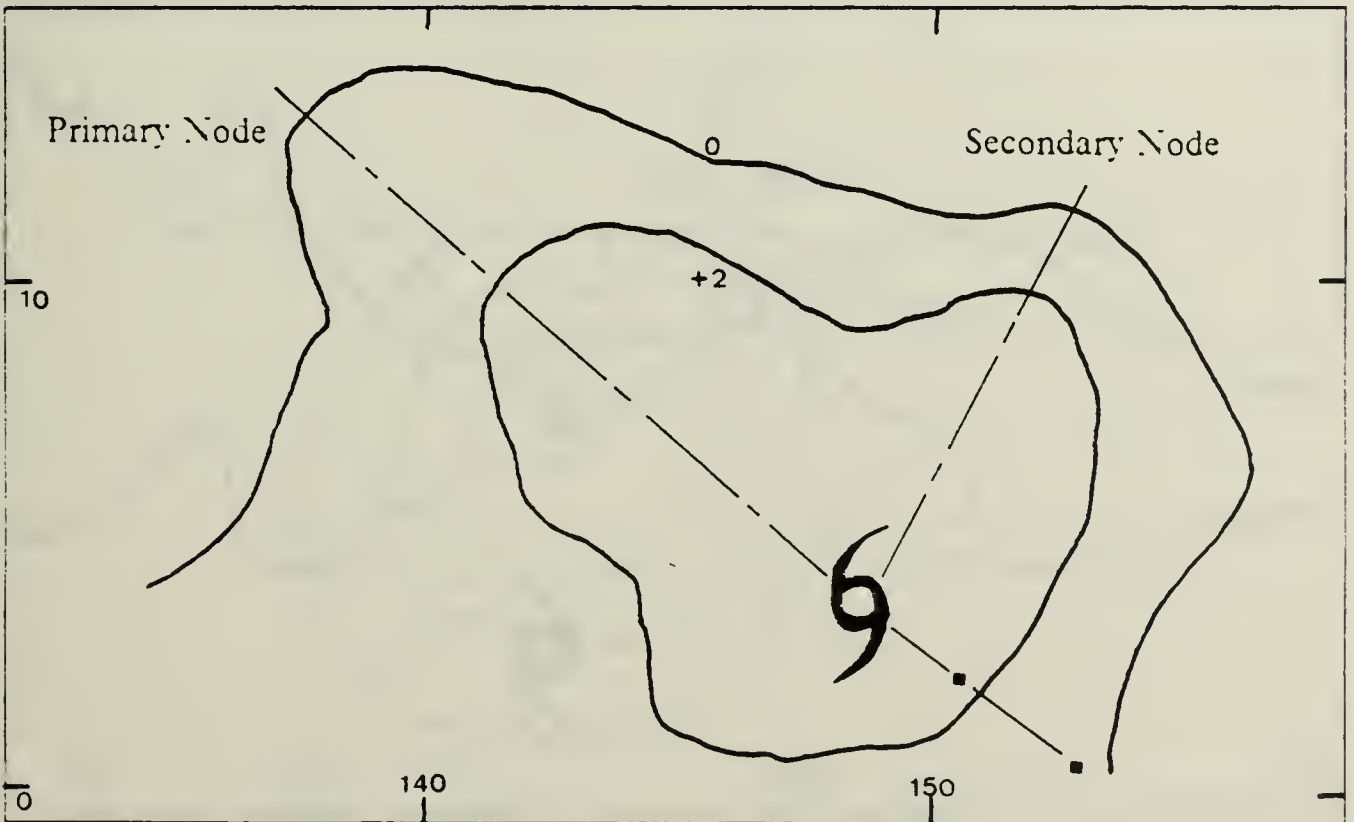


Fig. 3.2b Relative vorticity contour - node pattern.

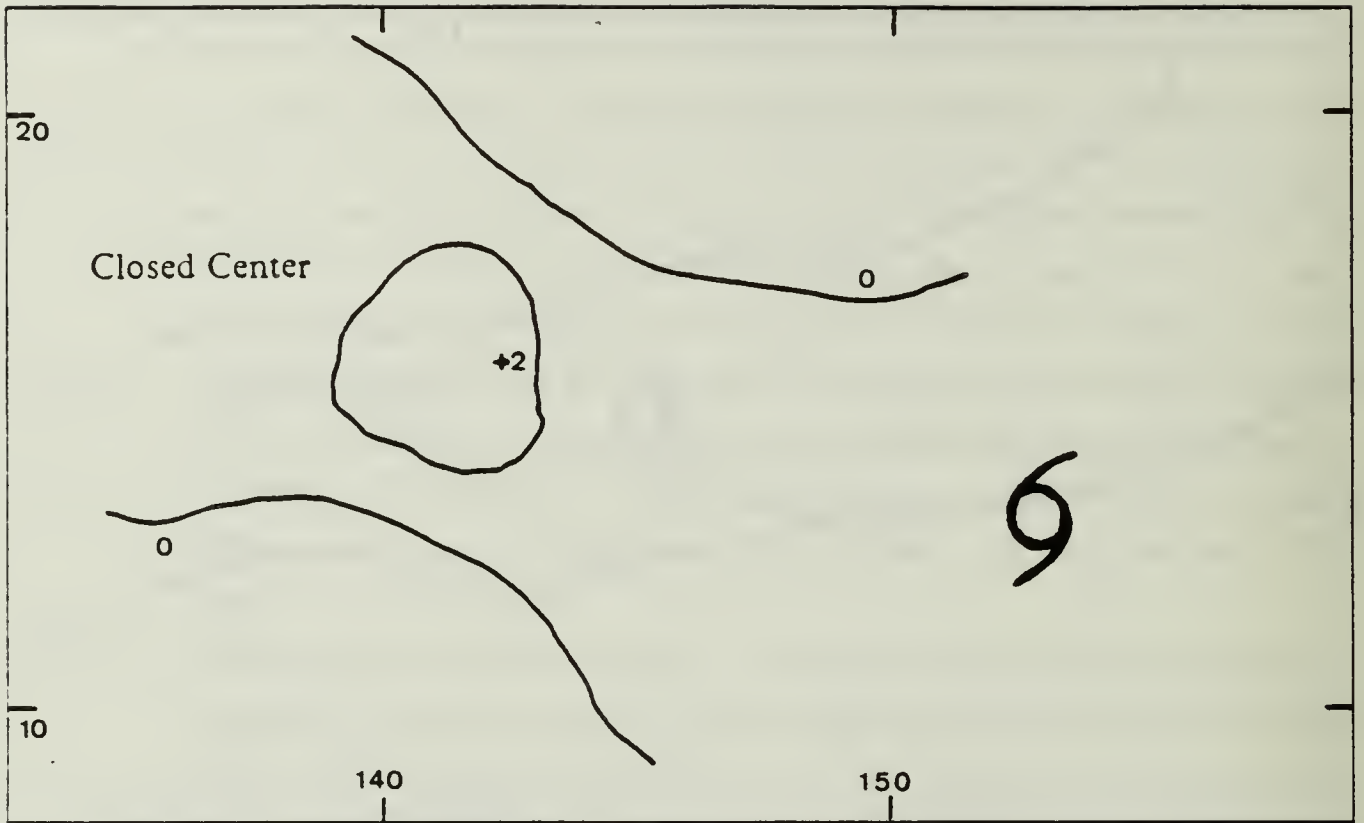


Fig. 3.2c Closed relative vorticity contour pattern.

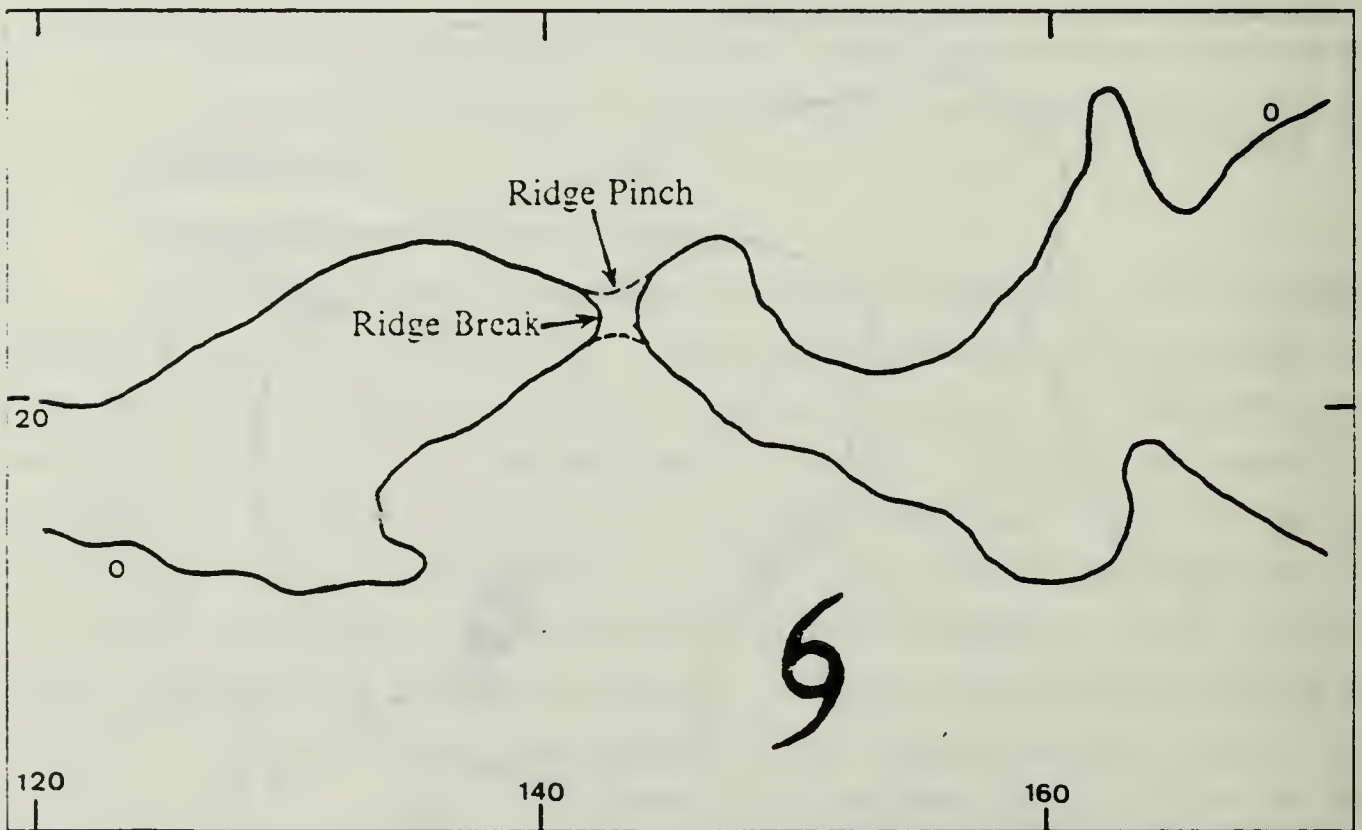


Fig. 3.2d Pinched or broken ridge contour pattern.

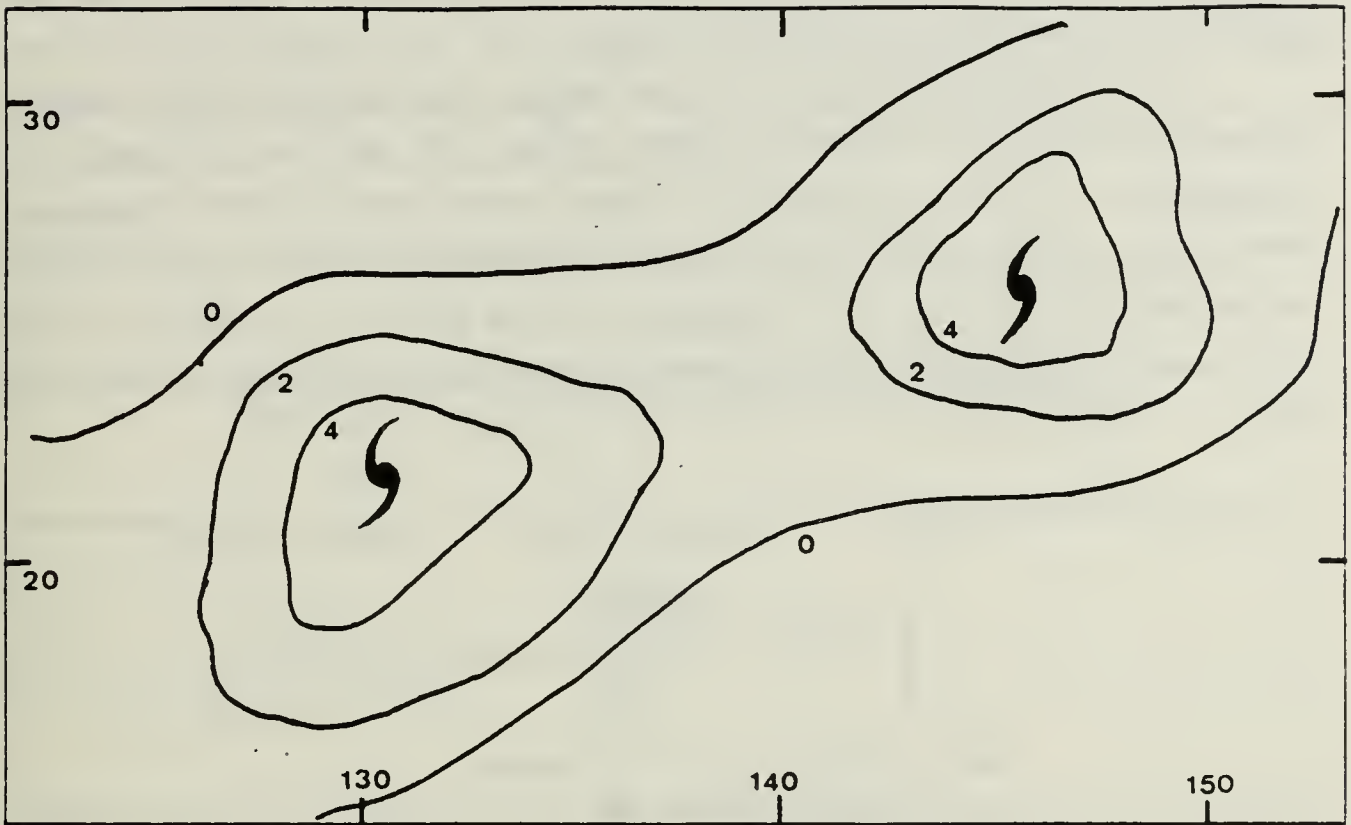


Fig. 3.2e Storm - storm interaction contour pattern.

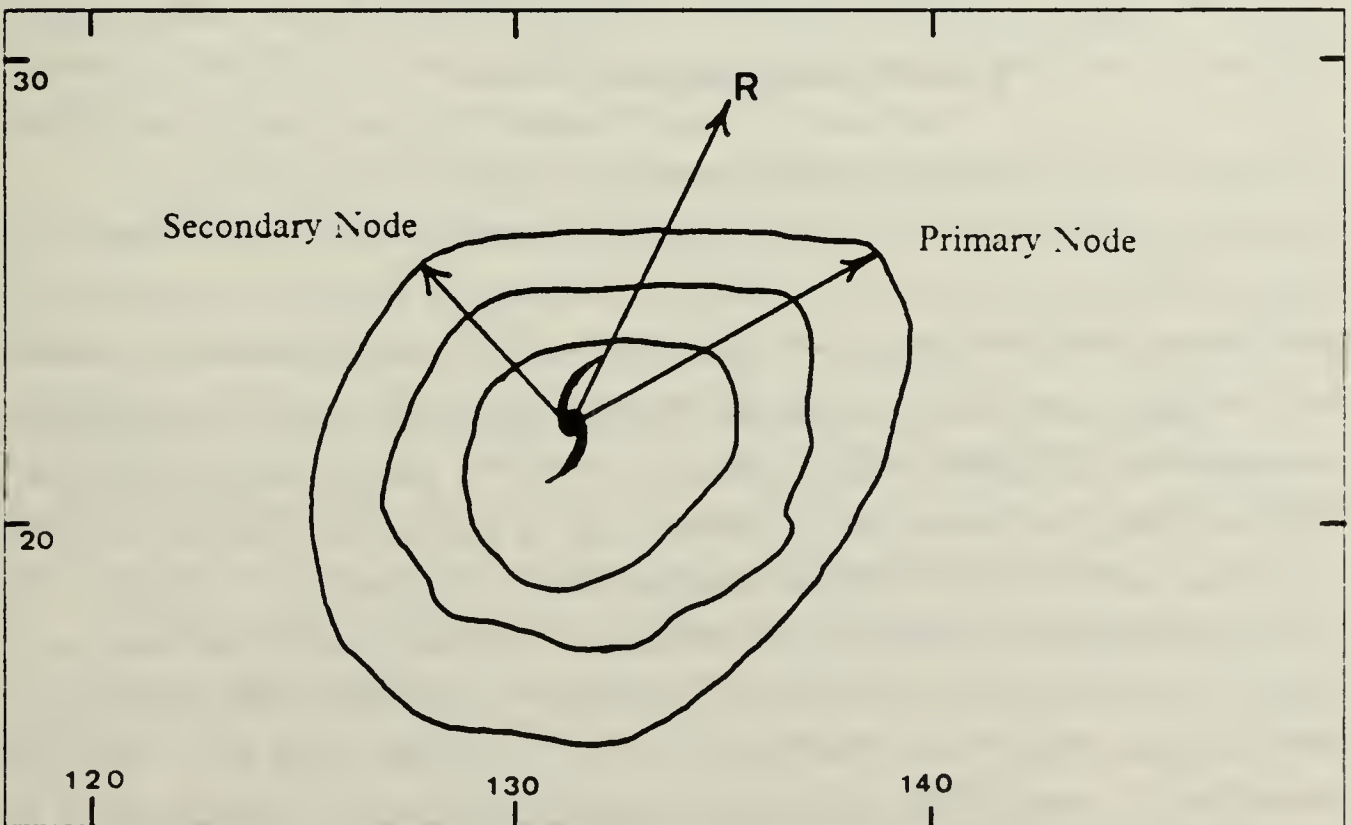


Fig. 3.2f Dual node-derived resultant vector pattern.

are chosen because the patterns of interaction among the storm and synoptic features are clearer with the earth's vorticity removed.

In the development phase of the research, a set of relative vorticity charts was plotted for the duration of Super Typhoon Marge. The best track for the 12 h old through the 72 h future positions were plotted on the charts to allow comparison of the vorticity pattern and the storm track. Unfortunately, the one chart set that was not available (12 UTC 05 Nov 1983) in the Marge series was 6 h after the time of recurvature. Table 4 gives the symbols used on the storm charts in the remainder of the study.

TABLE 4  
STORM CHART LEGEND

Best track positions (12 h intervals)	
Current position	●
12 h old position	■
Future positions	•
Forecast track positions (12 h intervals) *	
Positive vorticity contours	————
Negative vorticity contours	-----

Each chart is analyzed by first checking around the storm center location to determine the dominant contour pattern. In Fig. 3.3a, the first reported position of Typhoon Marge is located on the southern edge of a closed zero contour at 400 mb. The major pattern in the contours is a primary node in the zero and -2 contours, which has an orientation of approximately 310 degrees. Secondary nodes are found at 340 deg in the 0 contour and 325 deg in the -2 contour. Three distinct centers are found in the subtropical ridge, which is well to the north of the storm at this time. Notice that lines from the storm center through the primary and secondary nodes appear to pass

through the breaks between the centers in the subtropical ridge. The vorticity contours on the northern side of the ridge appear to have little relationship to the tropical cyclone as they are influenced more by the positive vorticity centers associated with two extratropical cyclones to the north of 40°N.

TABLE 5  
BEST TRACK - RELATIVE VORTICITY PATTERN  
ANGULAR CORRELATION EVALUATION CRITERIA

Included Angle (a)	Quality Assigned	Points
$0 < a < 5$	Excellent	6
$5 < a < 15$	Good	5
$15 < a < 30$	Fair	4
$30 < a < 60$	Poor	2
$60 < a$	None	0

To describe the correlation between the contour pattern and the best track, a comparison of the angle between the contour feature and the best track position is made. A point value is assigned according to the magnitude of the angle between the pattern axis and the best track. Table 5 gives the breakdown of points and a qualitative description for the ranges of the included angle (a) considered.

In applying the evaluation scheme to Fig. 3.3a, the closed zero contour that the center lies on is not considered. The orientation of the primary node in the open zero contour is evaluated as excellent (6 points) at 42 h and the secondary node is judged to be fair (4 points) at 42 h. These times are estimated by drawing an arc from the storm position and the maximum extent of the contour pattern to the best track, and interpolating along the best track at the intersection point (if the time is greater than 72 h, a value of 72 is assigned). For example, the primary and secondary nodes on the -2 contour are evaluated as excellent and good respectively at 72 h.

The vorticity contours in the 700 mb and 400:700 mb layer average fields (Fig. 3.3b and c) have less detail near the storm, although both have a node to the northwest in the zero contours. The 700 mb node in the zero contour is rated excellent at 58 h. The small +2 closed contour is evaluated as excellent at 12 h. The layer average (LAV) node in the zero contour is rated to be excellent at 48 h. Notice that a

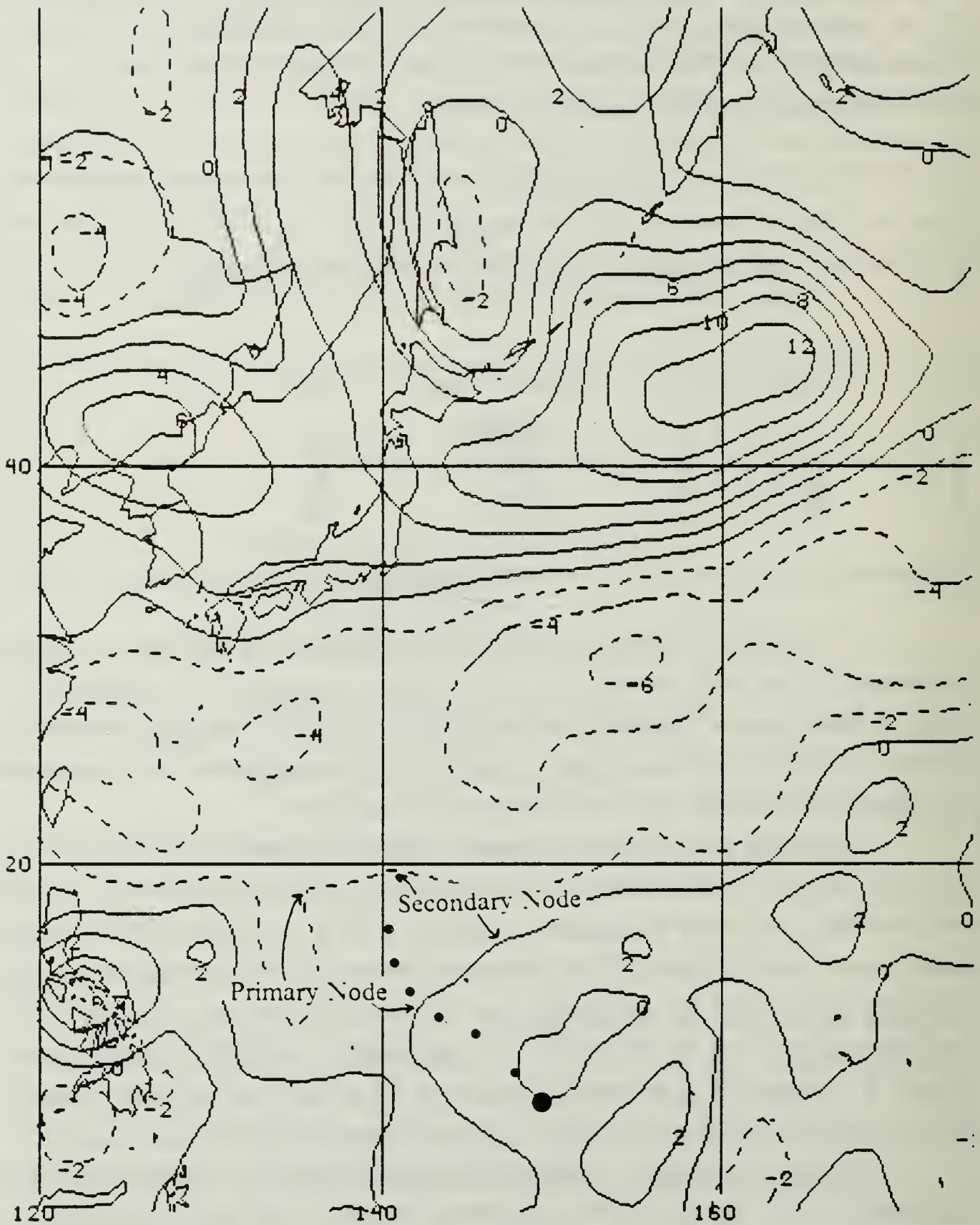


Fig. 3.3a Relative vorticity ( $\times 10^5 \text{s}^{-1}$ ) at 400 mb at 12 UTC 30 Oct 1983.

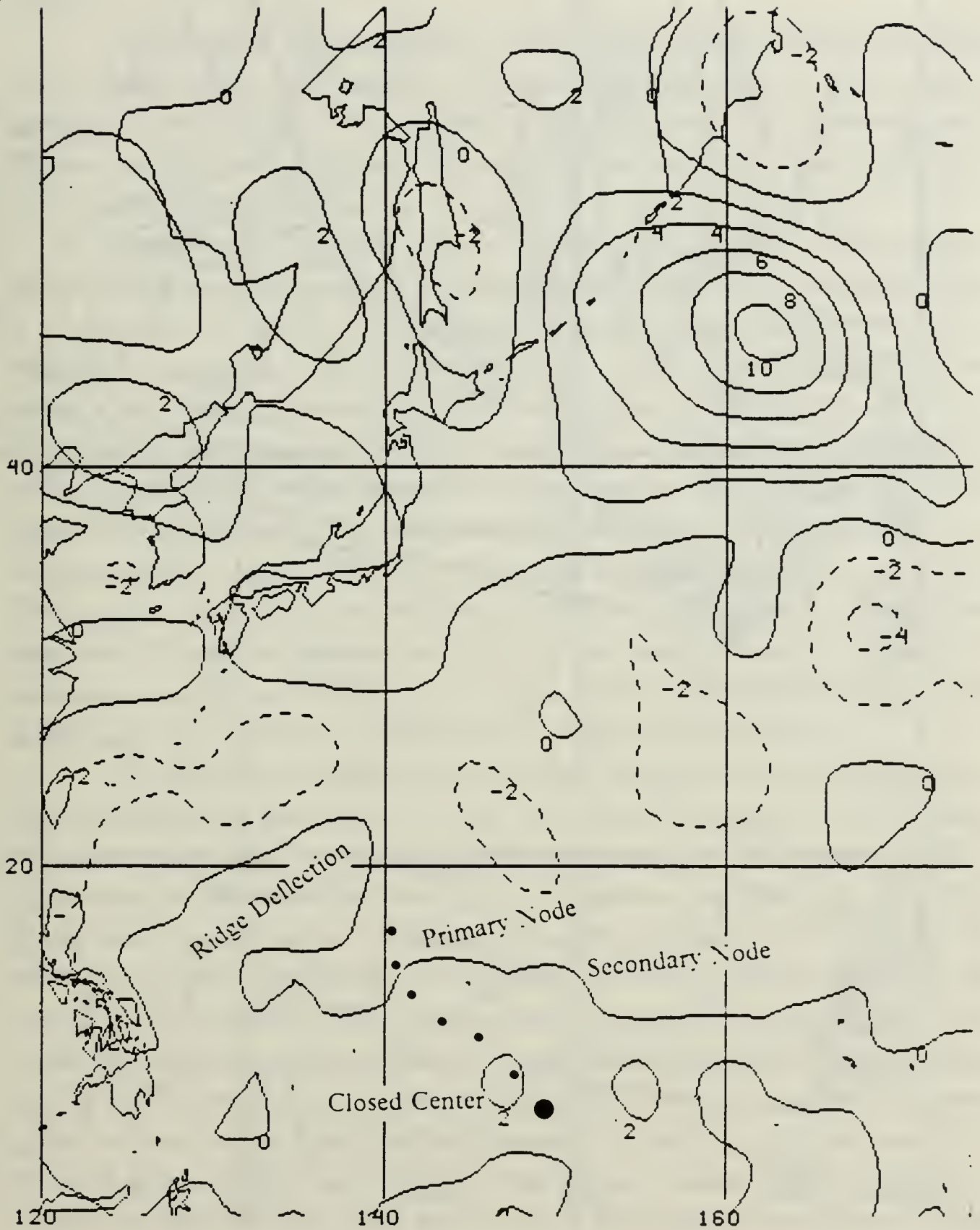


Fig. 3.3b Relative vorticity ( $\times 10^5 \text{ s}^{-1}$ ) at 700 mb at 12 UTC 30 Oct 1983.

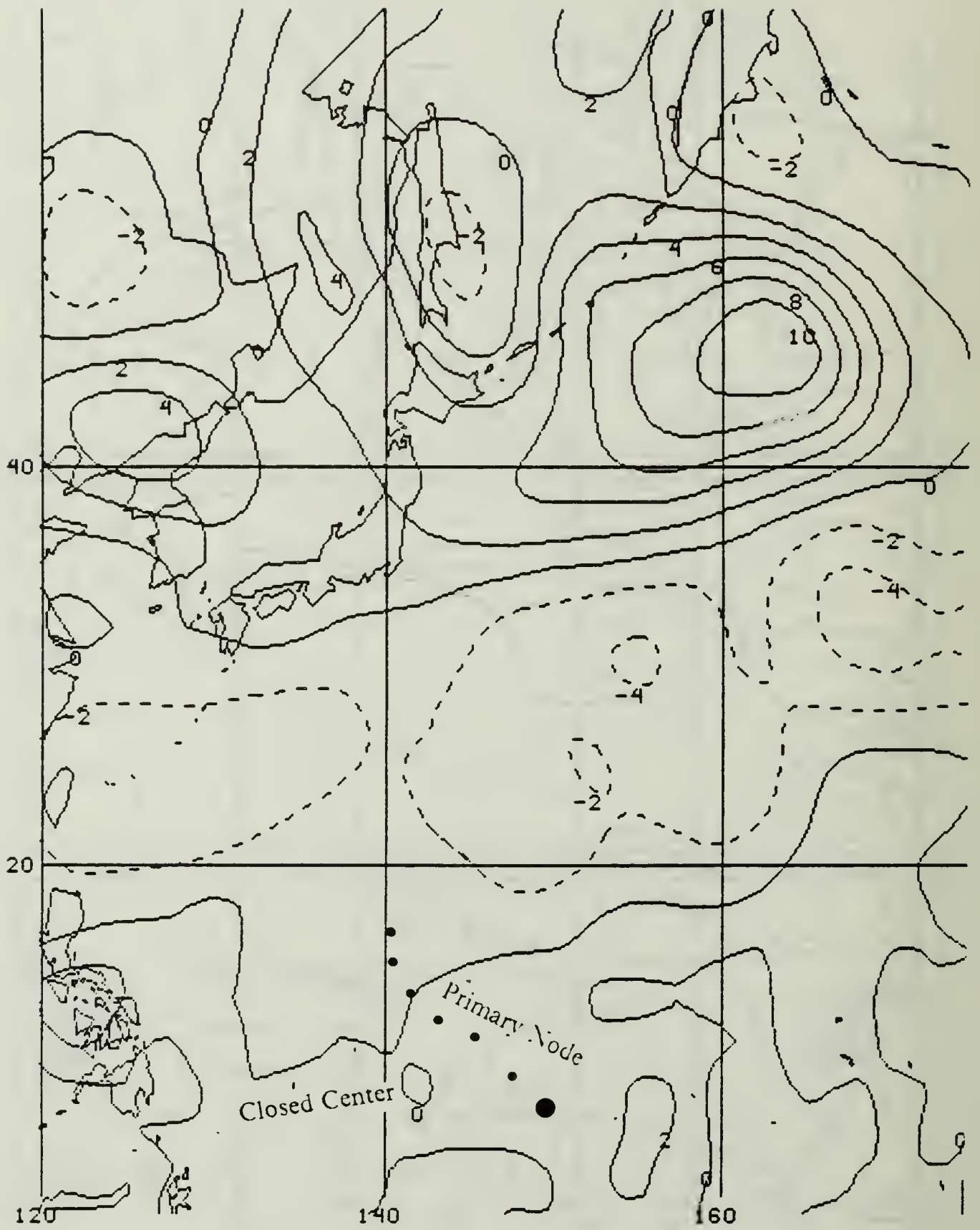


Fig. 3.3c Relative vorticity ( $\times 10^5 \text{ s}^{-1}$ ) in LAV at 12 UTC 30 Oct 1983.

distinct break in the ridge is defined by the -2 contour north of the 72 h best track position.

The movement and development of these basic patterns is followed through the next eight days in 12 h intervals to illustrate the progression of these synoptic pattern-track relationships. The objective is to determine if the synoptic pattern changes precede storm track changes consistently, which would allow them to be useful for forecasting the track change.

As development occurs in the next 12 h, a new +2 contour is found around the storm (Fig. 3.4a). Although the orientation of the zero contour nodes change little in 12 hours, the -2 node has moved slightly south and closer to the storm center in response to a strengthening of the subtropical ridge to the northwest. Notice that the change in the -2 node correlates with the direction change in the best track at 60-72 h. The strengthening of the ridge to the northeast seems to be linked to the passage of a vorticity center ( $45^{\circ}\text{N}$ ,  $170^{\circ}\text{E}$ ) moving to the east-northeast, with strengthening of the ridge following passage of the +12 center and weakening in proximity of the +6 center northwest of Marge. The 700 mb field (Fig. 3.4b) has changed little, other than a widening of the ridge in the meridional direction and the enclosure of the storm center by a +2 contour. Similarly, the LAV (Fig. 3.4c) has an enclosed vorticity center. Although the ridge has strengthened, the break in the ridge near  $25^{\circ}\text{N}$ ,  $140^{\circ}\text{E}$  has closed. This again suggests the storm may not continue the northerly track.

The primary (secondary) node on the zero contour at 400 mb becomes more (less) pronounced in the next 12 h (Fig. 3.5a). However, a large secondary node develops on the -2 contour. Although the new node on the -2 contour is larger than the one that has been tracked previously, it is considered as secondary due to the lack of past history for the feature. Furthermore, the new node does not correlate with the primary zero contour node or the storm track history well. At 700 mb (Fig. 3.5b), an expansion of the vorticity center occurs around the tropical cyclone, a closed zero contour develops and some weakening of the ridge occurs. A distinct change has taken place in the LAV chart (Fig. 3.5c) as a primary node in the zero contour has developed to the northwest of the storm center. This node is rated as a good correlation (5 points) at 60 h. However, the subtropical ridge has also widened slightly and a break has redeveloped to the north of the storm center in response to the mid-latitude trough pattern. The forecaster would have to evaluate whether this break in the ridge would signal continued recurvature, or whether the development of a strong primary node to the northwest would indicate a turn to the west.

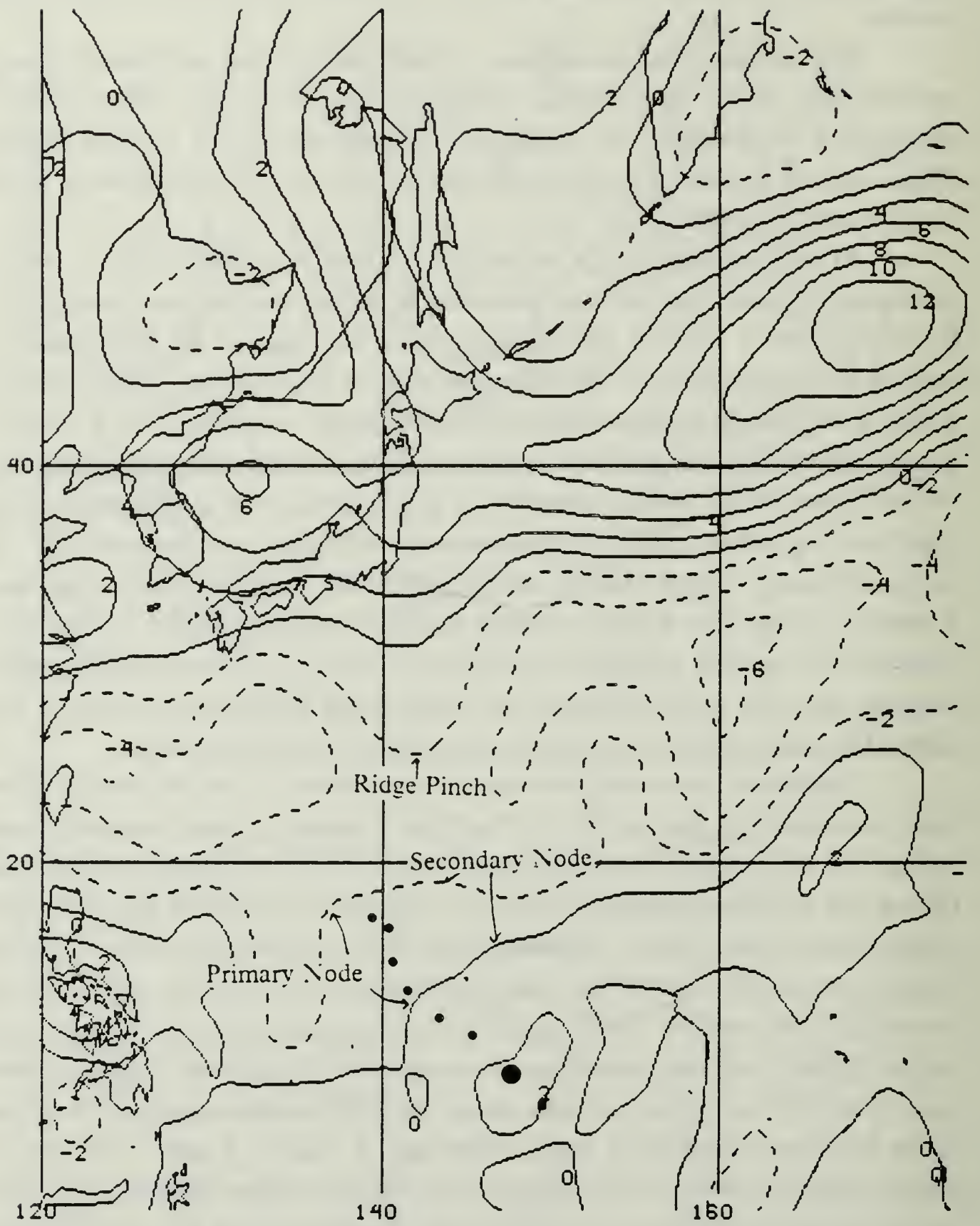


Fig. 3.4a Relative vorticity ( $\times 10^5 \text{s}^{-1}$ ) at 400 mb at 00 UTC 31 Oct 1983.

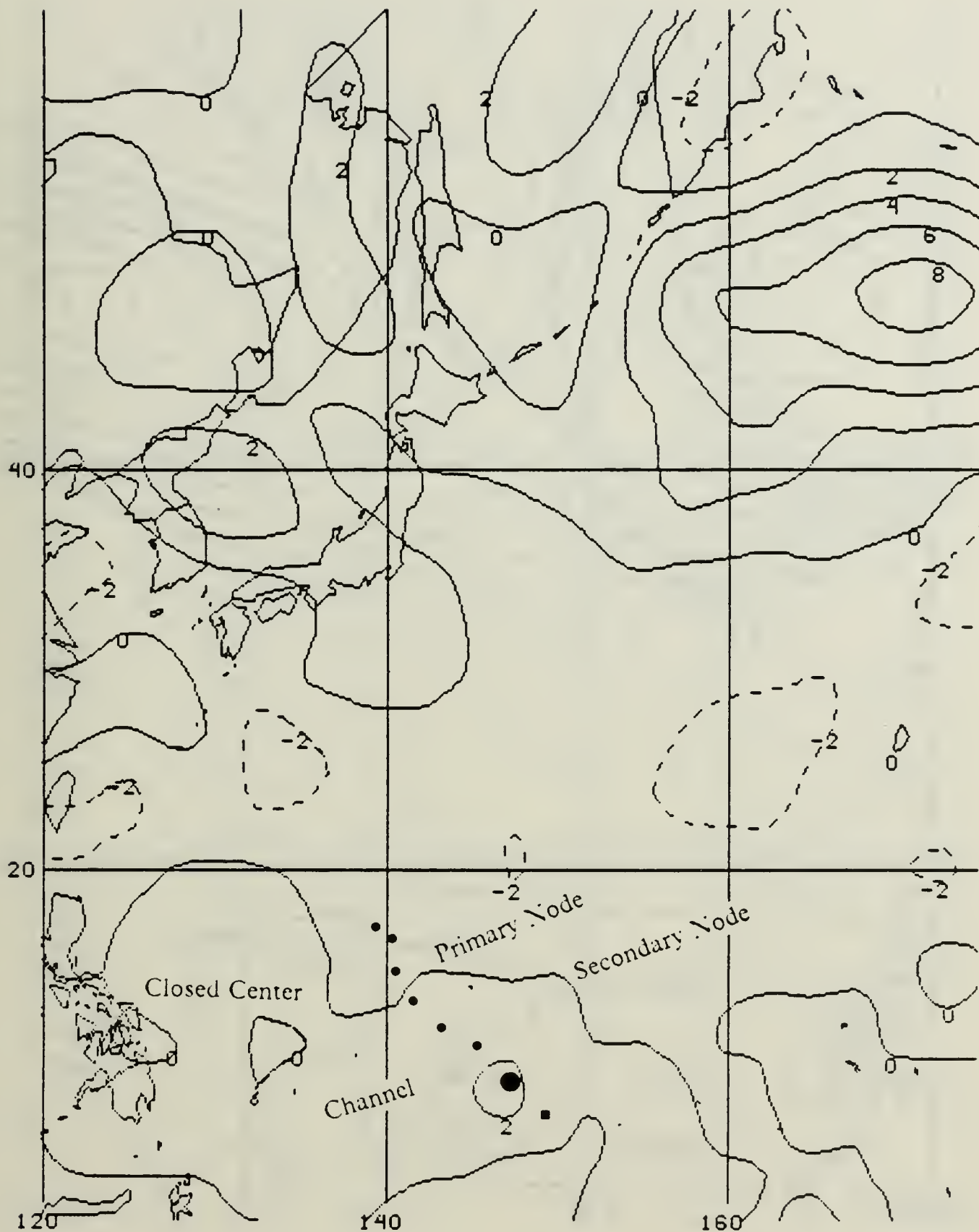


Fig. 3.4b Relative vorticity ( $\times 10^5 \text{s}^{-1}$ ) at 700 mb at 00 UTC 31 Oct 1983.

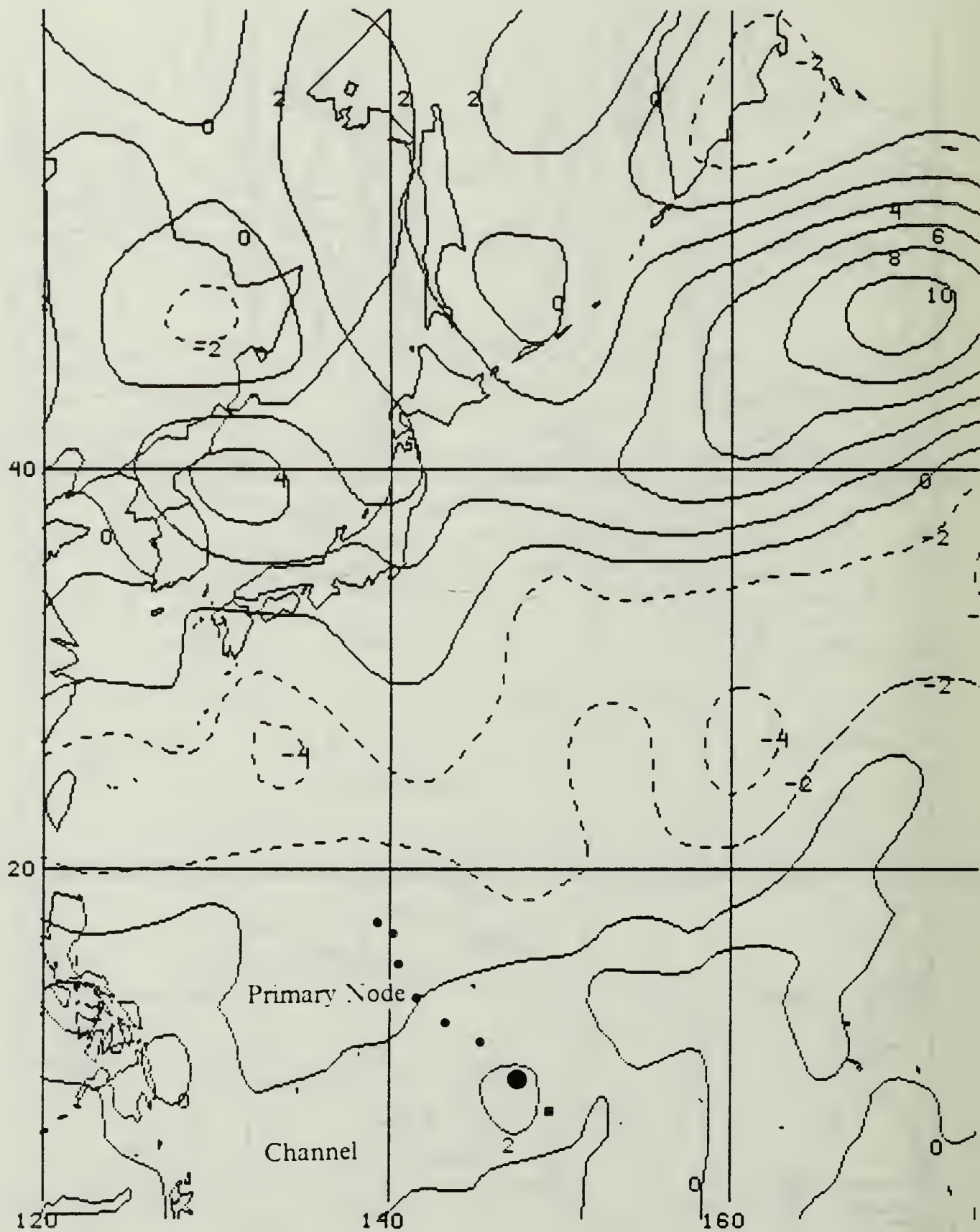


Fig. 3.4c Relative vorticity ( $\times 10^5 \text{s}^{-1}$ ) in LAV at 00 UTC 31 Oct 1983.

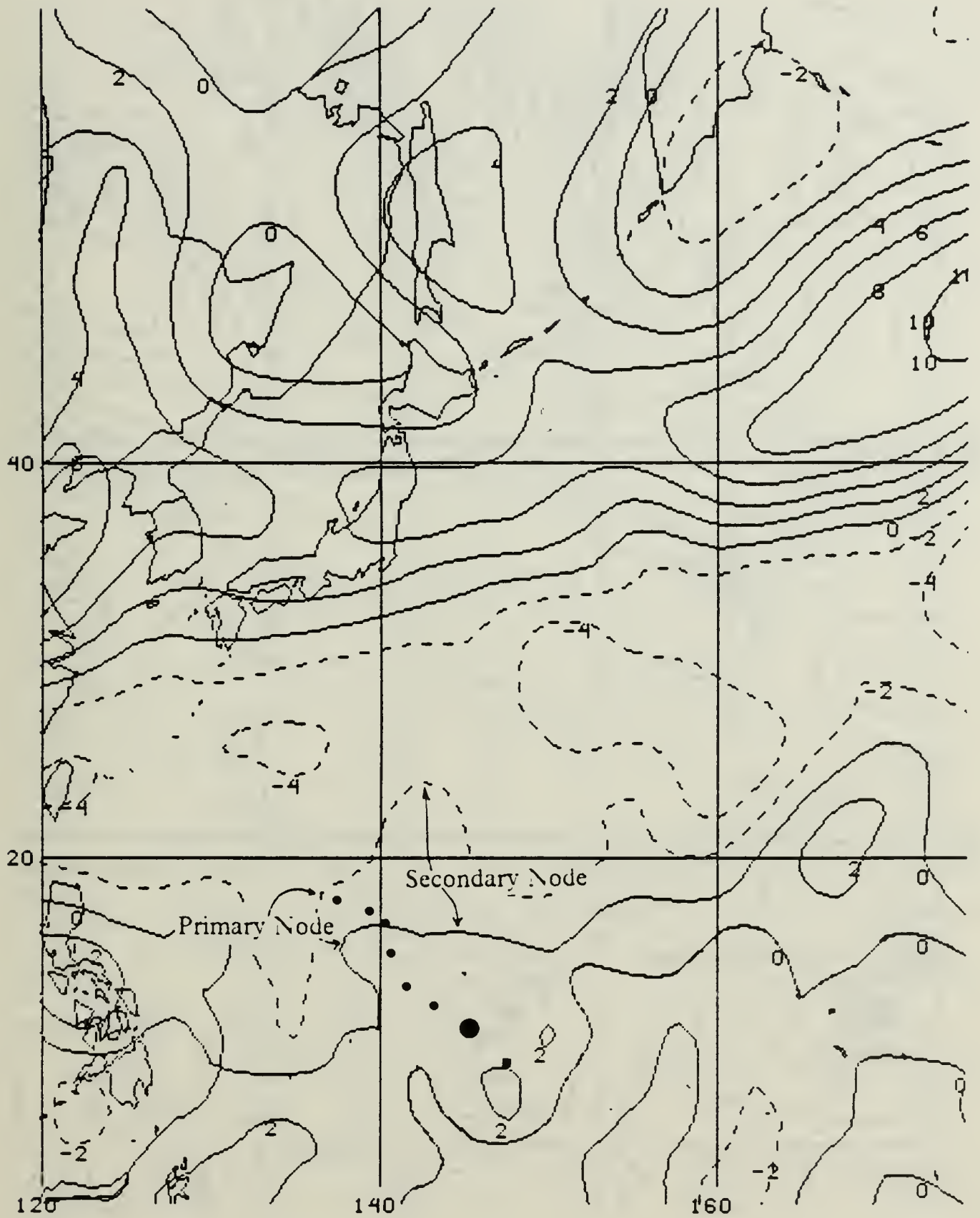


Fig. 3.5a Relative vorticity ( $\times 10^5 \text{s}^{-1}$ ) at 400 mb at 12 UTC 31 Oct 1983.

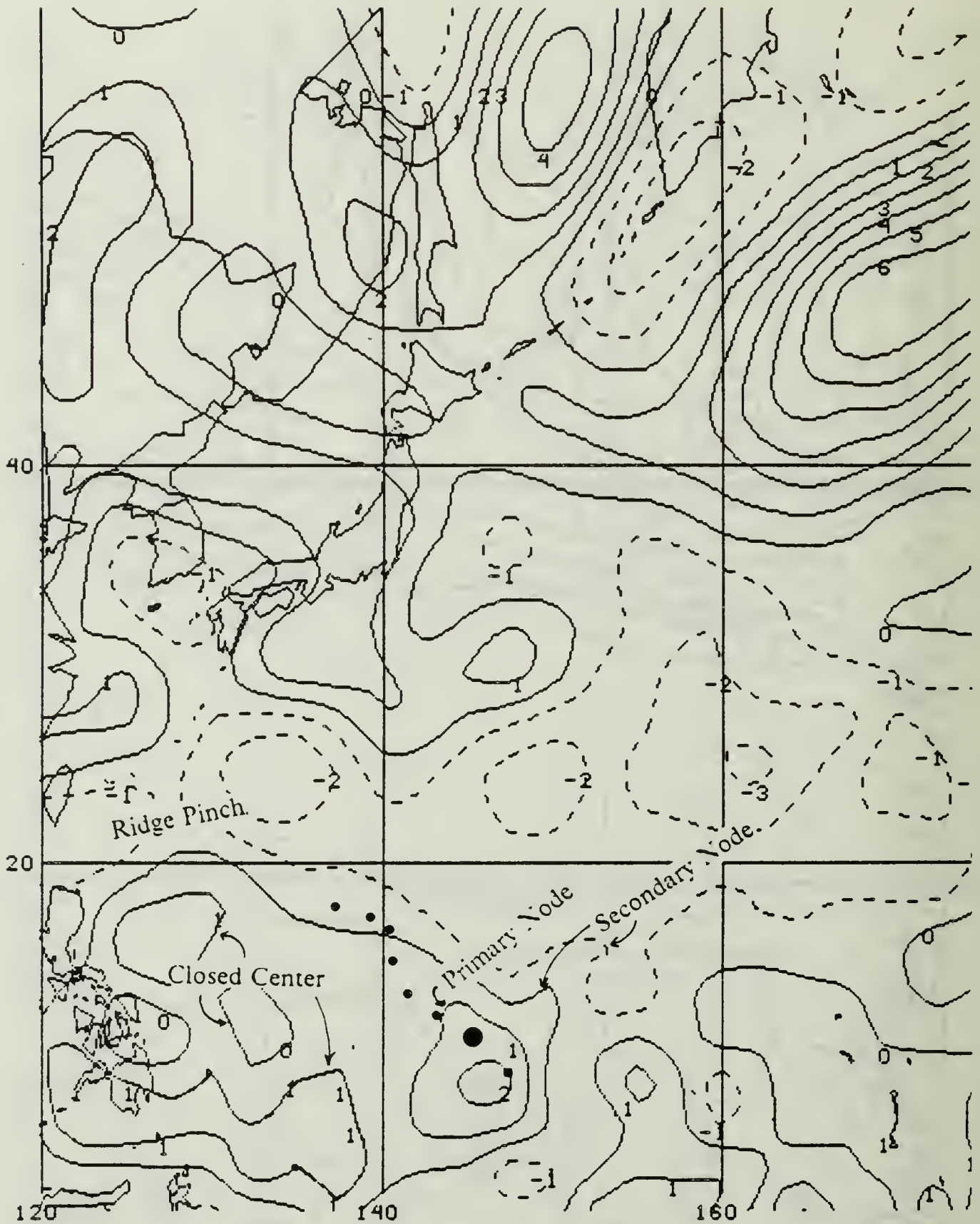


Fig. 3.5b Relative vorticity ( $\times 10^5 \text{ s}^{-1}$ ) at 700 mb at 12 UTC 31 Oct 1983.

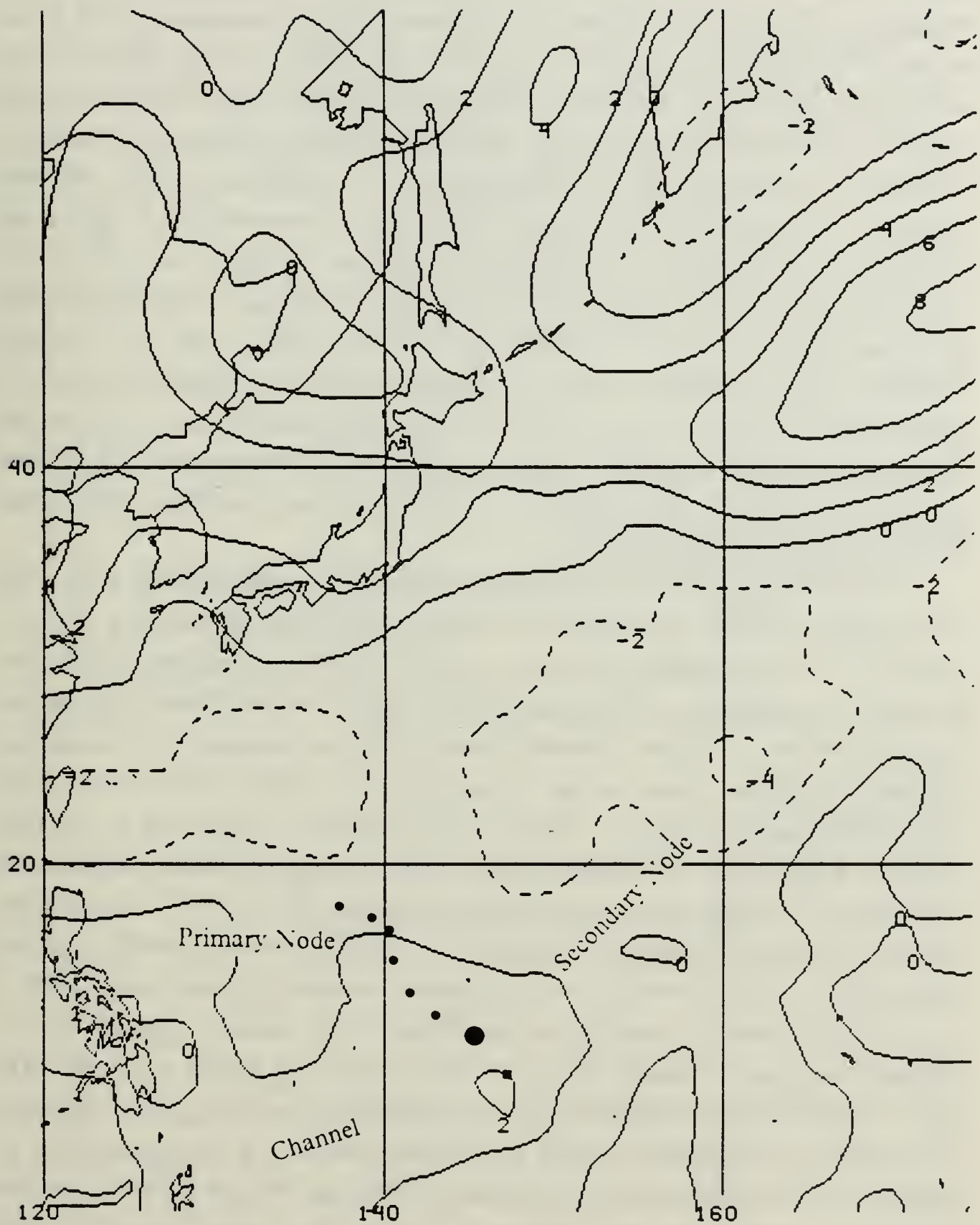


Fig. 3.5c Relative vorticity ( $\times 10^5 \text{s}^{-1}$ ) in LAV at 12 UTC 31 Oct 1983.

At 00 UTC 01 Nov 83, the 400 mb relative vorticity field (Fig. 3.6a) has slight changes including a +2 closed contour around the tropical storm center and strengthening of the ridge to the north of the center. Although continued growth of the secondary node in the -2 contour is observed, the tropical cyclone appears to be embedded in the primary node that in this case is associated with sustained motion toward the northwest. In Fig. 3.6b, the continued expansion of the vorticity center of the storm is evident as well as the appearance of a pronounced node in the zero contour to the northwest. The large vorticity gradient oriented NW to SE to the northwest of the storm would seem to suggest continued movement to the northwest. The LAV pattern (Fig. 3.6c) also shows slight changes. Although the subtropical ridge break has closed, a definite pinched ridge pattern remains, and the meridional separation of the -2 contours is reduced. The zero contour has changed little and a +2 contour has enclosed the center. The -2 contour changes would seem to indicate that recurvature should be anticipated at this time. However, the zero contour at all levels continues to display a major axis in the northwest-southeast direction, which would indicate movement to the northwest.

At 12 UTC 1 Nov 83, a significant change occurs at 400 mb (Fig. 3.7a) as the zero contour now has a pronounced secondary node similar to the node in the -2 contour. Thus, the direction of the major axis of the pattern is less clear than before. However, these nodes are quite far north of the tropical cyclone. Also, note that the major axis of the +2 closed contour around the center remains in the northwest-southeast orientation. Based on the persistence of the primary node and the recent track of the storm, no change is made in the primary node designation at this time. The 700 mb chart (Fig. 3.7b) shows a direct link to the higher latitudes has developed in the form of a narrow channel through the ridge near 22°N, 130°E. The LAV chart (Fig. 3.7c) has a more conservative change in the contour pattern with only a gradual growth of the secondary node on the zero contour. Although the ridge to the north of the center is quite broad, the ridge to the west-northwest appears to be narrowing in response to a positive vorticity center now over Honshu and moving to the east. This center eventually will create the path to the mid-latitudes that STY Marge will follow in recurvature. In hindsight, the key to the present situation is to recognize that the opportunity for recurvature into the weakness in the ridge will not occur. Only a feint to the north actually occurred, presumably because the primary vorticity channel oriented NW-SE was a dominant factor rather than the possible influence of the more distant secondary

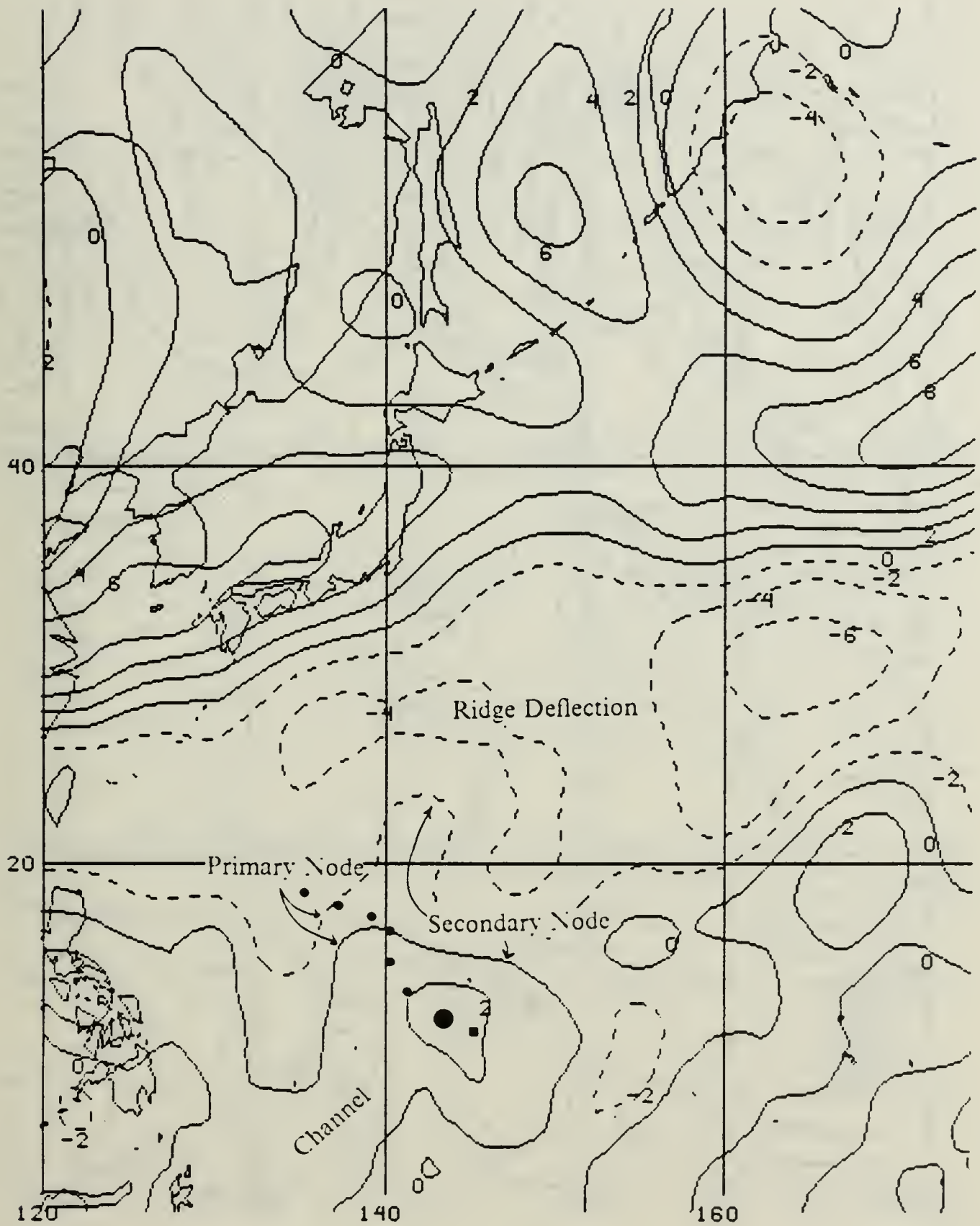


Fig. 3.6a Relative vorticity ( $\times 10^5 \text{s}^{-1}$ ) at 400 mb at 00 UTC 01 Nov 1983.

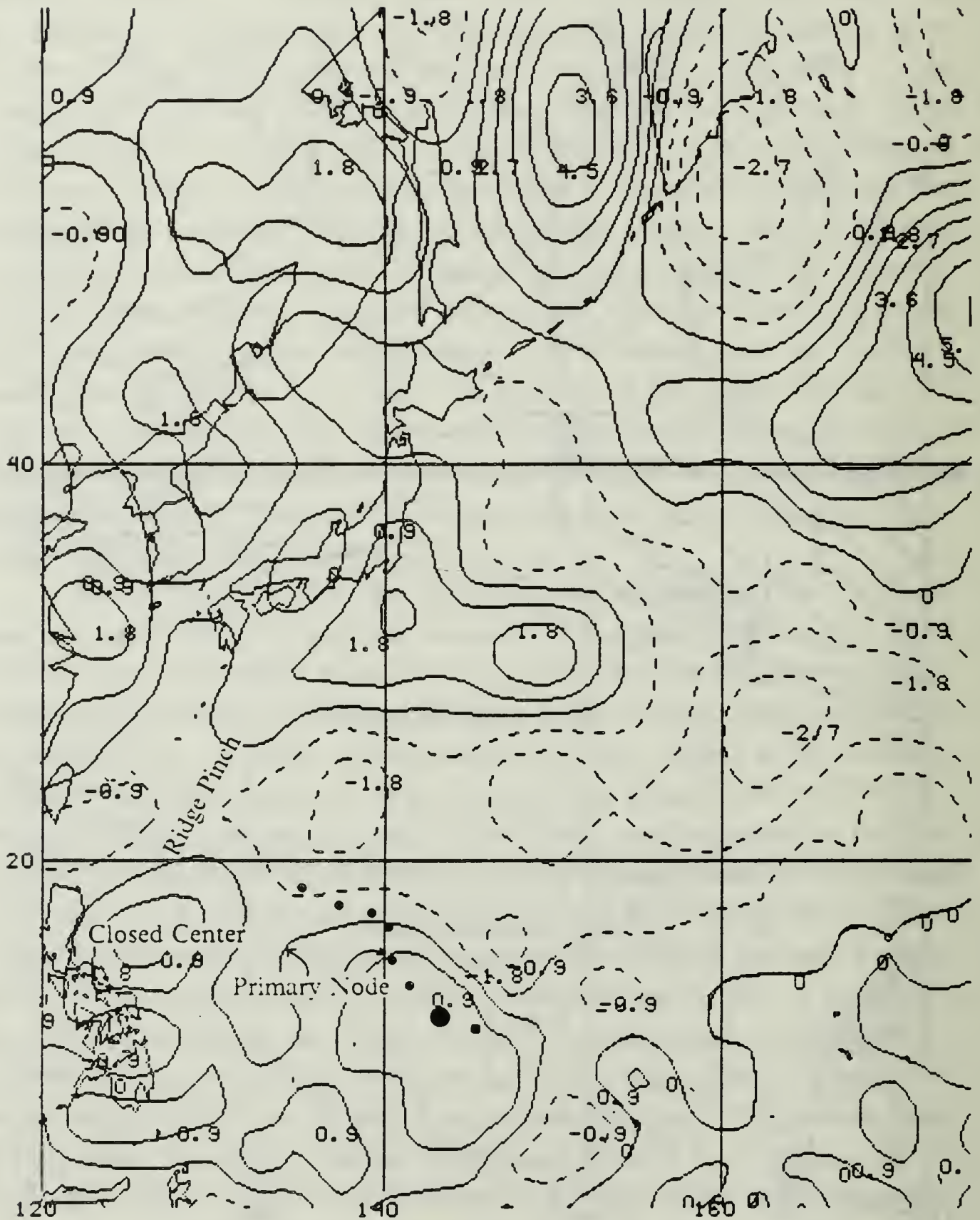


Fig. 3.6b Relative vorticity ( $\times 10^5 s^{-1}$ ) at 700 mb at 00 UTC 01 Nov 1983.

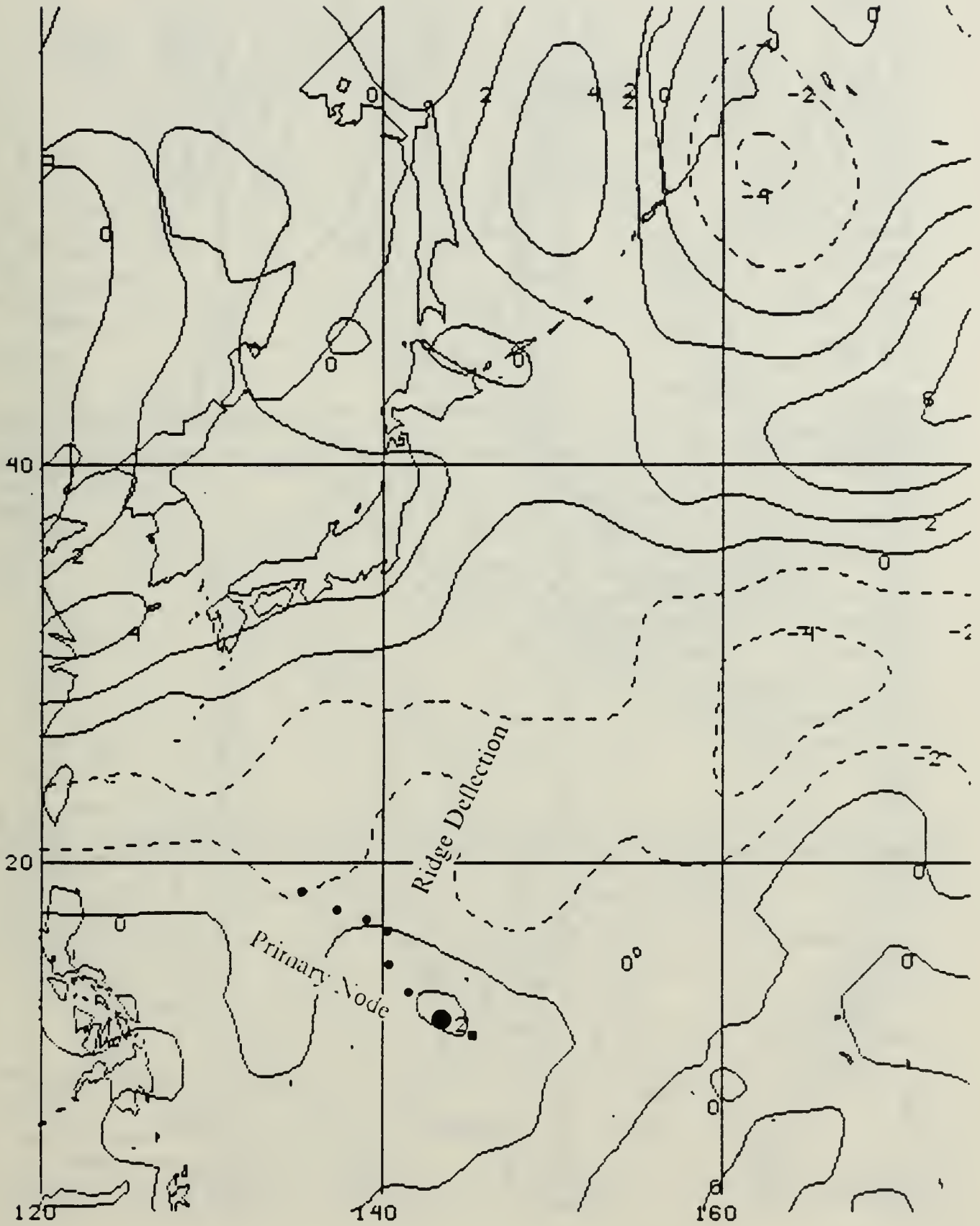


Fig. 3.6c Relative vorticity ( $\times 10^5 \text{ s}^{-1}$ ) in LAV at 00 UTC 01 Nov 1983.

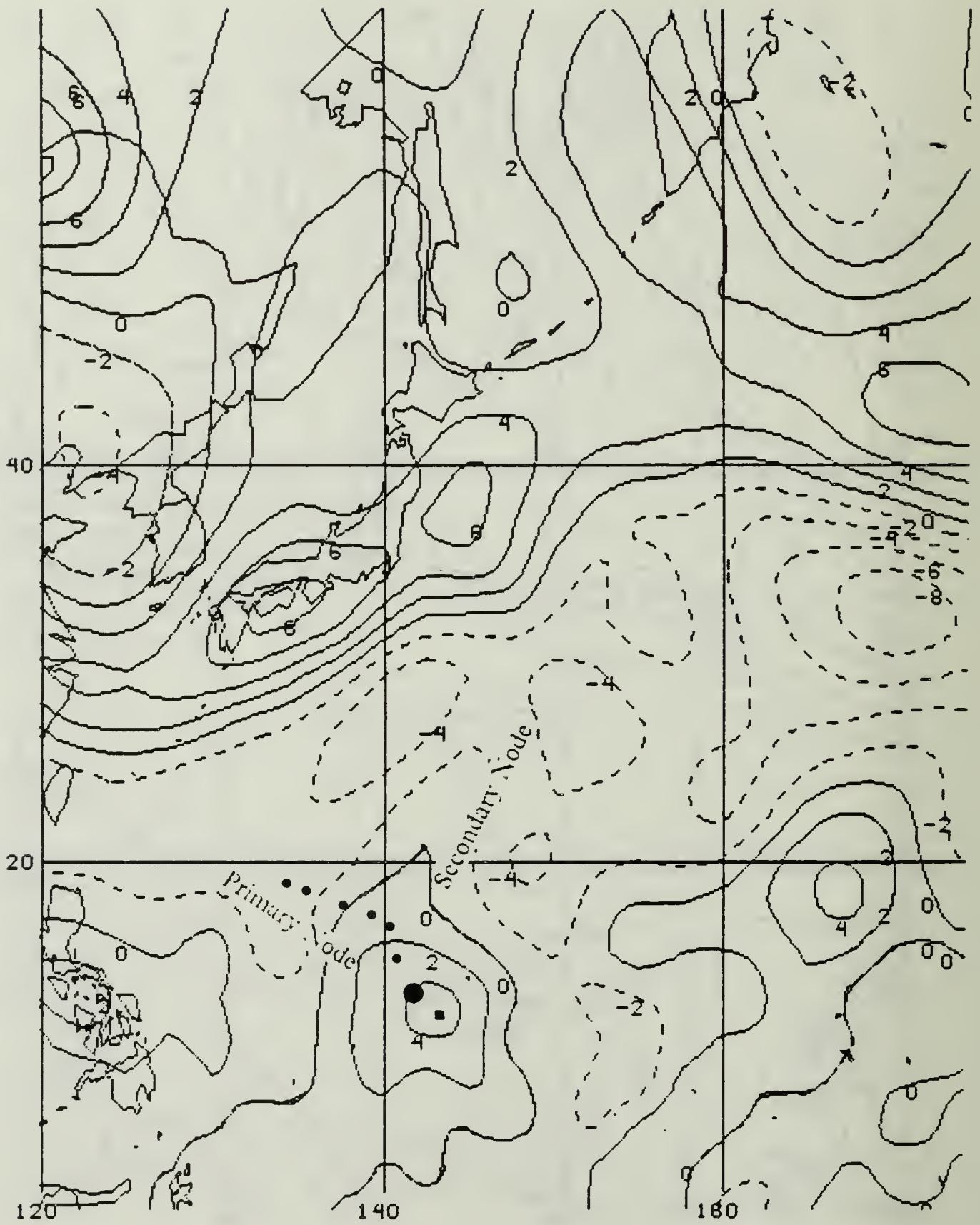


Fig. 3.7a Relative vorticity ( $\times 10^5 \text{s}^{-1}$ ) at 400 mb at 12 UTC 01 Nov 1983.

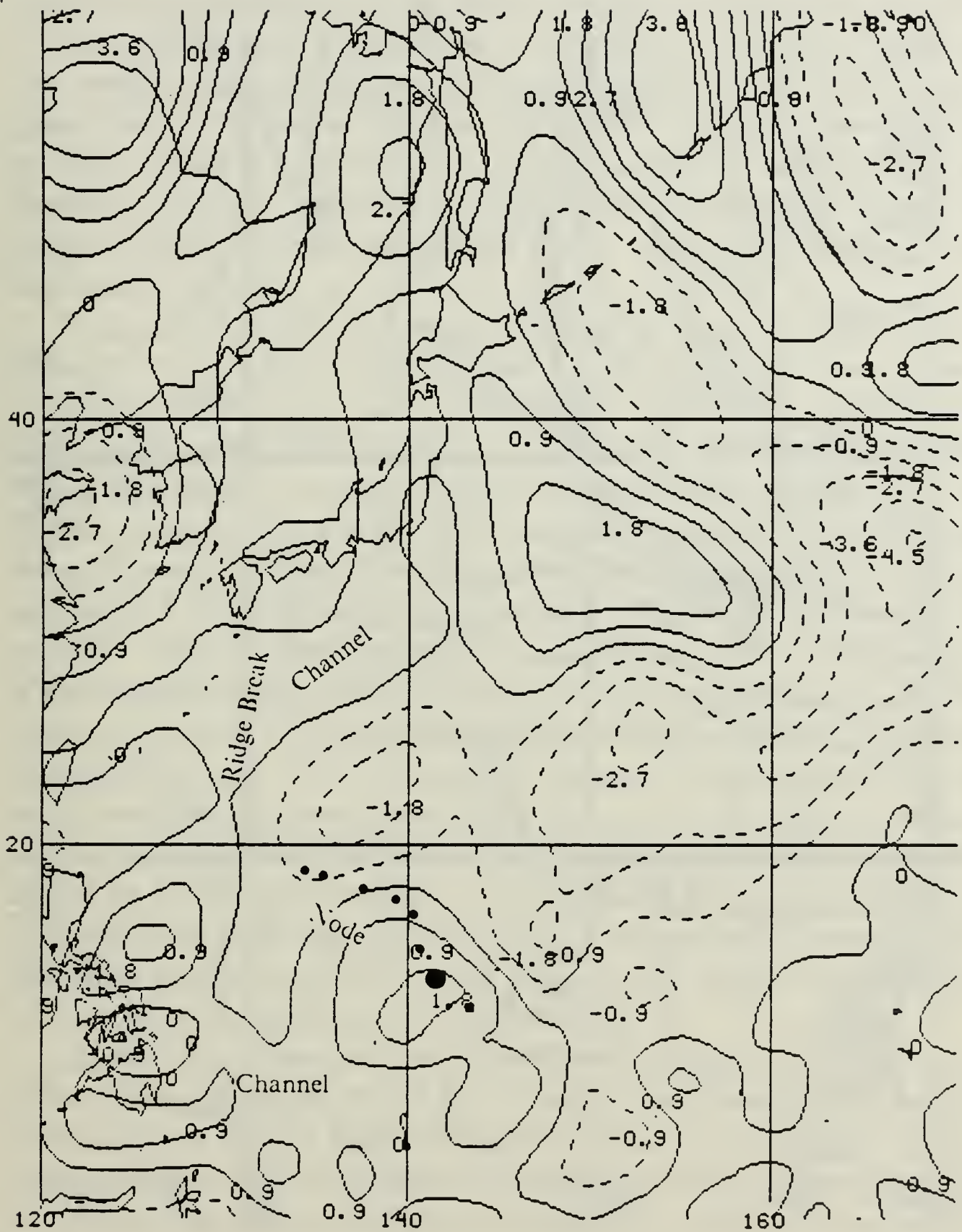


Fig. 3.7b Relative vorticity ( $\times 10^5 \text{s}^{-1}$ ) at 700 mb at 12 UTC 01 Nov 1983.

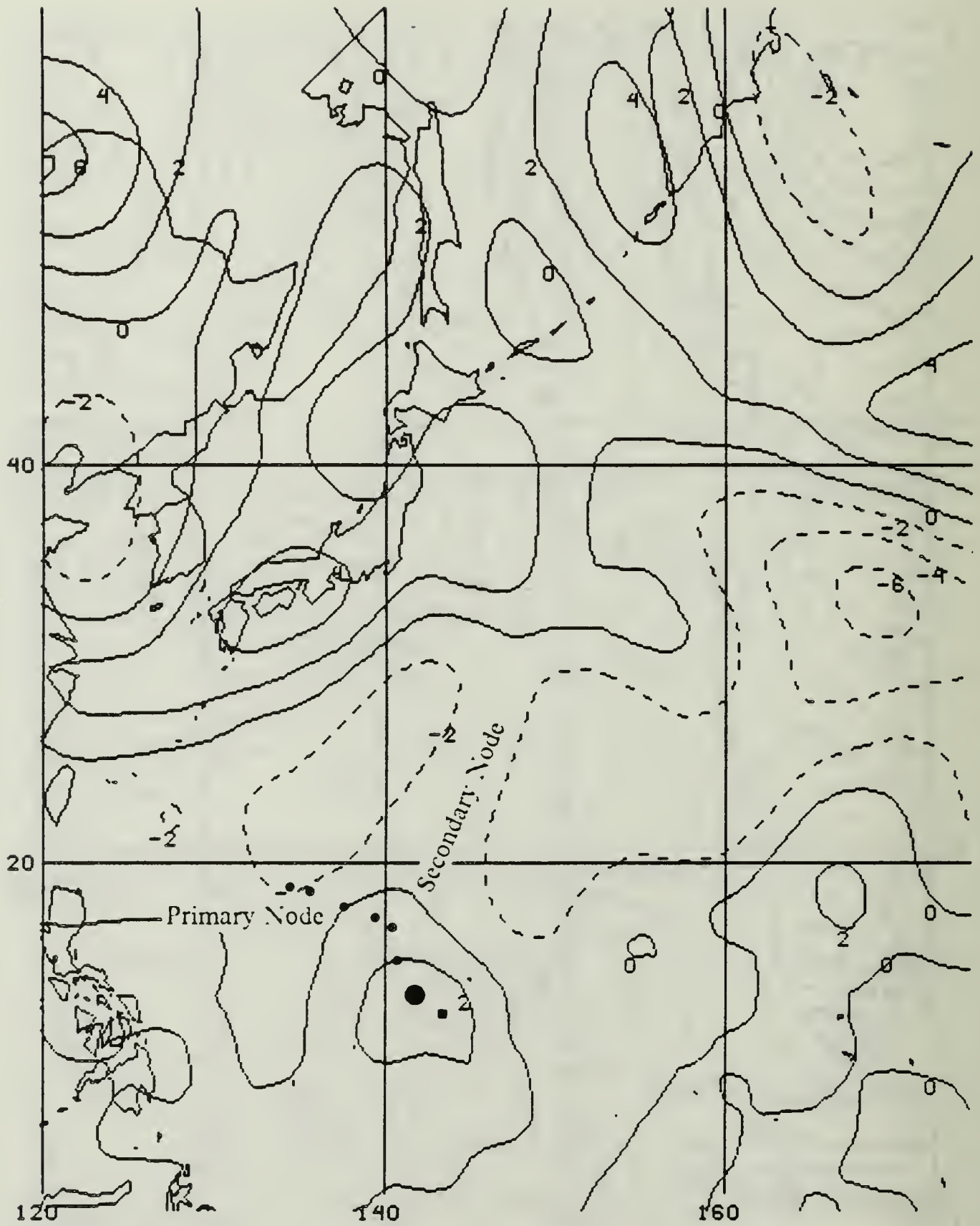


Fig. 3.7c Relative vorticity ( $\times 10^5 \text{s}^{-1}$ ) in LAV at 12 UTC 01 Nov 1983.

The next chart sequence (00 UTC 02 Nov 83) shows a return to a definite northwest track orientation in the 400 mb and LAV charts. The sharp secondary node is no longer present in the zero contour at 400 mb (Fig. 3.8a). The 700 mb chart (Fig. 3.8b) shows the further development of the channel pattern near 20°N, 130°E, which connects with the +2 vorticity center south of Honshu. Although a clear opening in the ridge is evident to the northwest in the LAV (Fig. 3.8c), the small positive center detected on the previous LAV chart has moved to the south of Honshu. Nevertheless, a weak cell in the subtropical ridge remains directly between the mid-latitude trough and the tropical cyclone.

At 12 UTC 02 Nov 83, strong indications of recurvature are seen in all three charts (Fig. 3.9). In Fig. 3.9a (400 mb), the primary node on the zero contour is clearly to the west-northwest. This primary node on the zero contour shows excellent correlation to the best track (6 points) at 36 h. However, a definite shift is seen in the primary node on the -2 contour in response to the continued strengthening of the positive vorticity center near 32°N, 142°E (good rating 5 points at 72 h). This change in the -2 contour nearly breaks the ridge at 24°N, 135°E. By contrast, the secondary node on the -2 contour shows little change at this time. Recurvature is expected late in the period, which is confirmed by the good (5 points) rating at 72 h. The cyclone center is in a channel of positive vorticity at 700 mb (Fig. 3.9b), with the channel wall (zero contour) to the north nearly describing the eventual recurvature path 66 h before the recurvature takes place. The LAV (Fig. 3.9c) indicates the impending recurvature in another way. With the eastward retreat of the -2 contour that previously separated the positive vorticity center to the north from the tropical cyclone center, the distance between the zero contours separating the centers is reduced as the positive center south of Honshu moves to the east-northeast. Although a clear pathway to the mid-latitudes appeared to develop in this case, the early portion of the track was toward the west-northwest along the primary node in the zero contour.

The changes in the individual levels (Fig. 3.10a and b) at 00 UTC 03 Nov 83 are somewhat confusing. At 400 mb (Fig. 3.10a), the ridge strengthens substantially, which leaves only a narrow break to the northeast of the storm center that is aligned with the secondary node in the zero contour. A reduction of the primary node in the zero contour is also evident. The channel at 700 mb (Fig. 3.10b) that had persisted for 36 h has closed, which leaves a weakness in the ridge similar to that at 400 mb. The LAV chart (Fig. 3.10c) reflects the alignment of weaknesses at the upper and lower

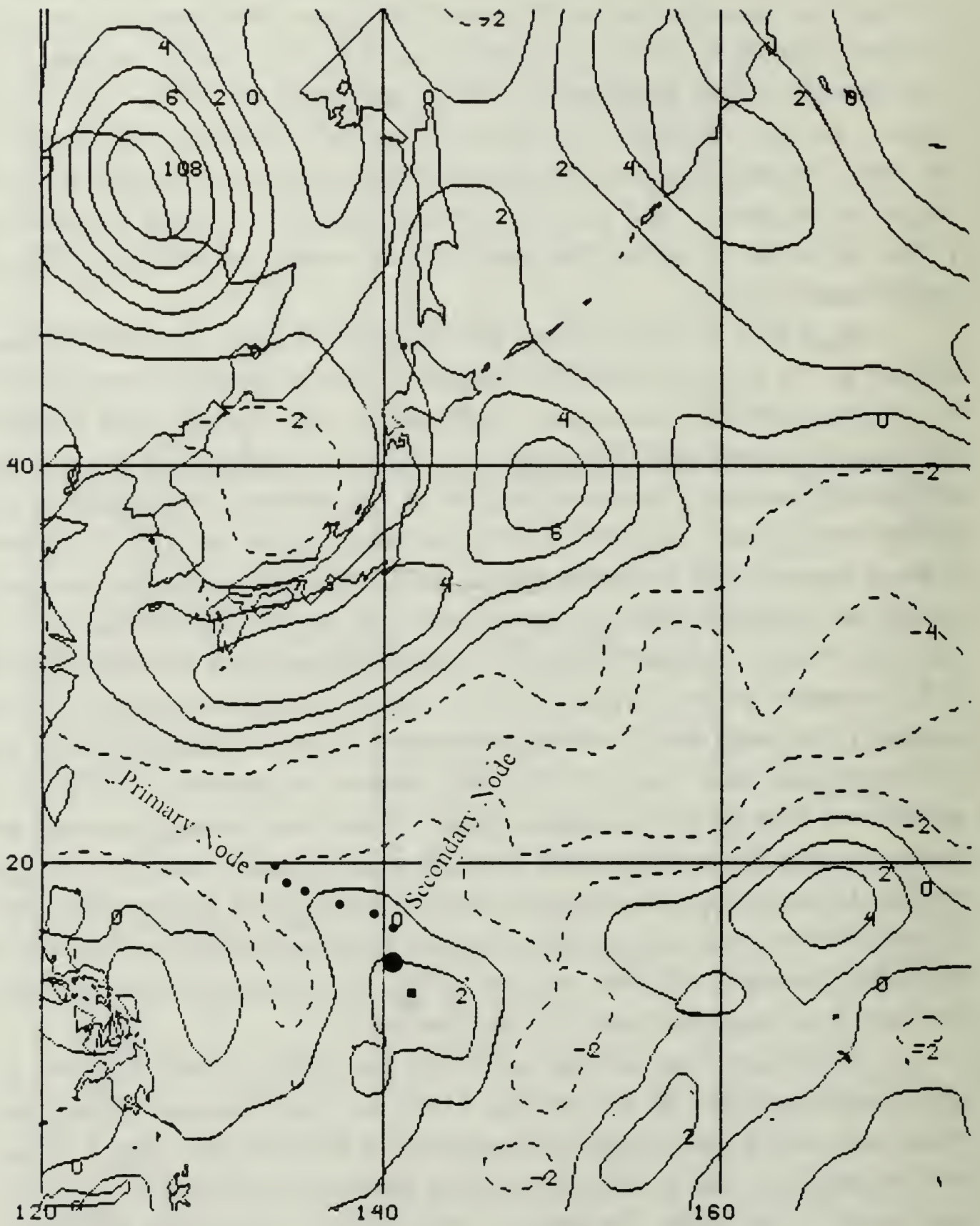


Fig. 3.8a Relative vorticity ( $\times 10^5 \text{s}^{-1}$ ) at 400 mb at 00 UTC 02 Nov 1983.

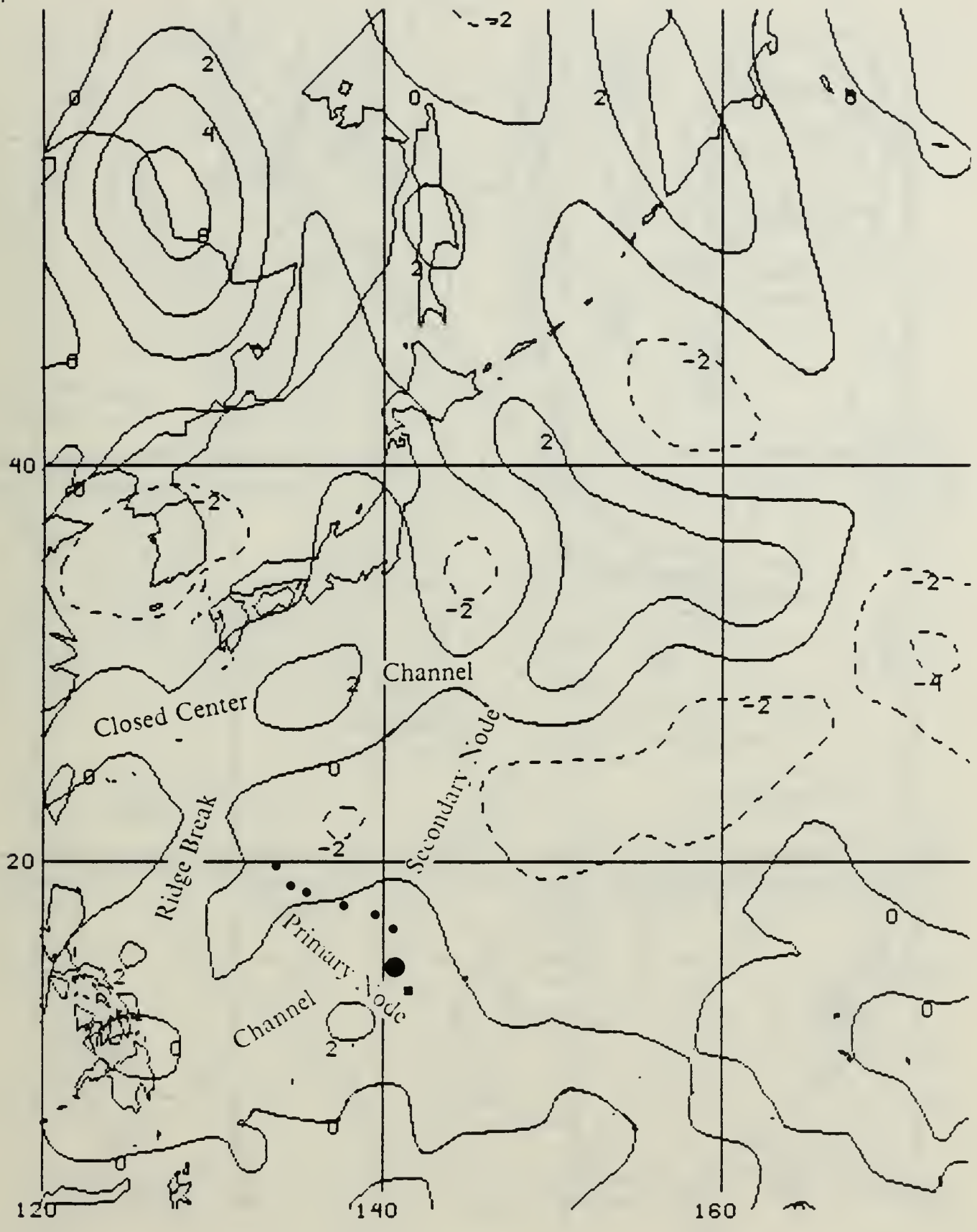


Fig. 3.8b Relative vorticity ( $\times 10^5 \text{s}^{-1}$ ) at 700 mb at 00 UTC 02 Nov 1983.

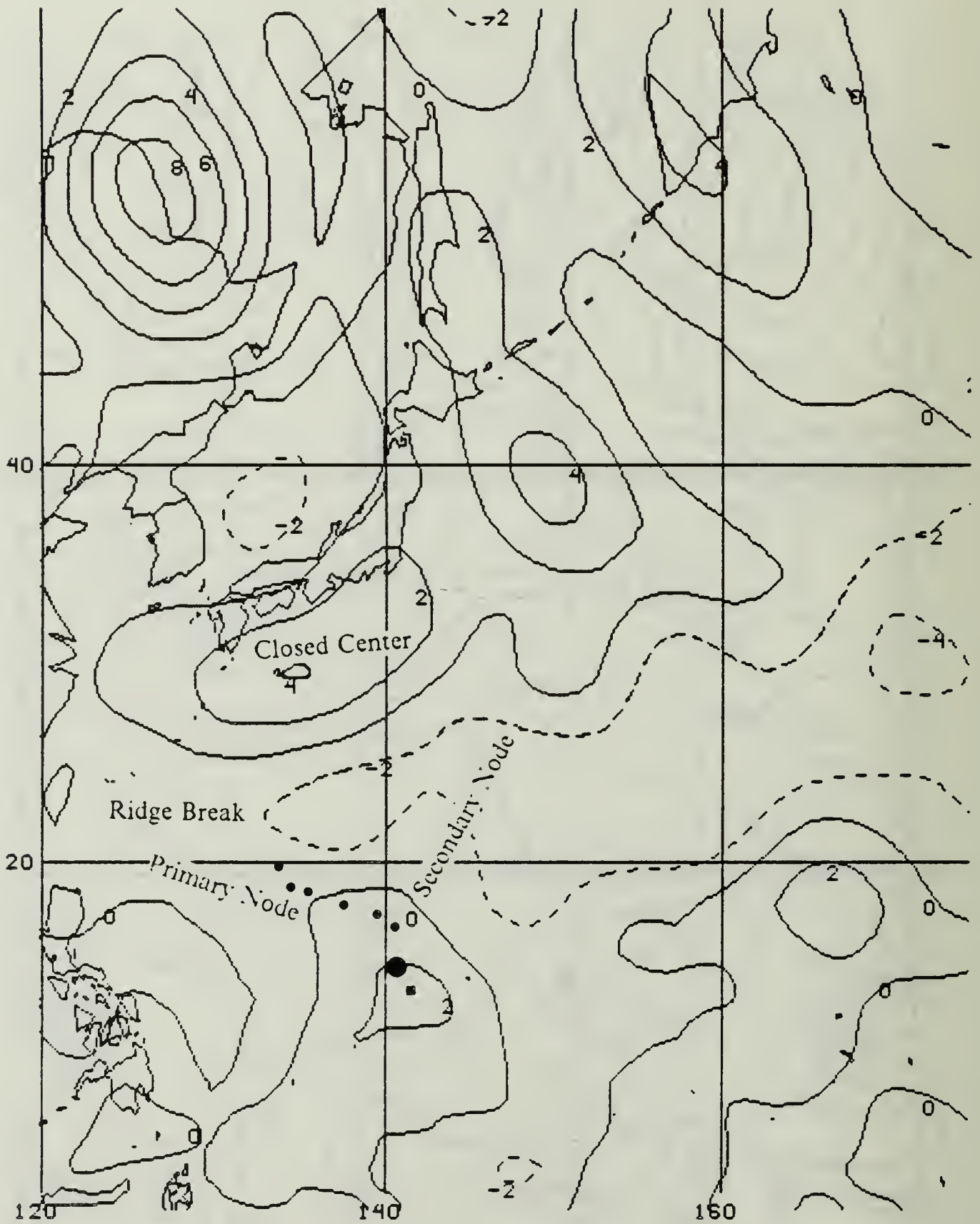


Fig. 3.8c Relative vorticity ( $\times 10^5 \text{s}^{-1}$ ) in LAV at 00 UTC 02 Nov 1983.

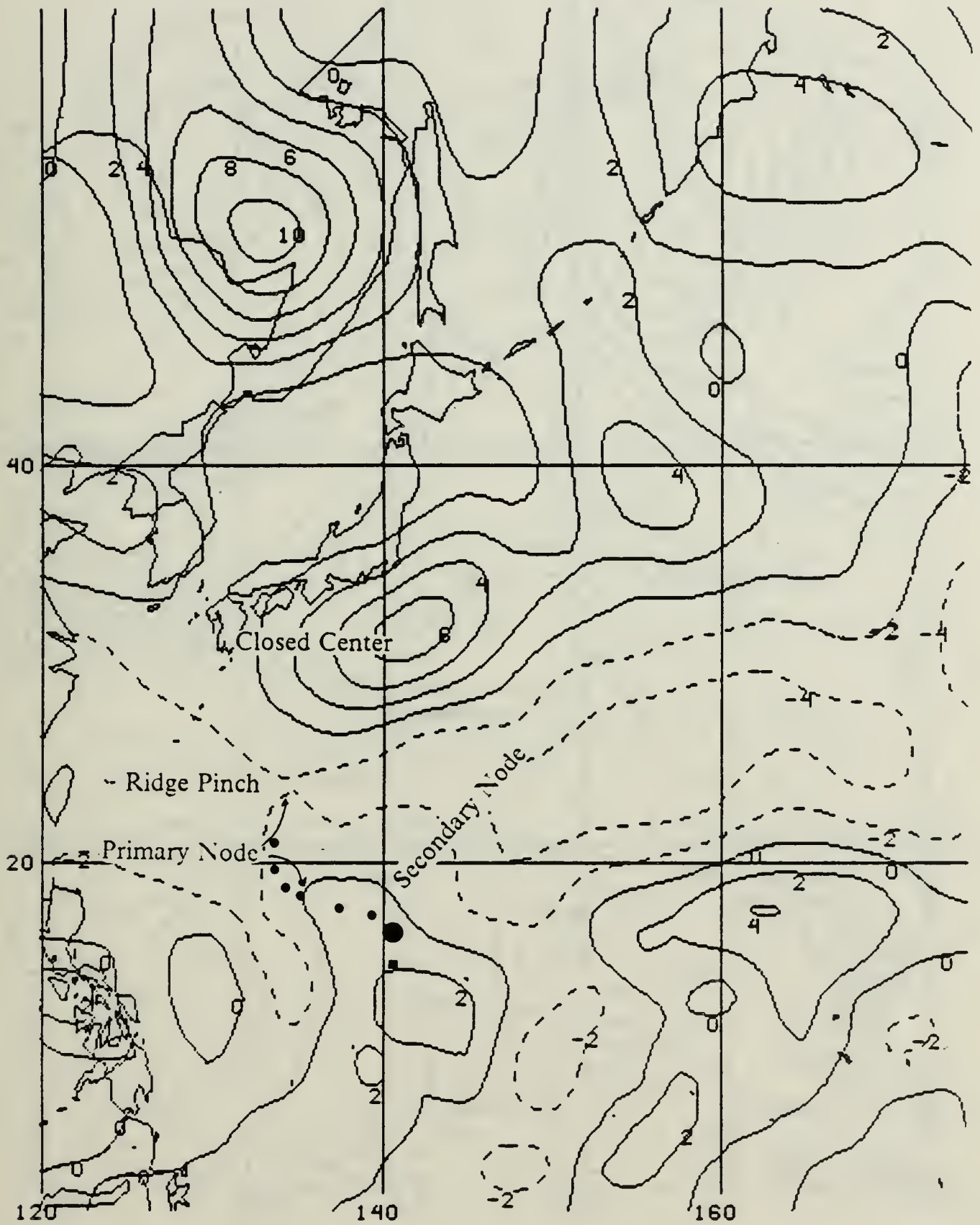


Fig. 3.9a Relative vorticity ( $\times 10^5 \text{s}^{-1}$ ) at 400 mb at 12 UTC 02 Nov 1983.

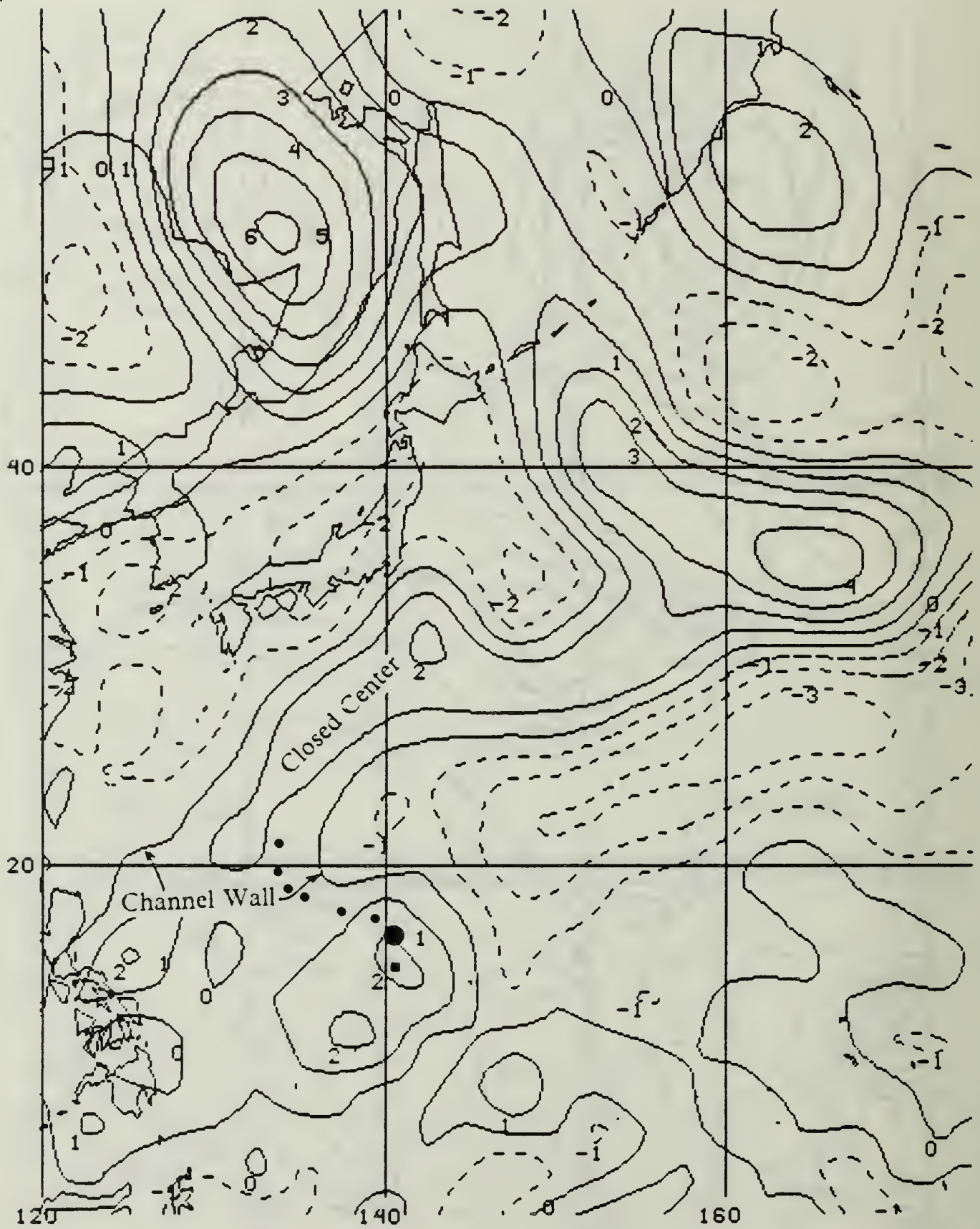


Fig. 3.9b Relative vorticity ( $\times 10^5 \text{ s}^{-1}$ ) at 700 mb at 12 UTC 02 Nov 1983.

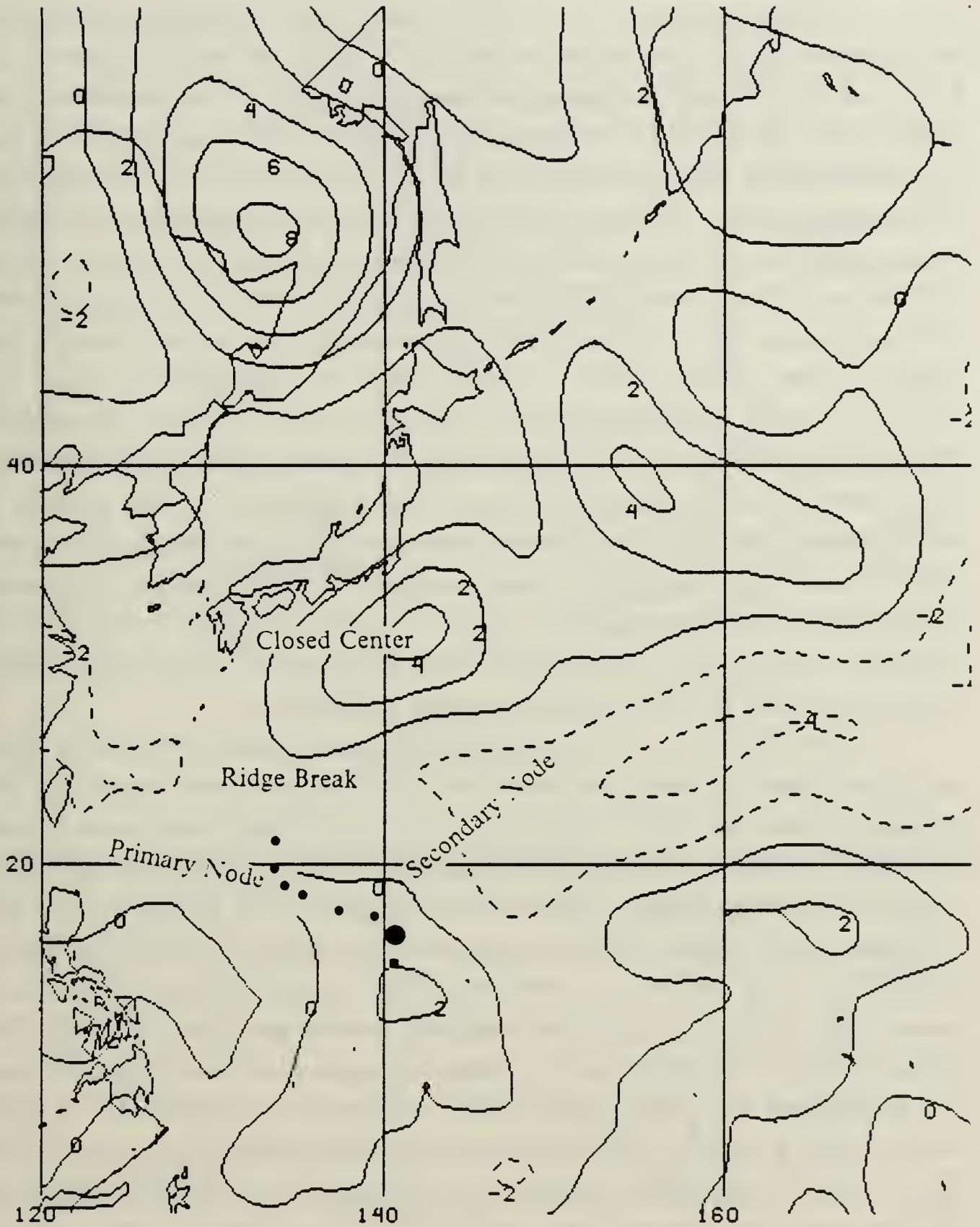


Fig. 3.9c Relative vorticity ( $\times 10^5 \text{s}^{-1}$ ) in LAV at 12 UTC 02 Nov 1983.

bounds of the layer, and also indicates a flattening of the primary node on the 0 contour, as well as an increase in the secondary node amplitude.

All three charts at 12 UTC 03 Nov 83 show strong recurvature tendencies as the indications of 24 h previous are reconfirmed. The 400 mb and LAV charts (Fig. 3.11 a and c) both show substantial increases in the node to the northeast of the cyclone center. At 400 mb, the primary node still shows excellent correlation with the best track (6 points) but the time factor has been reduced to about 30 h. Not only have the secondary nodes in the 0 and -2 contours increased in amplitude, they are aligned with each other along an axis that is nearly parallel with the post-recurvature track of STY Marge. The LAV chart (Fig. 3.11c) shows a greater flattening of the primary node in the zero contour (rated as excellent or 6 points at 36 h) and a marked increase in the amplitude of the secondary node. A line drawn from the cyclone center through the secondary node and the greatest southward extent of the zero contour to the north of the ridge also correlates well with the post-recurvature storm track. At 700 mb (Fig. 3.11b), the return of the southwest-northeast channel defined by the zero contours is clearly indicated. The axis of the channel correlates well with the patterns in the other two layers and the post-recurvature track. Consequently, the key question at this stage is not whether recurvature will occur, but when? At the present speed and direction of the storm, it would arrive at the flattened portion of the nearest zero contour in about 30 h. A turn toward the north should be expected at that time.

At 00 UTC 4 Nov 83, the designation of a new primary node must be made on all three charts. Although the present track of the cyclone is still aligned with the old primary node, the positive vorticity area around the cyclone center has a distinct shift in the orientation of the major axis toward the northeast. Thus, the old secondary node becomes the new primary node. Although the 400 mb and LAV charts (Fig. 3.12a and c) show similar patterns with large nodes to the northeast, an additional pattern is also present. The -4 contour on the 400 mb and the -2 contour on the LAV display a pinched ridge pattern (Fig. 3.2d) that aligns well with the post-recurvature path. The 700 mb chart (Fig. 3.12b) includes an extended channel pattern far to the northeast that encompasses the "wake" of the positive vorticity center that started as a small center south of Korea (Fig. 3.6c) and tracked to the east-northeast to the north of STY Marge. The low center passed to the north of STY Marge at 12 UTC 02 Nov 83 (Fig. 3.9c) and passed from the chart area after 12 UTC 03 Nov 83. That is, a frontal trough remains at 700 mb along the expected recurvature path. This feature splits the

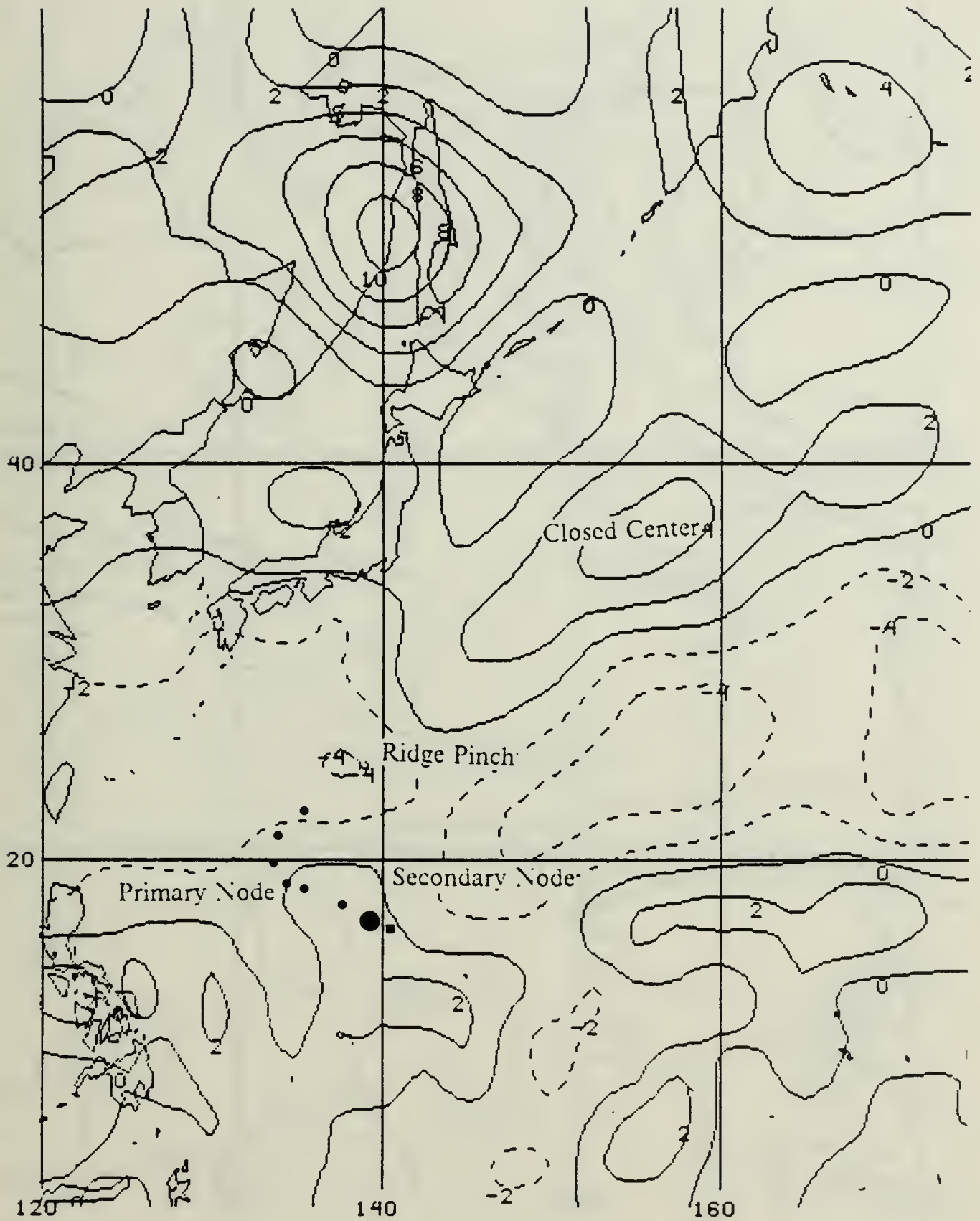


Fig. 3.10a Relative vorticity ( $\times 10^5 \text{s}^{-1}$ ) at 400 mb at 00 UTC 03 Nov 1983.

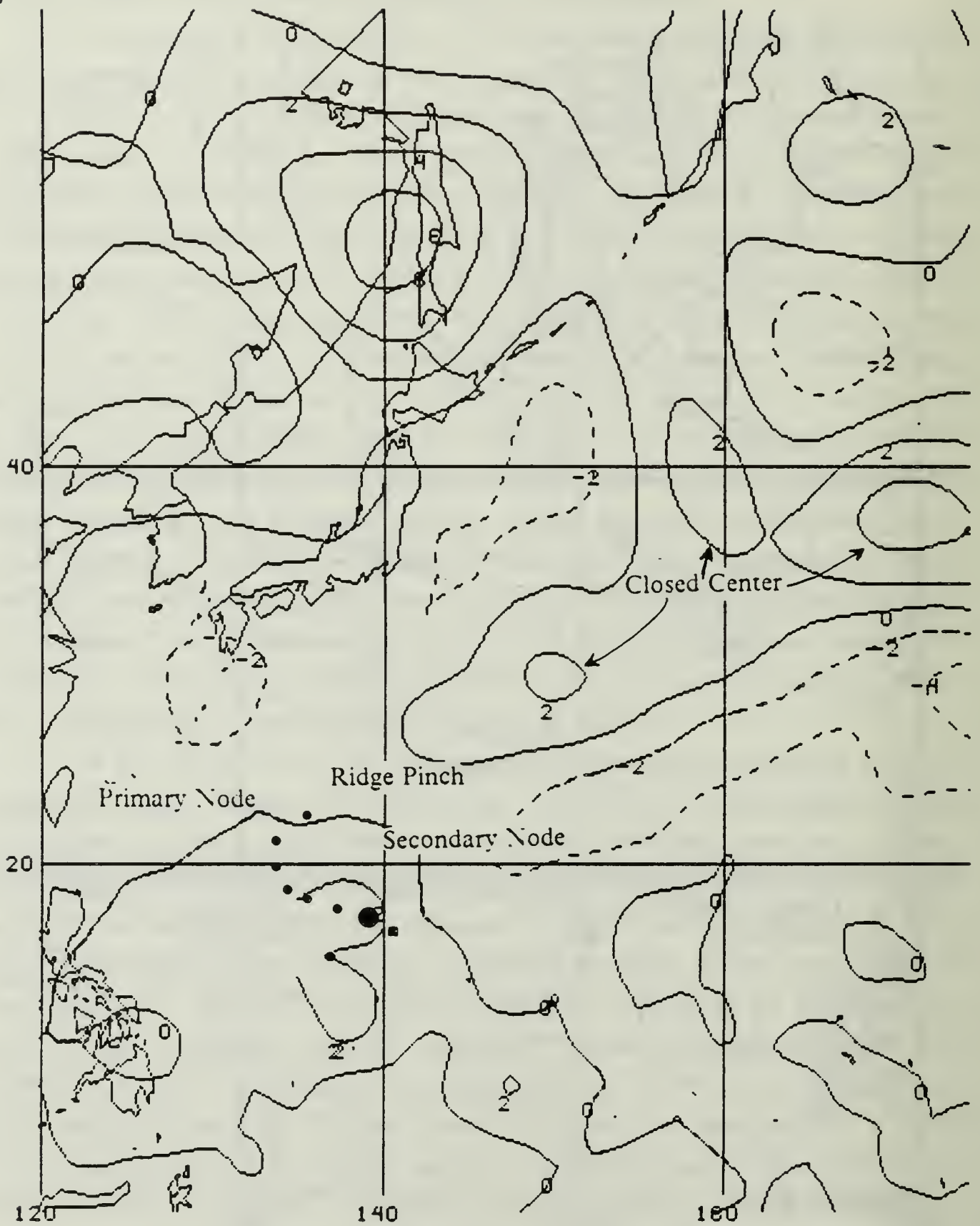


Fig. 3.10b Relative vorticity ( $\times 10^5 \text{s}^{-1}$ ) at 700 mb at 00 UTC 03 Nov 1983.

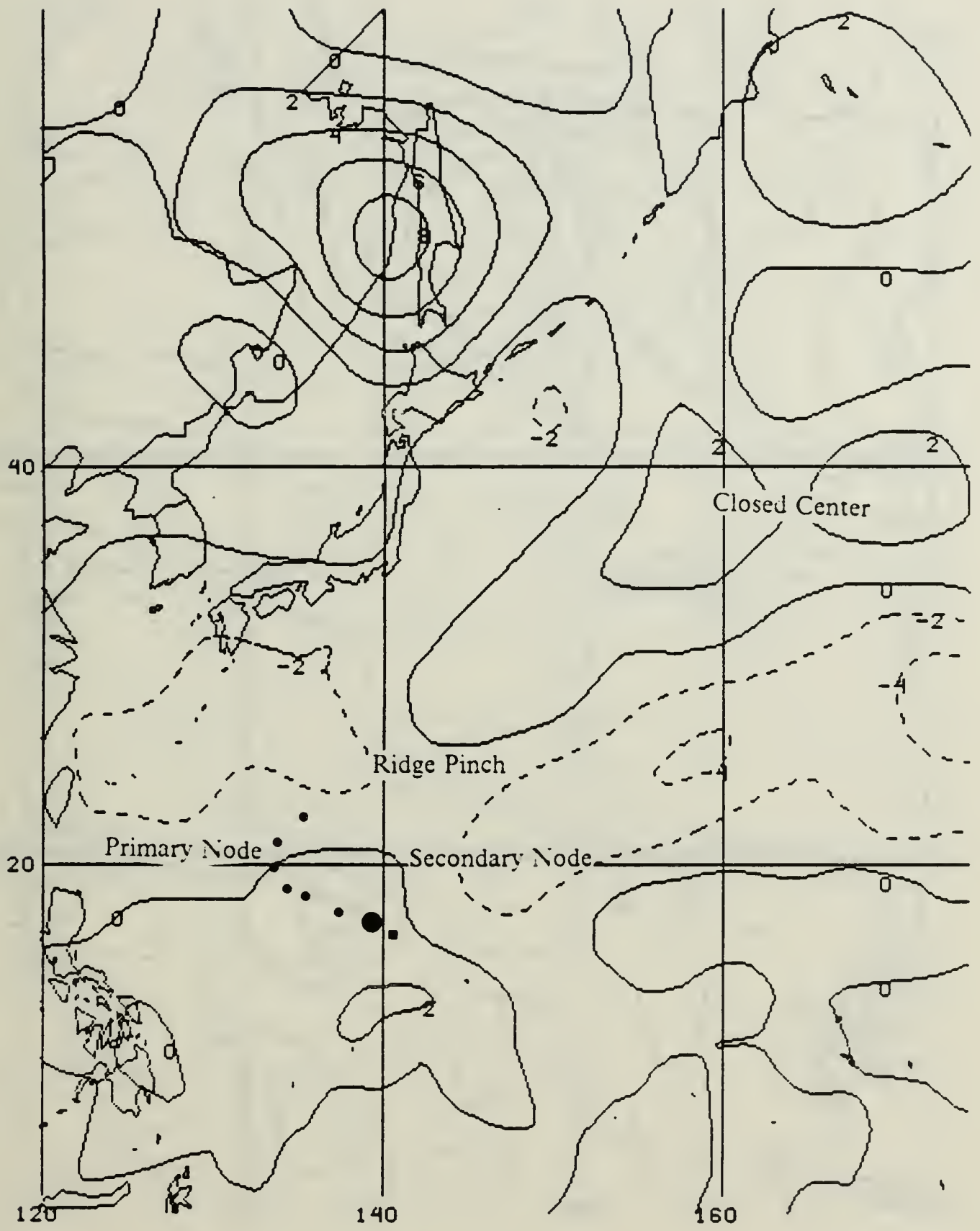


Fig. 3.10c Relative vorticity ( $\times 10^5 \text{s}^{-1}$ ) in LAV at 00 UTC 03 Nov 1983.

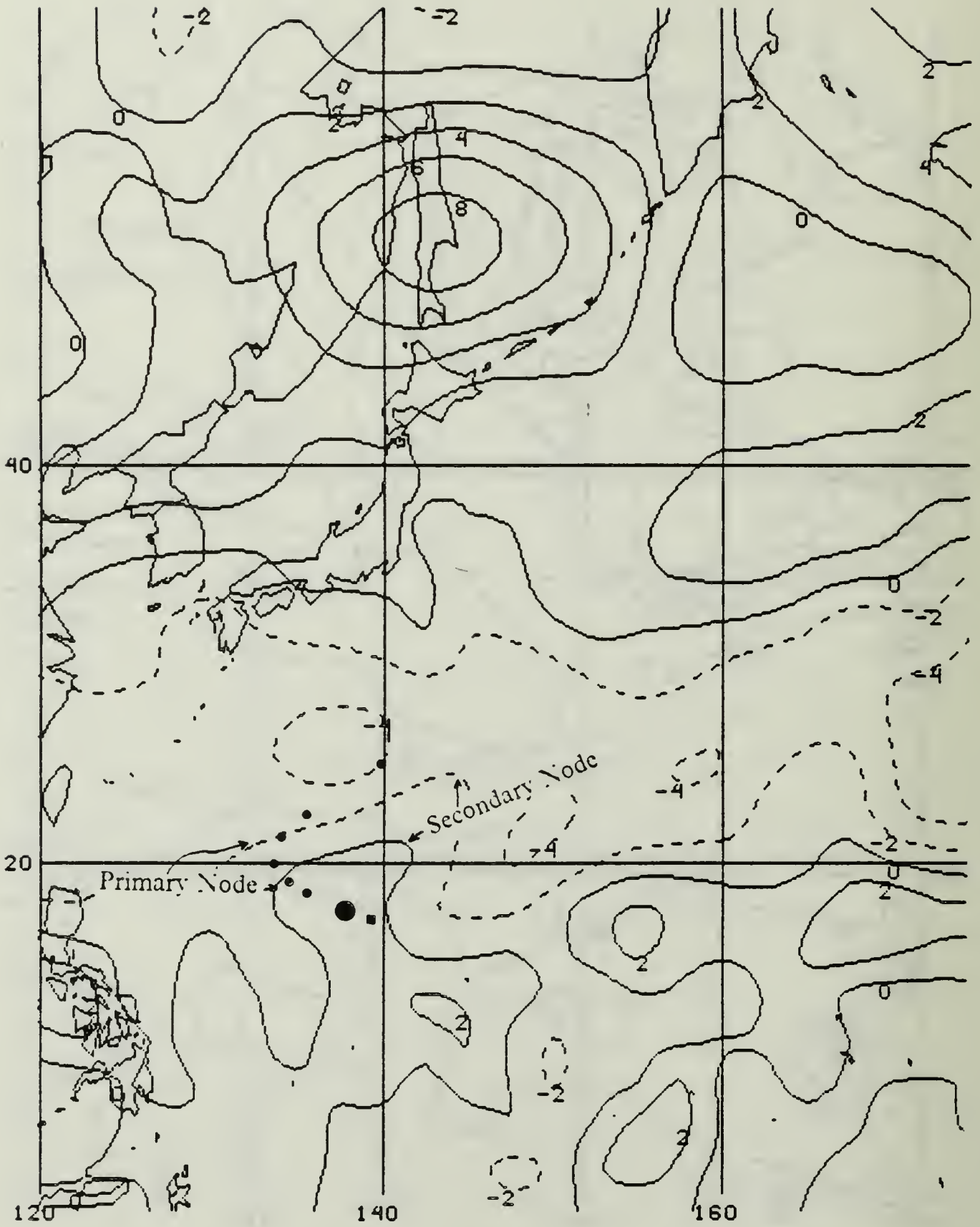


Fig. 3.11a Relative vorticity ( $\times 10^5 \text{s}^{-1}$ ) at 400 mb at 12 UTC 03 Nov 1983.

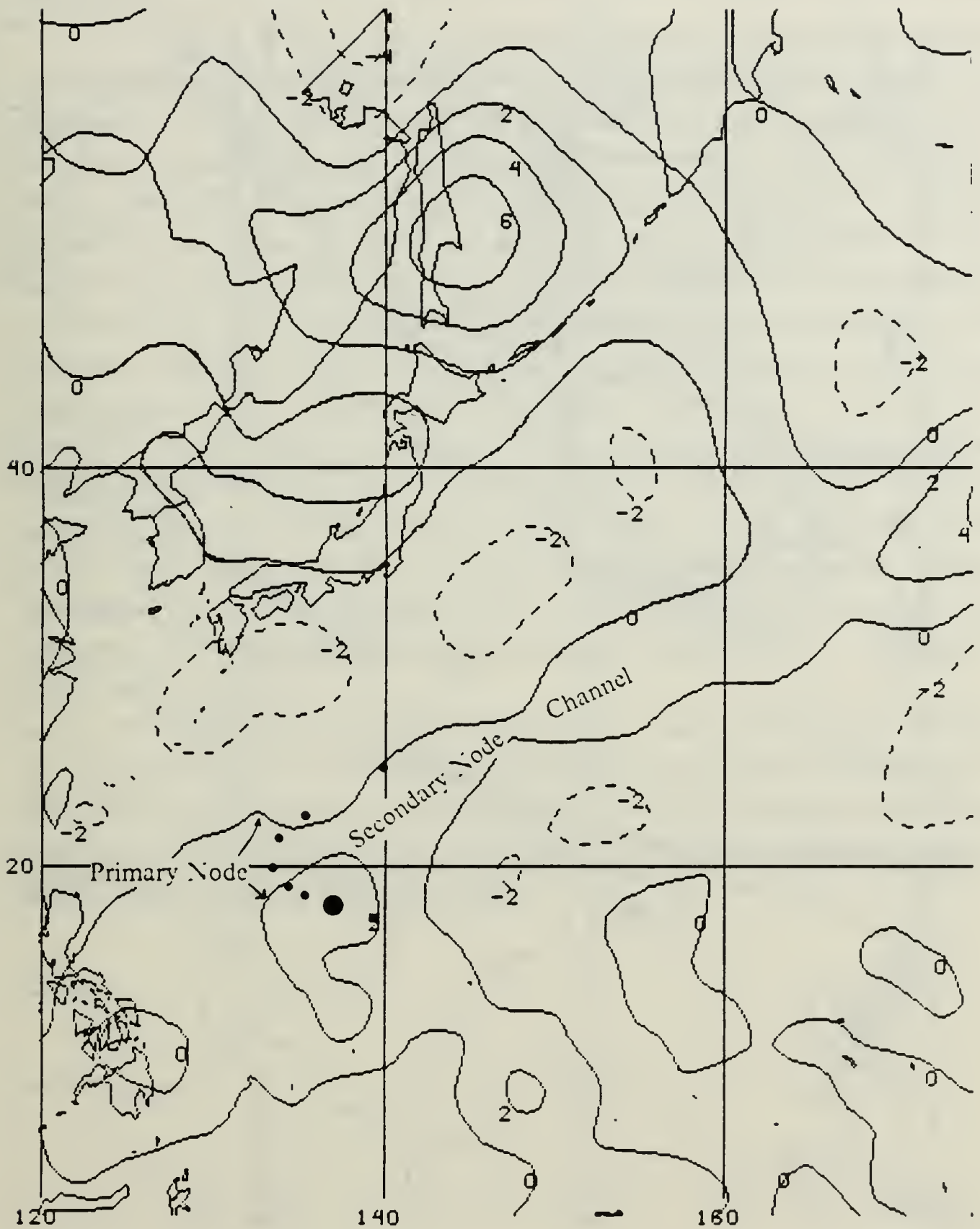


Fig. 3.11b Relative vorticity ( $\times 10^5 \text{ s}^{-1}$ ) at 700 mb at 12 UTC 03 Nov 1983.

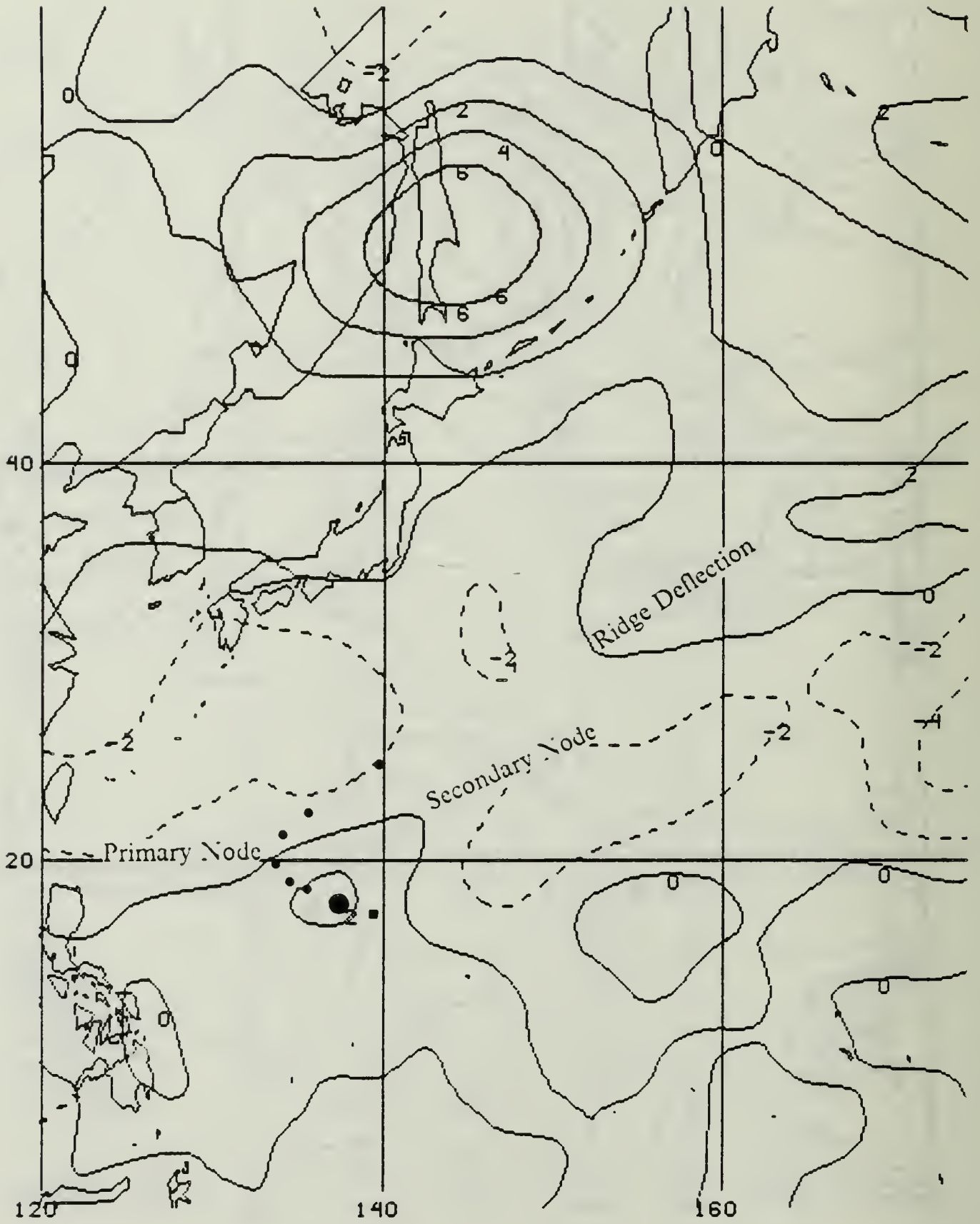


Fig. 3.11c Relative vorticity ( $\times 10^5 \text{s}^{-1}$ ) in LAV at 12 UTC 03 Nov 1983.

subtropical ridge around 25°N and the mid-latitude ridge that extends southward from 40°N, 160°E.

By 12 UTC 04 Nov 83, an extensive node of positive vorticity has penetrated into the subtropical ridge during the past 24-36 h. In Fig. 3.13a (400 mb), the node axis continues to be nearly parallel to the best track after recurvature with a slight right bias. Thus, the recurvature track appears to punch directly through a rather substantial ridge at 400 mb. However, Marge is clearly approaching the ridge axis at 700 mb (Fig. 3.13b). The zero contour around Marge at 700 mb and the one associated with the mid-latitude positive vorticity band are much closer than those at 400 mb or previously at 700 mb (Fig. 3.12b). This indicates that the subtropical ridge is narrowing at the lower levels more than at 400 mb at this time. Both lower and upper-level charts need to be examined in these baroclinic (vertically-sheared) conditions. The LAV chart (Fig. 3.13c) has a combination of a broad node to the northwest and a narrowing of the subtropical ridge. The LAV node axis is not as clearly correlated with the post-recurvature track as is the 400 mb depiction. This poor correlation may be due to the layer averaging routine that does not use a mass weighted scheme, but rather a simple averaging of the two input level values. That is, the 700 mb level should have much more weight in the LAV fields because it represents a deeper layer of the atmosphere that is steering the storm.

Over the next 12 h, the trends continue in all three charts (Fig. 3.14 a, b and c). A continued reduction of the distance separating the zero contours of the ridge is seen. The next 12 h period is not available as the 12 UTC 05 Nov 83 fields are missing from the archived GBA data. Thus, the transition at the time of recurvature between 00 and 12 UTC cannot be observed for Marge.

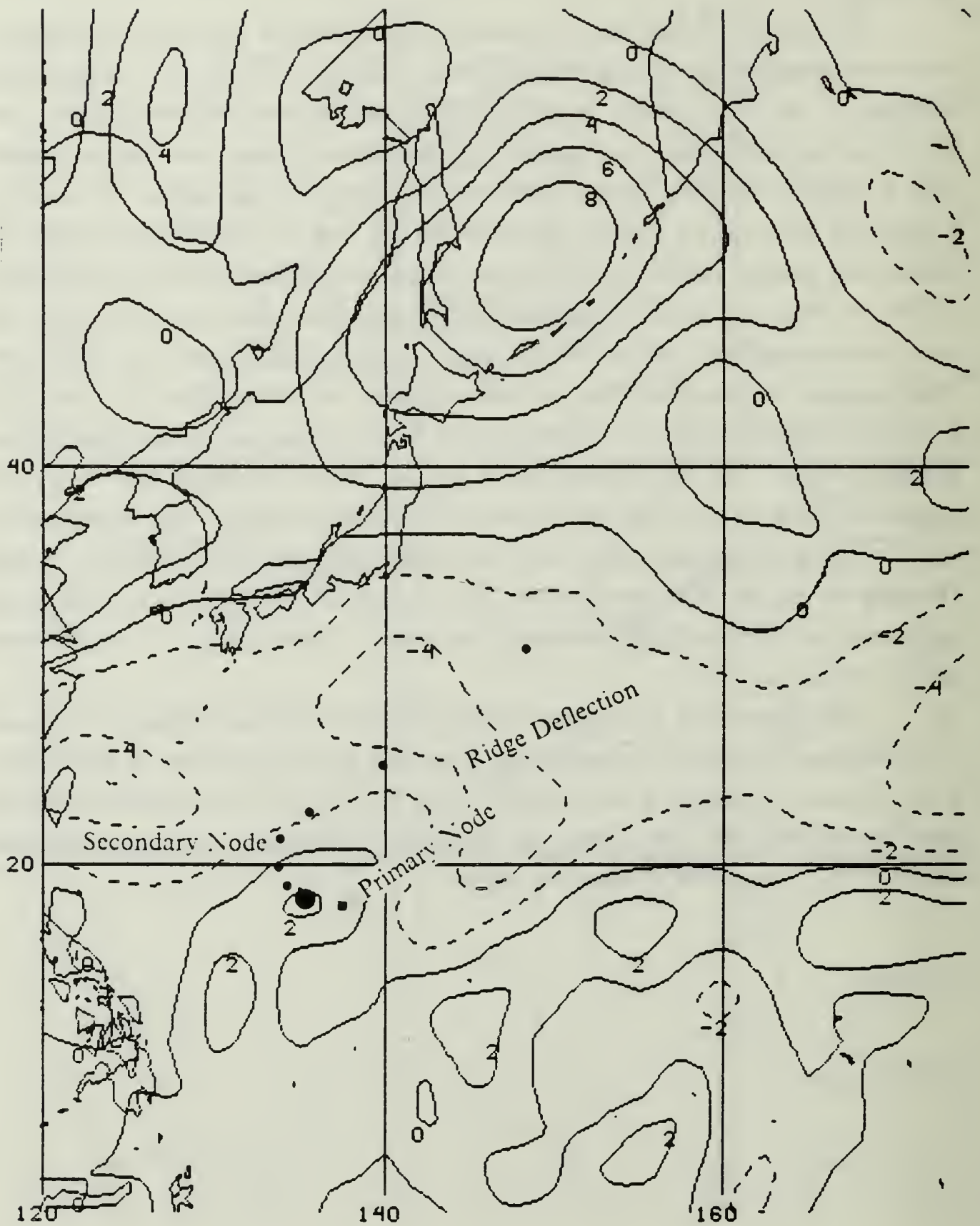


Fig. 3.12a Relative vorticity ( $\times 10^5 \text{s}^{-1}$ ) at 400 mb at 00 UTC 04 Nov 1983.

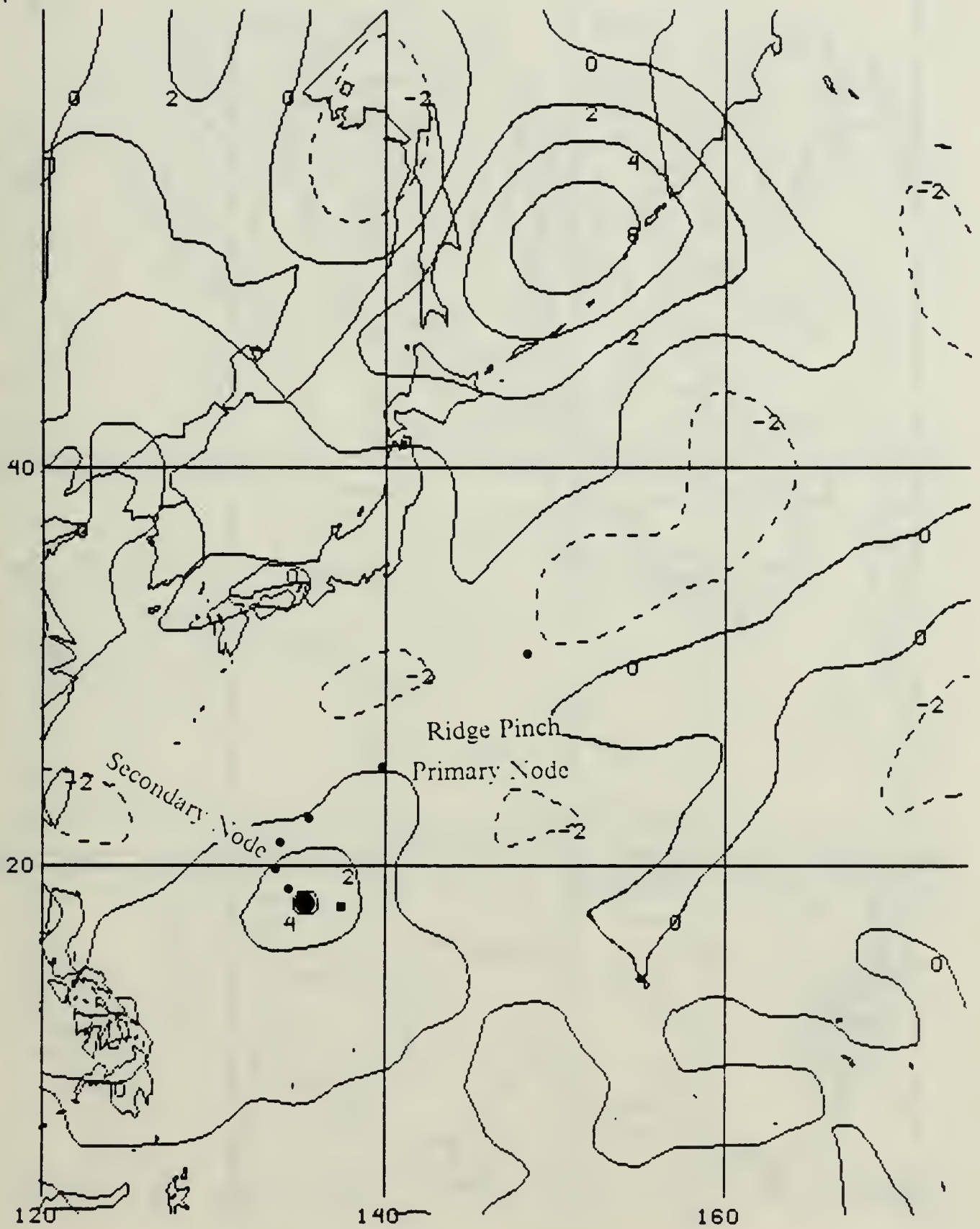


Fig. 3.12b Relative vorticity ( $\times 10^5 \text{s}^{-1}$ ) at 700 mb at 00 UTC 04 Nov 1983.

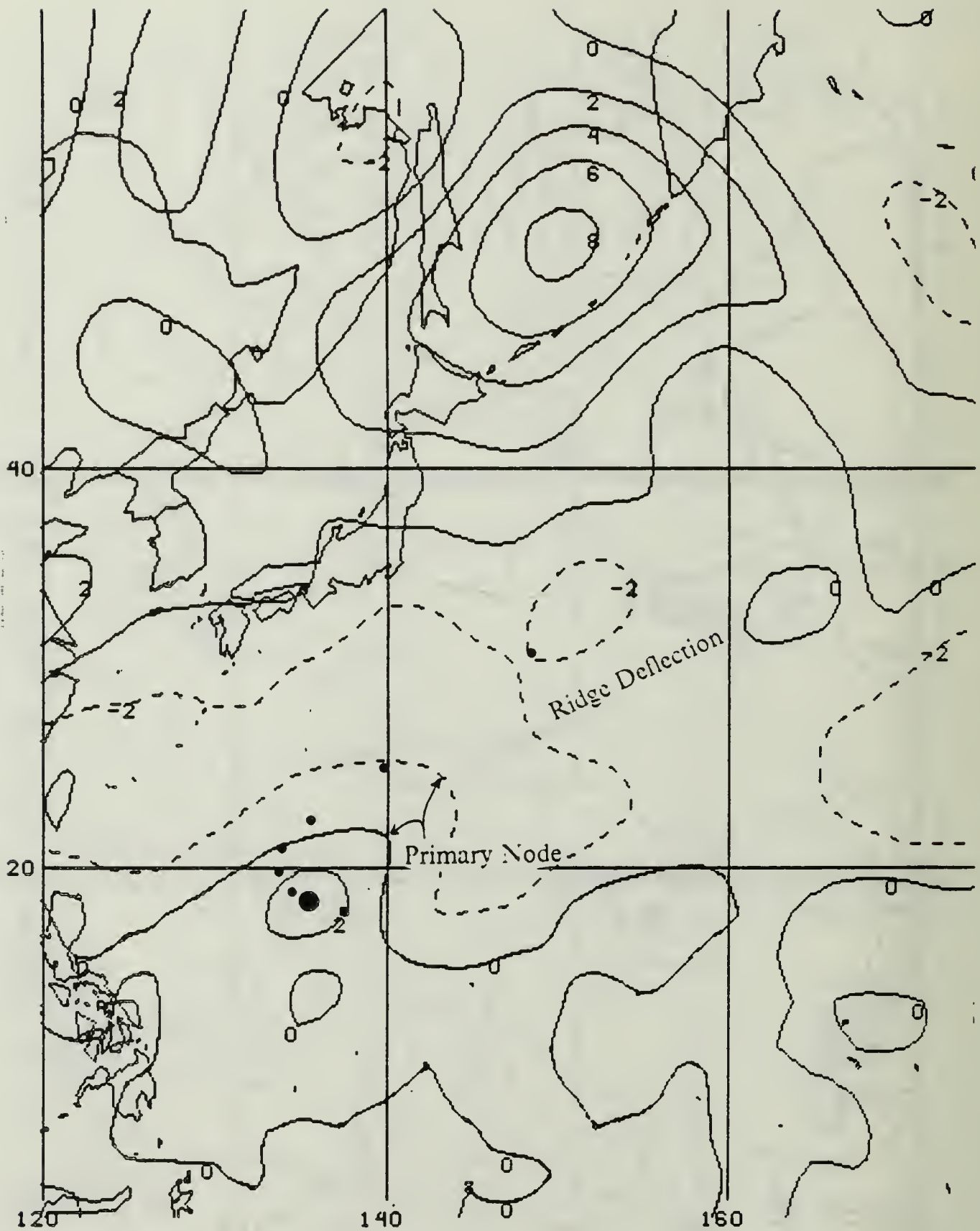


Fig. 3.12c Relative vorticity ( $\times 10^5 \text{s}^{-1}$ ) in LAV at 00 UTC 04 Nov 1983.



Fig. 3.13a Relative vorticity ( $\times 10^5 \text{ s}^{-1}$ ) at 400 mb at 12 UTC 04 Nov 1983.

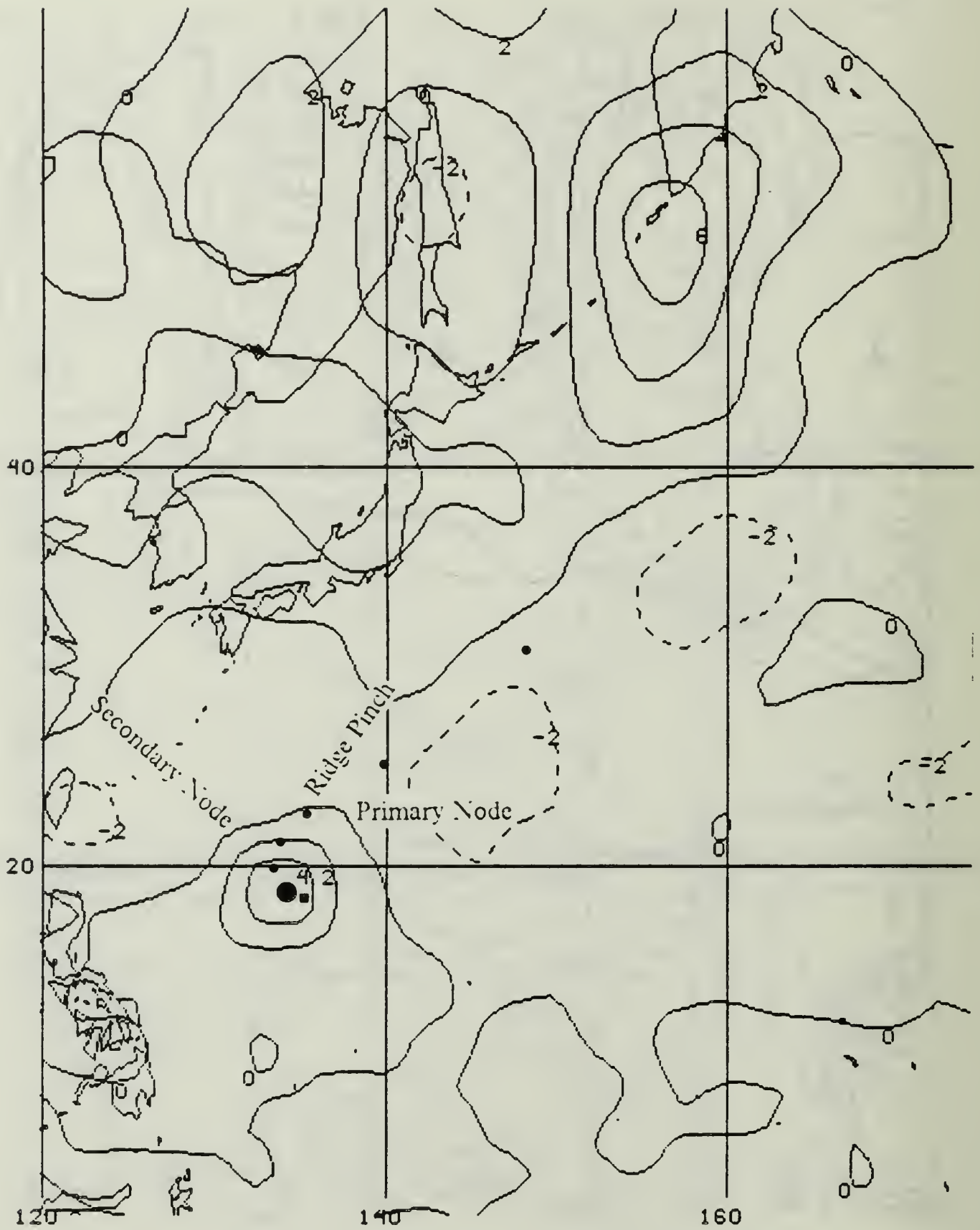


Fig. 3.13b Relative vorticity ( $\times 10^5 \text{s}^{-1}$ ) at 700 mb at 12 UTC 04 Nov 1983.

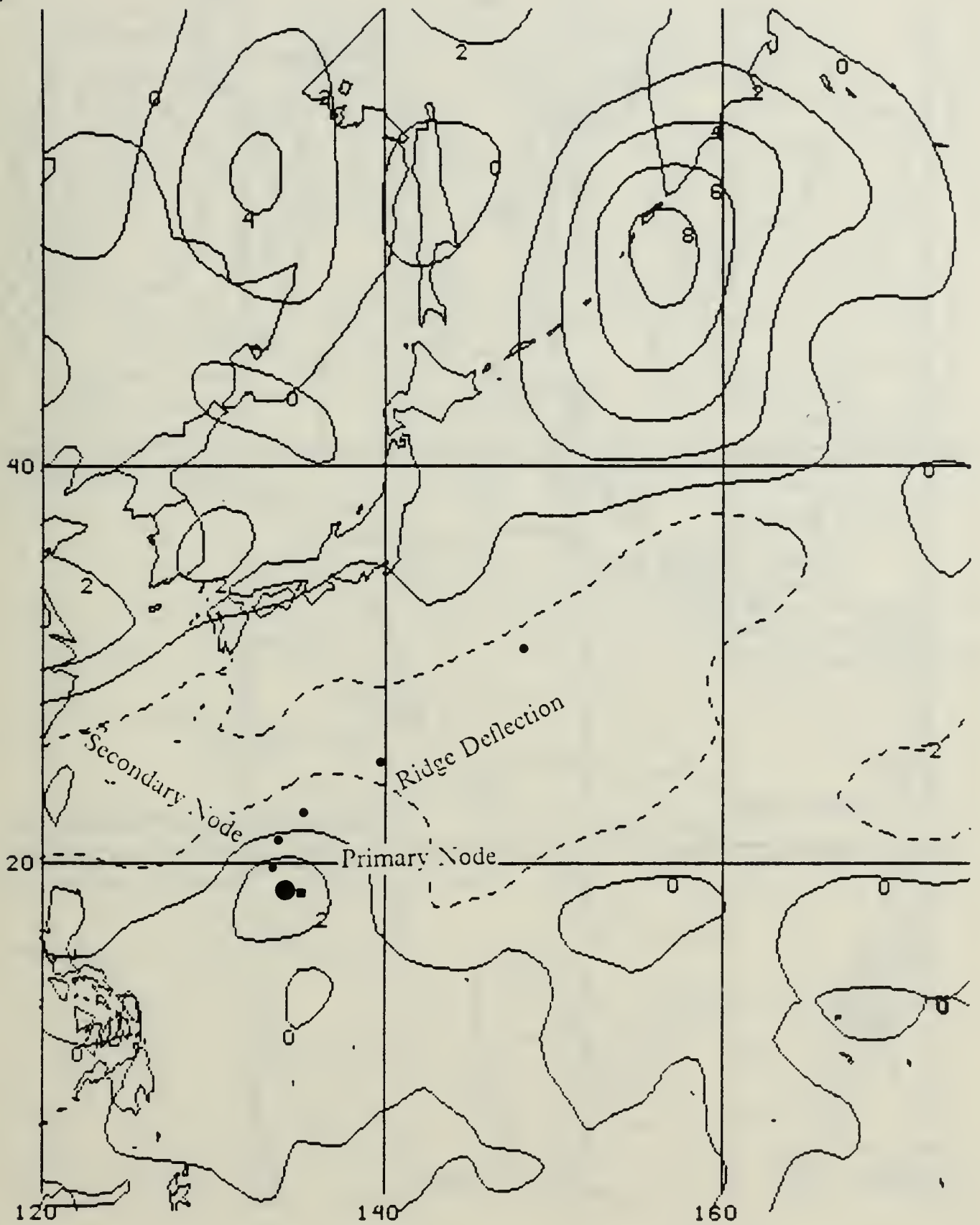


Fig. 3.13c Relative vorticity ( $\times 10^5 \text{s}^{-1}$ ) in LAV at 12 UTC 04 Nov 1983.

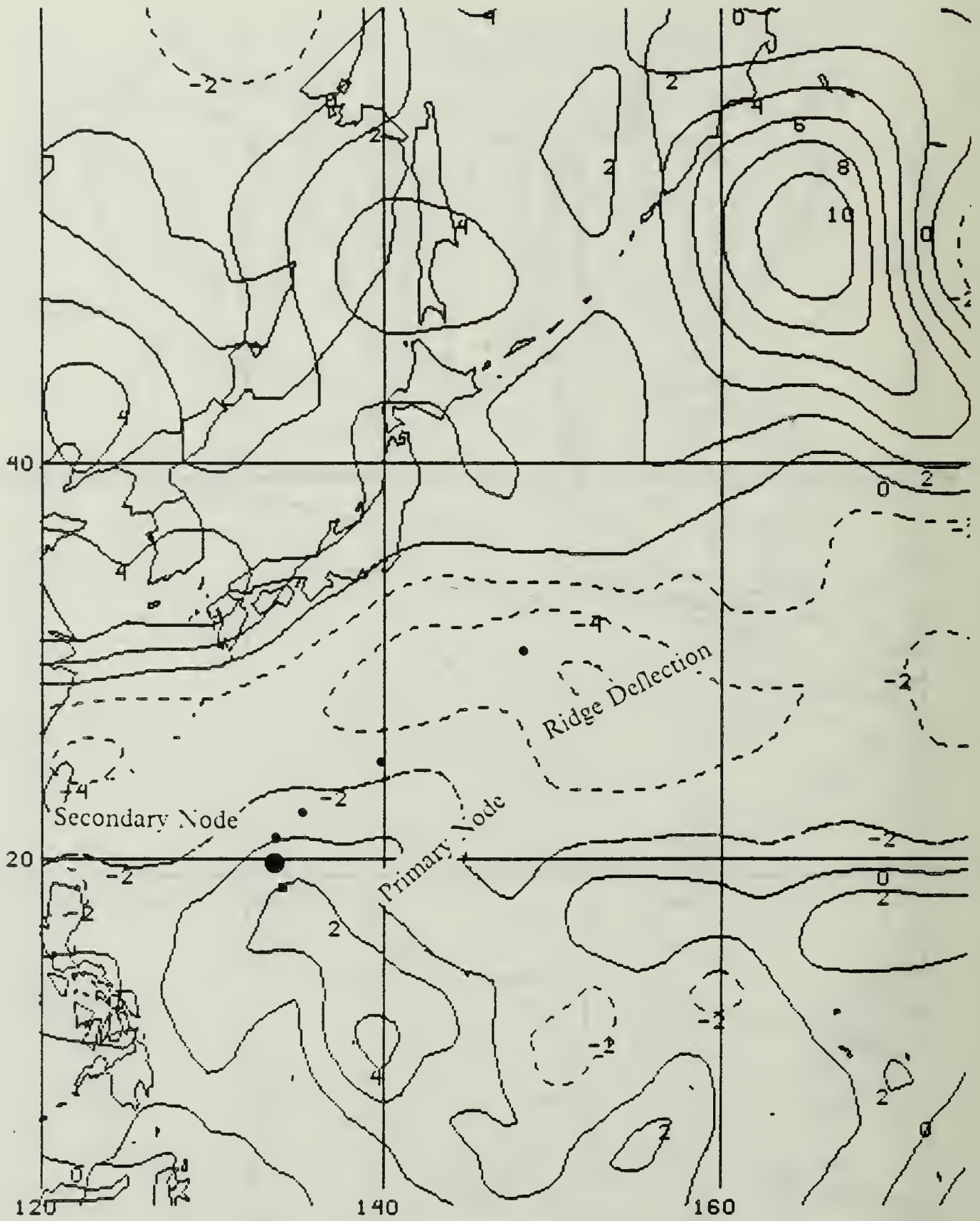


Fig. 3.14a Relative vorticity ( $\times 10^5 \text{ s}^{-1}$ ) at 400 mb at 00 UTC 05 Nov 1983.



Fig. 3.14b Relative vorticity ( $\times 10^5 \text{ s}^{-1}$ ) at 700 mb at 00 UTC 05 Nov 1983.

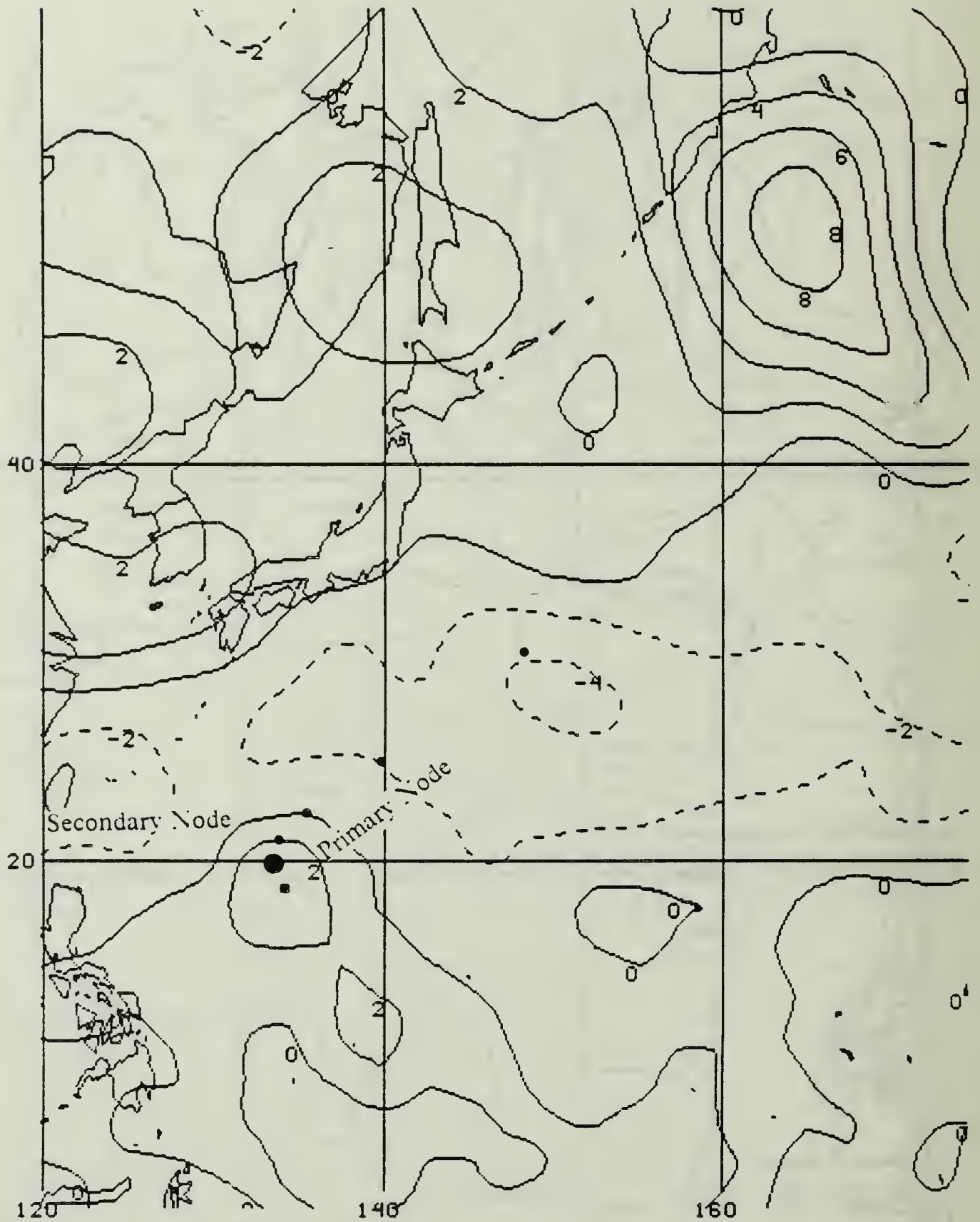


Fig. 3.14c Relative vorticity ( $\times 10^5 \text{ s}^{-1}$ ) in LAV at 00 UTC 05 Nov 1983.

A major development of a positive vorticity center at 400 mb (Fig. 3.15a) occurs over southern Japan at 00 UTC 06 Nov 83. Consequently, only a very narrow ridge separates the tropical cyclone and the mid-latitude circulation. At 700 mb (Fig. 3.15b), a +2 contour surrounds both the tropical and mid-latitude systems with a large node in the zero contour on the east side of a north-south channel. The +2 closed center in the node has excellent correlation with the cyclone's final best track position. The LAV (Fig. 3.15c) includes two distinct centers in a positive vorticity channel with about 300 n mi separation of the +2 contours around the centers. A reflection of the 700 mb node is present in the -2 contour to the east. Again, a more representative vertical weighting in the LAV would probably display the recurvature conditions more accurately.

Over the next 24 h, the track of STY Marge appears to be determined by that of the mid-latitude system tracking to the east-northeast. At 400 mb (Fig. 3.16a and 3.17a), the tropical center seems to be moving slightly faster than the mid-latitude system. In the 700 mb charts (Fig. 3.16b and 3.17b), only one vorticity center is depicted. Notice the extreme vorticity gradient between the tropical cyclone and the ridge to the east. The best track tropical cyclone position is to the southeast of the large center. The LAV charts show a blend of the two levels as expected (Fig. 3.16c and 3.17c).

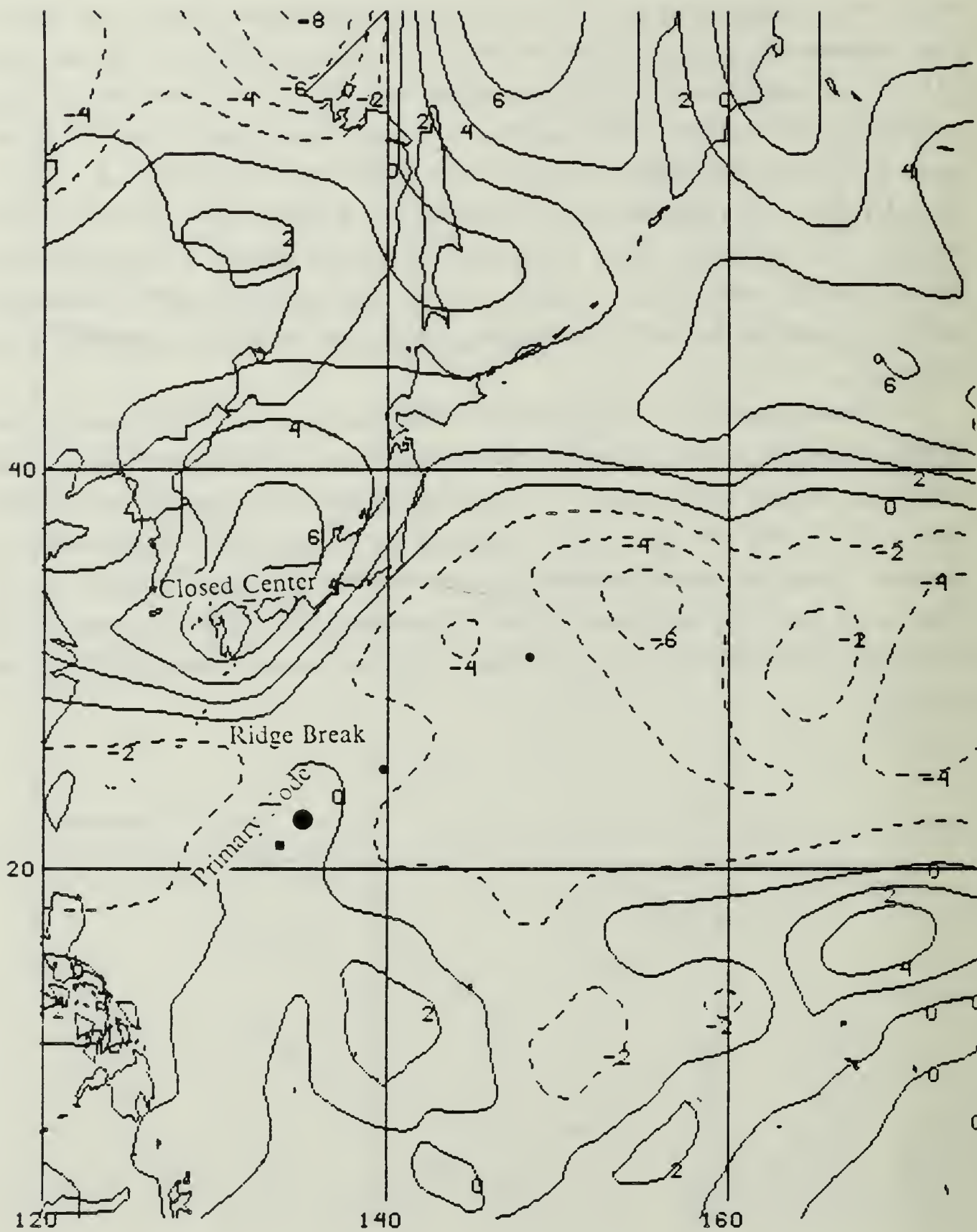


Fig. 3.15a Relative vorticity ( $\times 10^5 \text{s}^{-1}$ ) at 400 mb at 00 UTC 06 Nov 1983.

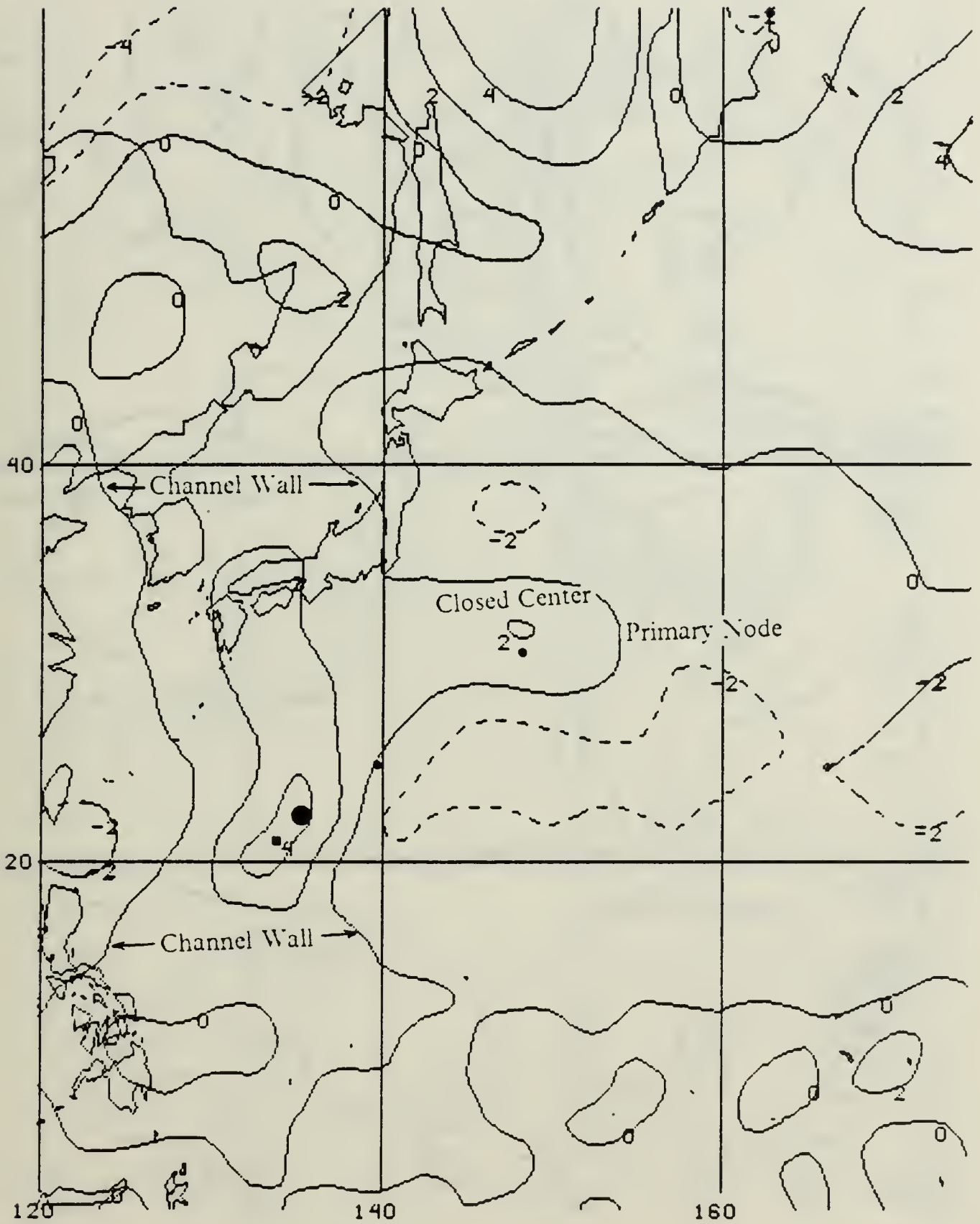


Fig. 3.15b Relative vorticity ( $\times 10^5 s^{-1}$ ) at 700 mb at 00 UTC 06 Nov 1983.

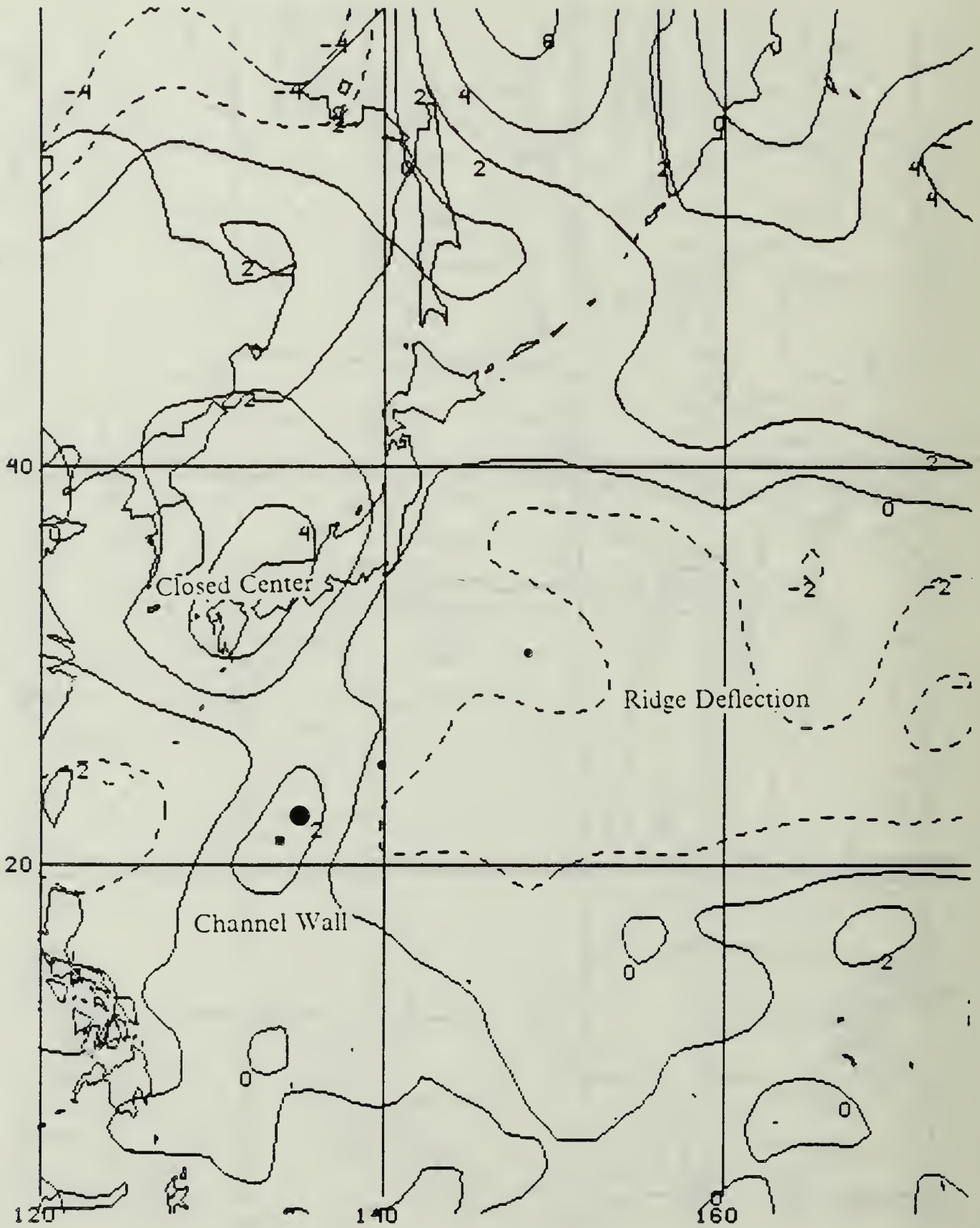


Fig. 3.15c Relative vorticity ( $\times 10^5 \text{s}^{-1}$ ) in LAV at 00 UTC 06 Nov 1983.

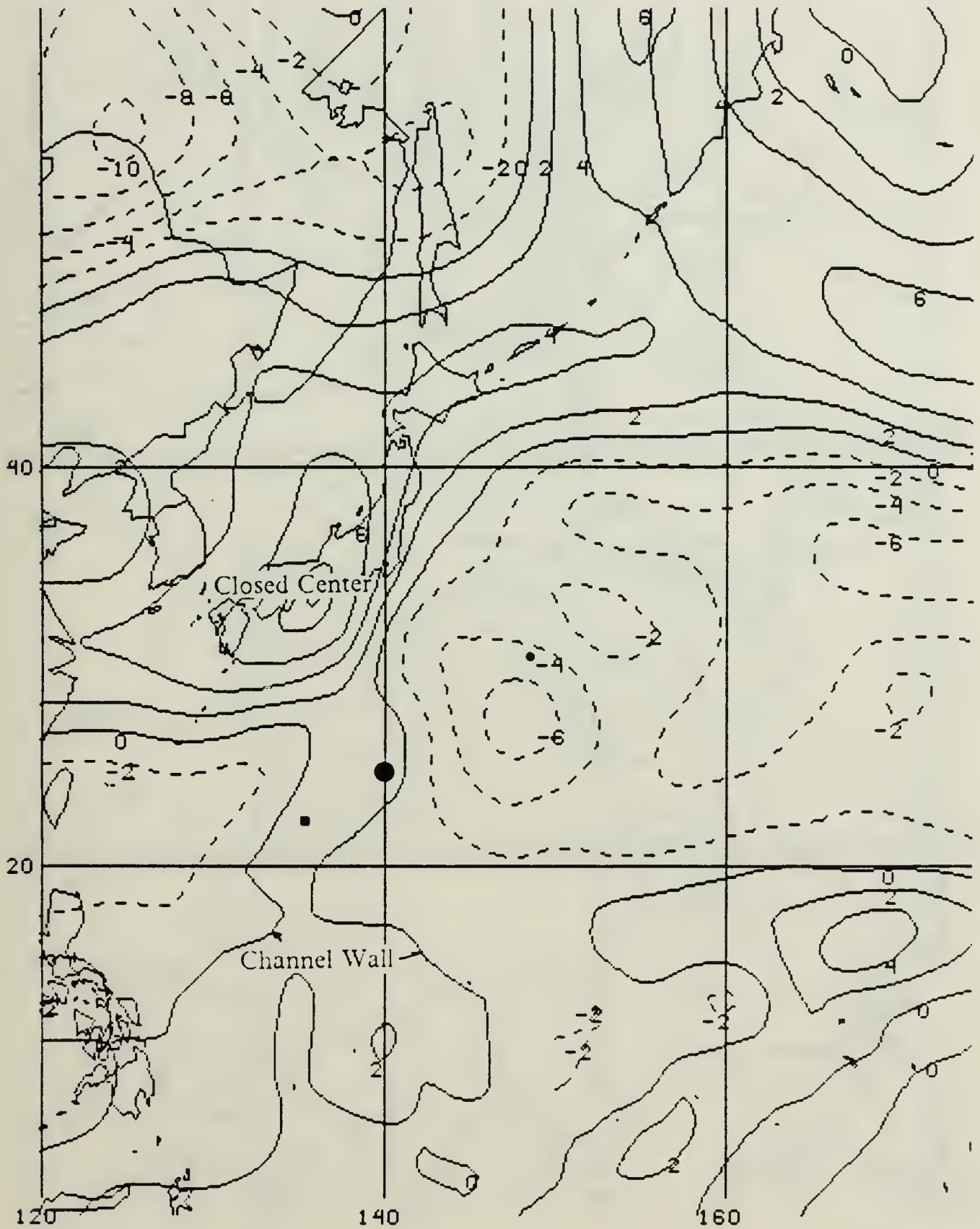


Fig. 3.16a Relative vorticity ( $\times 10^5 \text{ s}^{-1}$ ) at 400 mb at 12 UTC 06 Nov 1983.

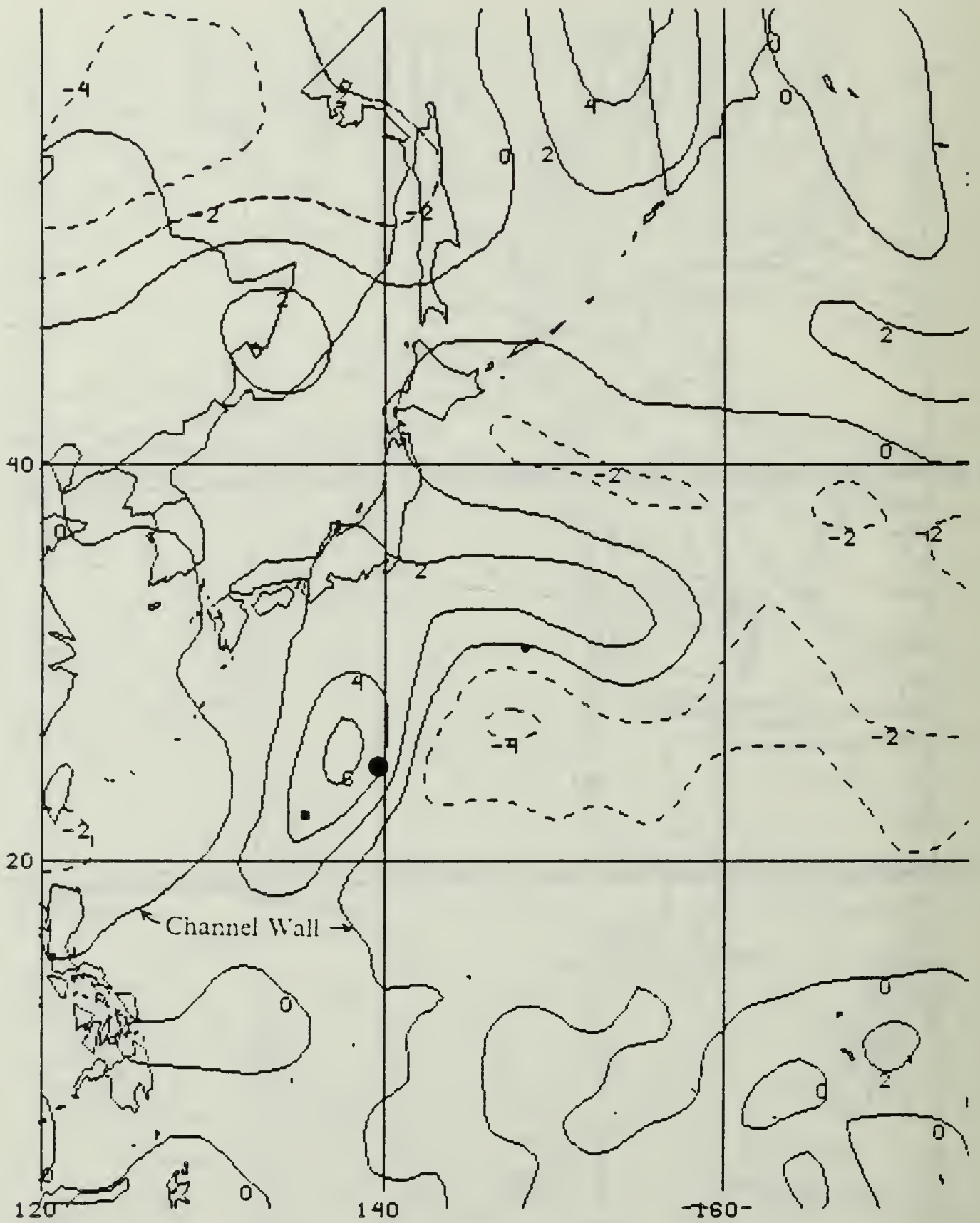


Fig. 3.16b Relative vorticity ( $\times 10^5 \text{ s}^{-1}$ ) at 700 mb at 12 UTC 06 Nov 1983.



Fig. 3.16c Relative vorticity ( $\times 10^5 \text{s}^{-1}$ ) in LAV at 12 UTC 06 Nov 1983.

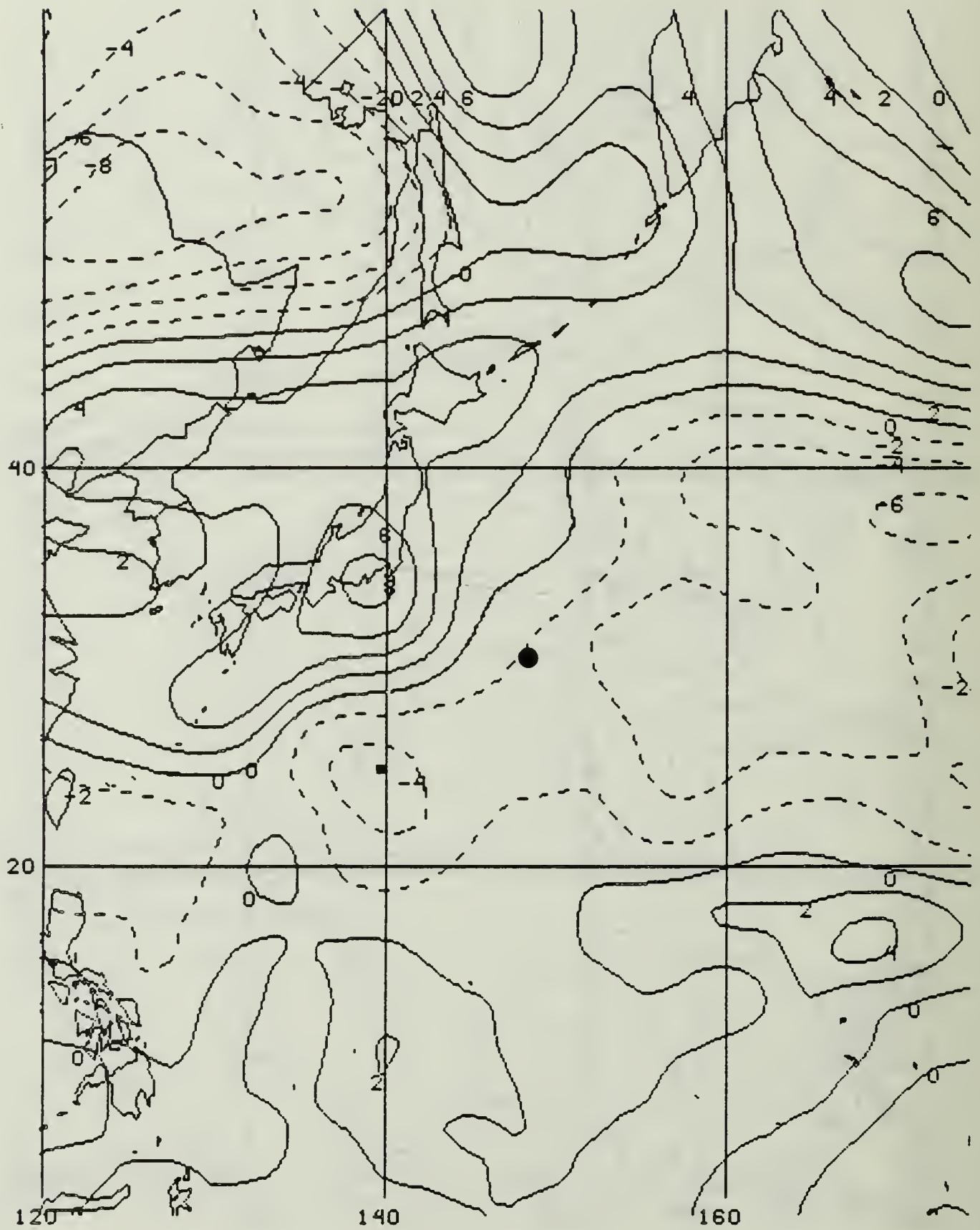


Fig. 3.17a Relative vorticity ( $\times 10^5 \text{s}^{-1}$ ) at 400 mb at 00 UTC 07 Nov 1983.

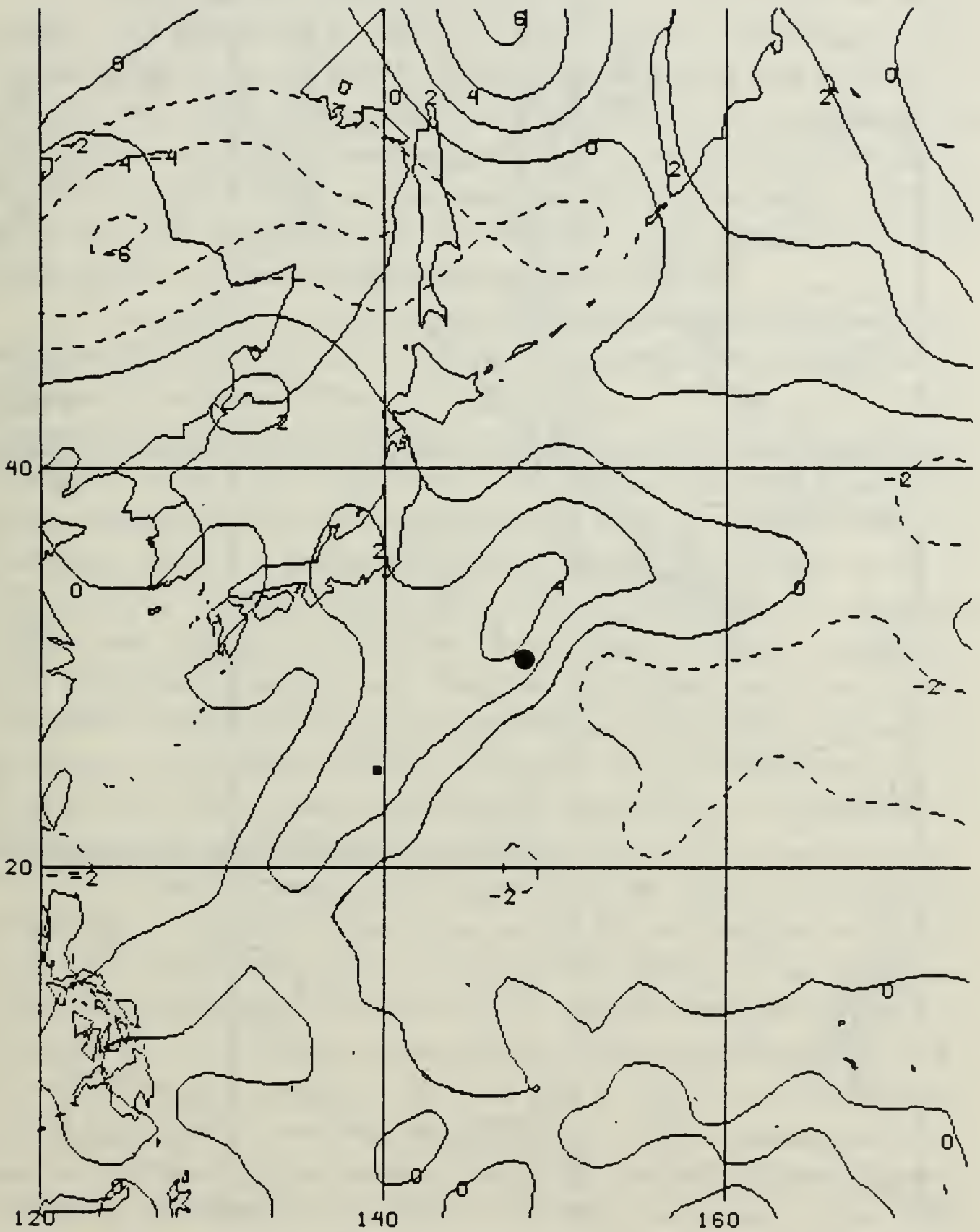


Fig. 3.17b Relative vorticity ( $\times 10^5 \text{s}^{-1}$ ) at 700 mb at 00 UTC 07 Nov 1983.

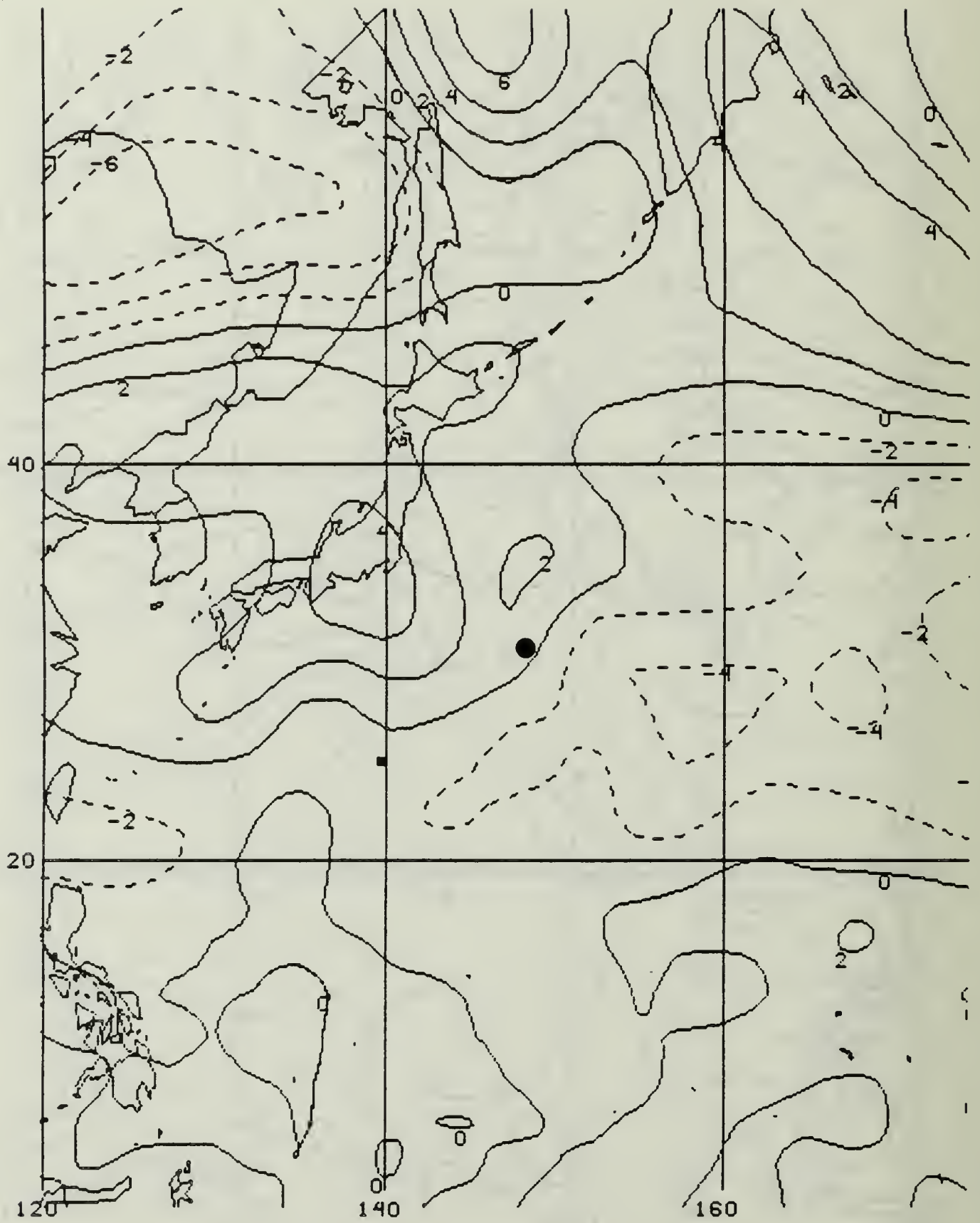


Fig. 3.17c Relative vorticity ( $\times 10^5 \text{ s}^{-1}$ ) in LAV at 00 UTC 07 Nov 1983.

### 3. Summary of the Relative Vorticity Analysis of STY Marge's Track

The development of the node pattern in the relative vorticity contours and the change in the pattern with time appear to give reasonable indications of the three critical changes in the track of STY Marge. The first step in the track occurred at 12 UTC 31 Oct 83 and was the smallest of the track changes. Each of the 400, 700 and LAV chart series indicated that the subtropical ridge was strong. The primary nodes in the vorticity patterns showing excellent correlation 18-30 h beyond the 20 deg left turn in the track. The strongest indicator was the 400 mb pattern, which provided the best indication of the conditions during the first step in the storm track.

The weakness in the ridge that accompanied the bending of the storm track to the right after 12 UTC on the 31st is evident in the 400 mb and LAV charts, but the pattern does not appear clearly at 700 mb. The ridge at 700 mb narrows to some degree but remains intact to the north of the cyclone center. The ridge break that develops to the northeast of Luzon is well to the west-northwest of the center. In this case, the pattern at 700 mb would indicate west-northwest movement rather than recurvature, about 48 h prior to the left turn at 12 UTC on 2 Nov 83. The 400 mb chart 24 h prior to the step in the storm track (Fig. 3.7a) could lead to a serious track forecast error if it was used without the other two charts. The sharp north-northeast node would seem to indicate that recurvature should take place at about 140°E. However, the 700 mb chart indicates a relatively strong ridge at 140°E with a weakness in the ridge to the west near 130°E. The average of the ridge weaknesses at the two levels would be at 135°E, which coincidentally would have been an excellent forecast as STY Marge eventually did recurve at about 134°E.

The critical recurvature period appears to be well represented in the relative vorticity fields as the 400 mb node pattern and the 700 mb channel pattern began to align in the vertical after the second track step. The transition of the primary node pattern from one oriented toward the NW to become oriented with the previous secondary node started 72 h prior to the recurvature, and was nearly complete 36-48 h prior to the turn to the northeast. This would seem to provide a useful forecast aid if such patterns appeared consistently. Finally, orientation of the node and channel axes gave an indication of the post-recurvature track. The question is whether the patterns observed in the relative vorticity fields of STY Marge are evident in other tropical cyclones. Table 6 gives the dominant vorticity pattern, rating value and time factor for each 12 h period for STY Marge.

TABLE 6  
RATING VALUES FOR SUPER TYPHOON MARGE

<u>Dtg.</u>	<u>+2</u>	<u>400 mb</u>			<u>700 mb</u>			<u>LAV</u>									
		<u>0(pri)</u>	<u>-2</u>	<u>0(sec)</u>	<u>+2</u>	<u>0</u>	<u>-2</u>	<u>+2</u>	<u>0(pri)</u>	<u>-2</u>	<u>0(sec)</u>						
103012		N/E/42	N/E/72	N/F/47	N/E/12	N/E/58			N/E/48								
3100	N/F/6	N/E/36	N/E/72	N/P/36		N/G/40			N/E/36	P/F/72							
12		N/G/60	N/E/72	N/P/30		N/F/72	P/E/72		N/G/60		N/None						
110100	N/E/12	N/G/48	N/E/60	N/None		N/F/66	P/E/72	N/E/6	N/G/48								
12	N/F/20	N/G/48	N/E/60	N/P/60		N/G/48	B/E/72	N/E/12	N/E/48		N/F/48						
0200		N/E/48	N/E/72	N/P/36		N/G/48			N/E/46		N/F/30						
12		N/E/36	N/E/72	N/P/24		C/G/72			N/E/60		N/None						
0300		N/E/36	N/E/60	N/P/18		N/G/72			N/E/48		N/None						
12		N/E/30	N/G/48	N/None	N/G/36	N/F/48			N/E/36		N/P/66						
0400		N/P/48	N/F/60	N/E/24	N/P/36	N/G/60			N/E/54	N/G/62	N/E/36						
12		N/P/36	N/F/48	N/E/12	N/F/30	N/E/40			N/F/36	N/G/48	N/P/24						
0500		N/P/30	N/G/40	N/E/12	N/G/24	N/E/30			N/F/12	N/G/24	N/E/36	N/None					
12	M	I	S	S	I	N	G	D	A	T	A	F	I	E	L	D	S
0600		N/F/6	N/E/28			O/E/48	N/G/48		N/P/6	N/F/16	N/G/48						
12		N/F/4	N/G/6			N/G/12	N/F/12			N/G/12							

(type of pattern/rating/time) N-node, P-ridge pinch, B-ridge break, C-channel, O-closed center  
E-excellent, G-good, F-fair, P-poor

## D. APPLICATION OF THE ANALYSIS TECHNIQUE TO OTHER STORMS

### 1. Dominant Vorticity Patterns

The relative vorticity contour pattern analysis described above is applied to the other 11 storms in the data set. It is not possible to describe these cases in the detail given above for STY Marge. Dominant and secondary contour patterns (Fig. 3.2) are identified and the angular difference (Table 5) between the pattern and the best track is measured, and the time interval over which the technique would provide useful guidance is estimated as above. Table 7 is a summary of the relative vorticity contour patterns observed in the storms.

TABLE 7  
RELATIVE VORTICITY CONTOUR PATTERNS OBSERVED

Storm	Dominant Patterns	Secondary Patterns
Marge	Node	Ridge deformation, Channel
Bess	Node, Channel	Ridge deformation, Resultant vector
Gordon	Node, Channel	Ridge deformation, Storm-storm (Faye)
Forrest	Ridge deformation, Node	Closed centers, Resultant vector
Lex	Node	Channel
Ida	Node	Closed centers, Resultant vector
Clara	Ridge deformation, Node	Closed centers, Storm-storm (Bill)
Thad	Ridge deformation, Channel	Closed centers
Vanessa	Node, Channel	Storm-storm (Thad, Warren)
Abby	Channel, Node	Ridge deformation, Closed centers, Storm-storm (Ben, Carmen) Resultant vector
Wayne	Node, Channel	
Ike	Channel, Closed centers	Node

The node pattern was found in 11 of the 12 tropical cyclones. Only Typhoon Thad did not show the node pattern. Thad was unusual in that it displayed a broken ridge from the start. The break gave an excellent indication of the 72 h position in Fig. 3.18. Official forecast errors were large due to numerical model predictions for strengthening of the ridge, which did not verify (Joint Typhoon Warning Center, 1984). The channel pattern (Fig. 3.2a) was the next most frequently occurring pattern. Channels were dominant in portions of the tracks of seven storms and secondary patterns in two other tropical cyclones. They were generally found in the low level field (700 mb) or in the late stages of a storm. The ridge deformation pattern (node intrusion, pinch, or break) was a dominant pattern in three storms (including Thad) and as a secondary pattern in four storms. The closed center pattern occurred almost as often as the ridge deformation pattern, but was a dominant pattern only in Typhoon Ike. The track of Ike (Fig. 3.19) is within the channel south of the zero contour toward the closed +2 center before Ike turned toward the node to the west of Luzon.

## 2. Cyclone-Cyclone Interaction

The interaction between tropical cyclones is a complex problem for the forecaster. A determination first has to be made whether or not an interaction is occurring. The key questions are at what distance between centers will the interaction begin and when will this interaction be strong enough to change either the track or intensity of one or both of the cyclones. According to Sandgathe (1987), storm-storm interaction takes place in four of the systems in the data set. STY Vanessa interacted to some degree with two other tropical cyclones, but the track of Vanessa (not shown) does not appear to have been influenced during these interactions. The first interaction was a reduction of upper-level outflow above the incipient Vanessa due to deformation of the upper-level field by the outflow of TY Thad (Joint Typhoon Warning Center, 1984). During the second interaction, Vanessa influenced the track of TY Warren, which was located in the South China Sea and had been tracking slowly westward. As STY Vanessa approached recurvature in the Philippine Sea, Warren turned rapidly to the east-northeast and increased in translation speed. This created a major forecast problem because of the potential danger to a group of ships leaving Subic Bay. Another storm-storm interaction between TY Clara and TY Bill resulted in little or no change in the track of Clara, but had a profound effect on Bill's track (not shown). The circulation and intensity of Clara at 12 UTC 18 Nov 1984 (Fig. 3.20) were very large compared to that of Bill. Clara's recurvature track was not changed by Bill, but Bill had a long track to the southeast under the influence of the circulation of Clara.

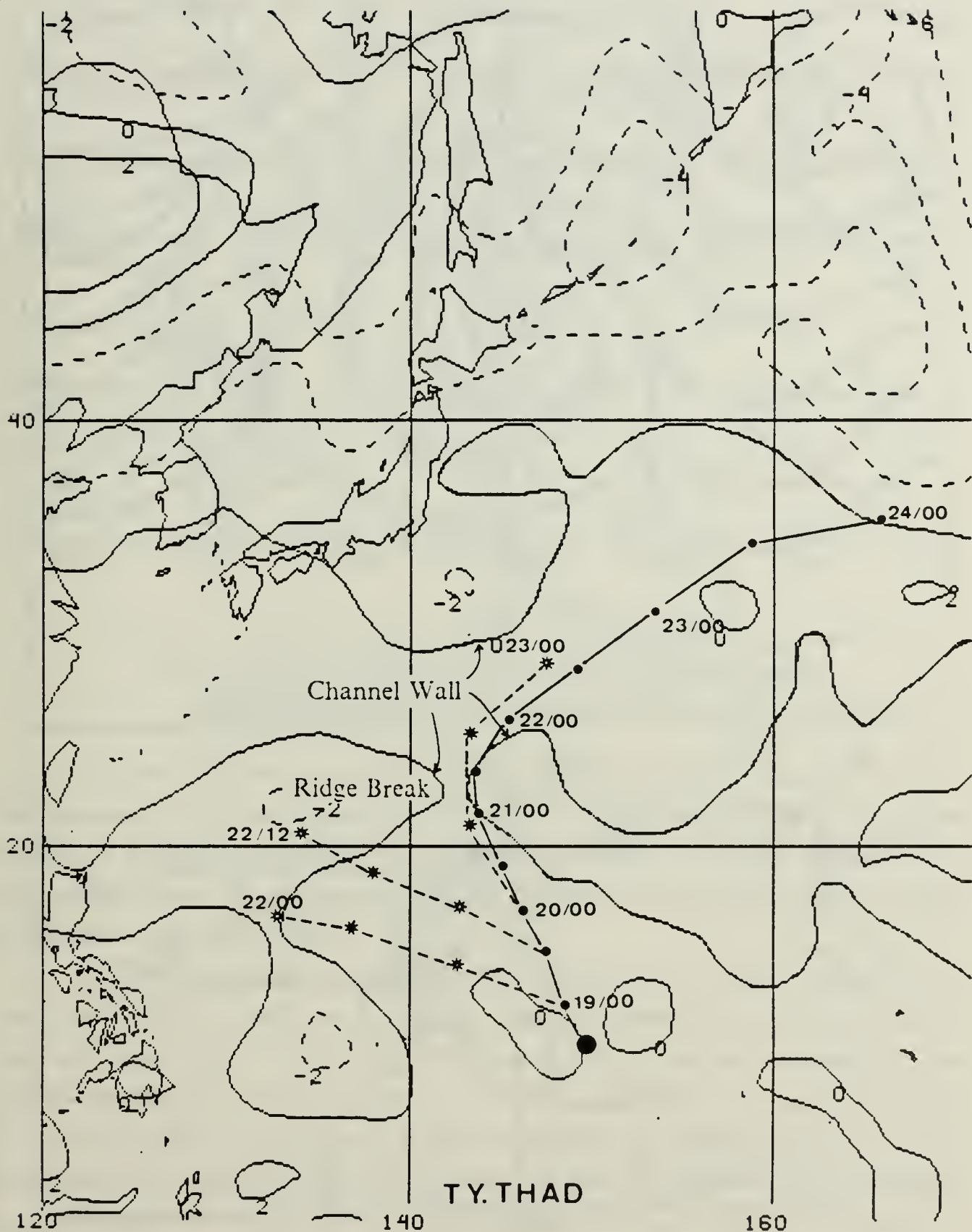


Fig. 3.18 Relative vorticity ( $\times 10^5 \text{ s}^{-1}$ ) in LAV at 12 UTC 18 Oct 1984 for Typhoon Thad. Forecast tracks are dashed with stars.

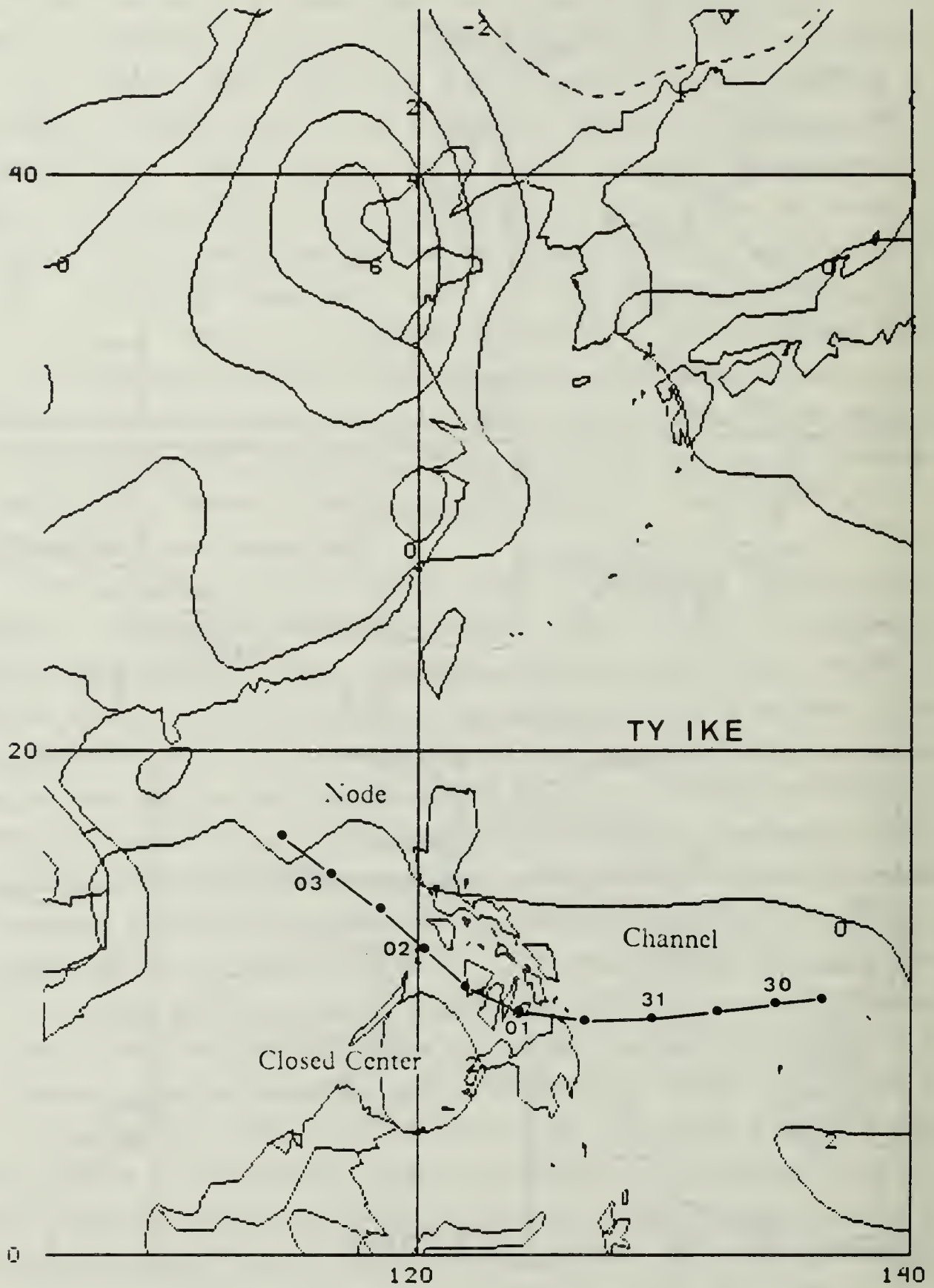


Fig. 3.19 Relative vorticity ( $\times 10^5 \text{ s}^{-1}$ ) in LAV at 12 UTC 30 Aug 1984 for Typhoon Ike.

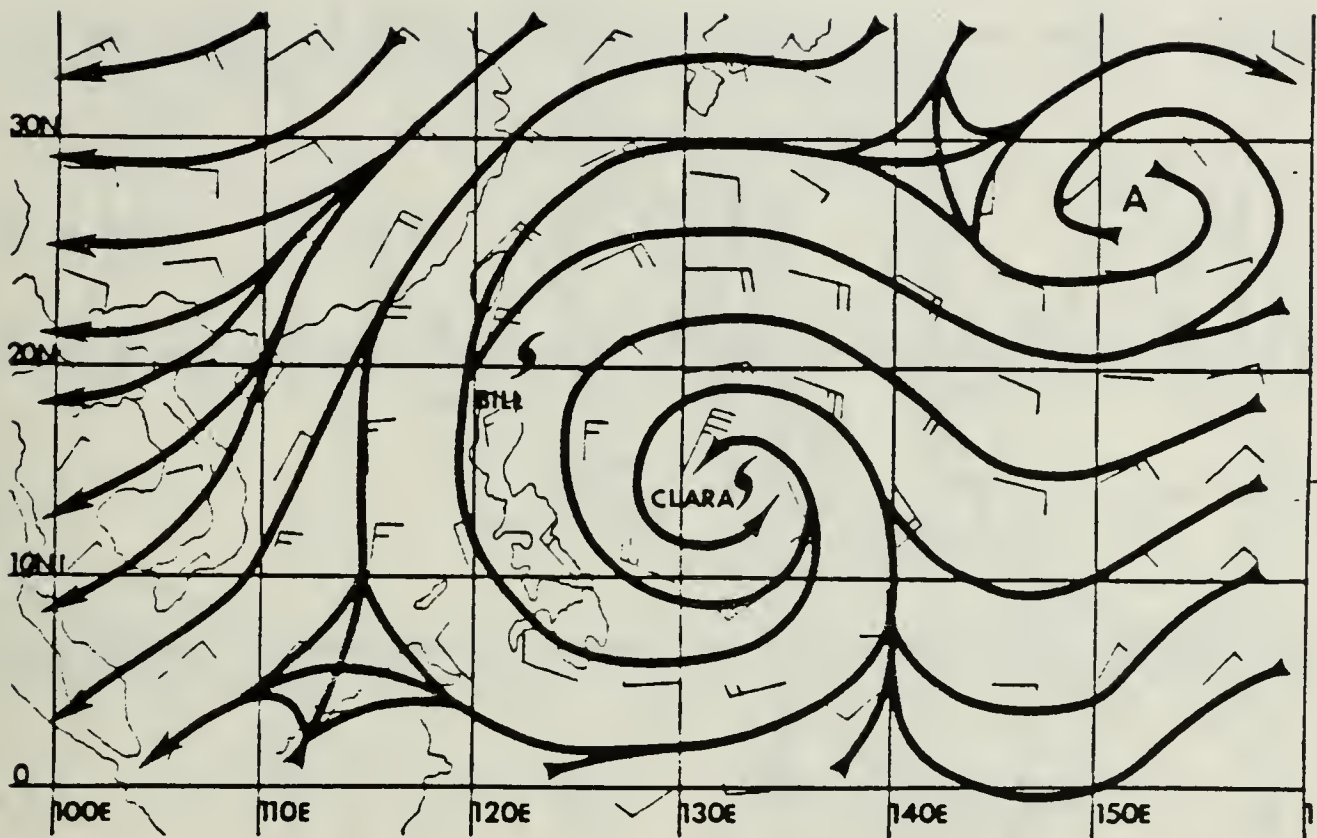


Fig. 3.20 Streamline analysis at 925 mb at 12 UTC 18 Nov 1984 illustrating Typhoon Bill and Typhoon Clara interaction (Joint Typhoon Warning Center, 1984).

Typhoon Gordon interacted with TY Faye at 00 UTC 30 Aug 82 (Fig. 3.21). The interaction is unusual because of the nearly 14 deg of latitude (840 n mi) distance at which it occurs. This distance seems particularly large considering that Faye is a very small cyclone. The interaction may be enhanced by the large positive vorticity (low) center northwest of Japan.

In the fourth case of cyclone-cyclone interaction, STY Abby interacts with two other cyclones at extended distances, and apparently before the other systems are even in warning status. Usually when cyclone-cyclone interaction is considered, two mature or nearly mature systems that are approximately 600 n mi apart are involved. STY Abby displays a very different pattern in the relative vorticity fields. About 36 h before the first warning on Tropical Storm (TS) Ben, an apparent interaction takes place between STY Abby (110 kt) and the tropical disturbance that would become TS Ben. The zero contour in the LAV field for 00 UTC 11 Aug 83 (Fig. 3.22a) surrounds Abby and a +2 center to the east from which Ben will develop. The zero contour also

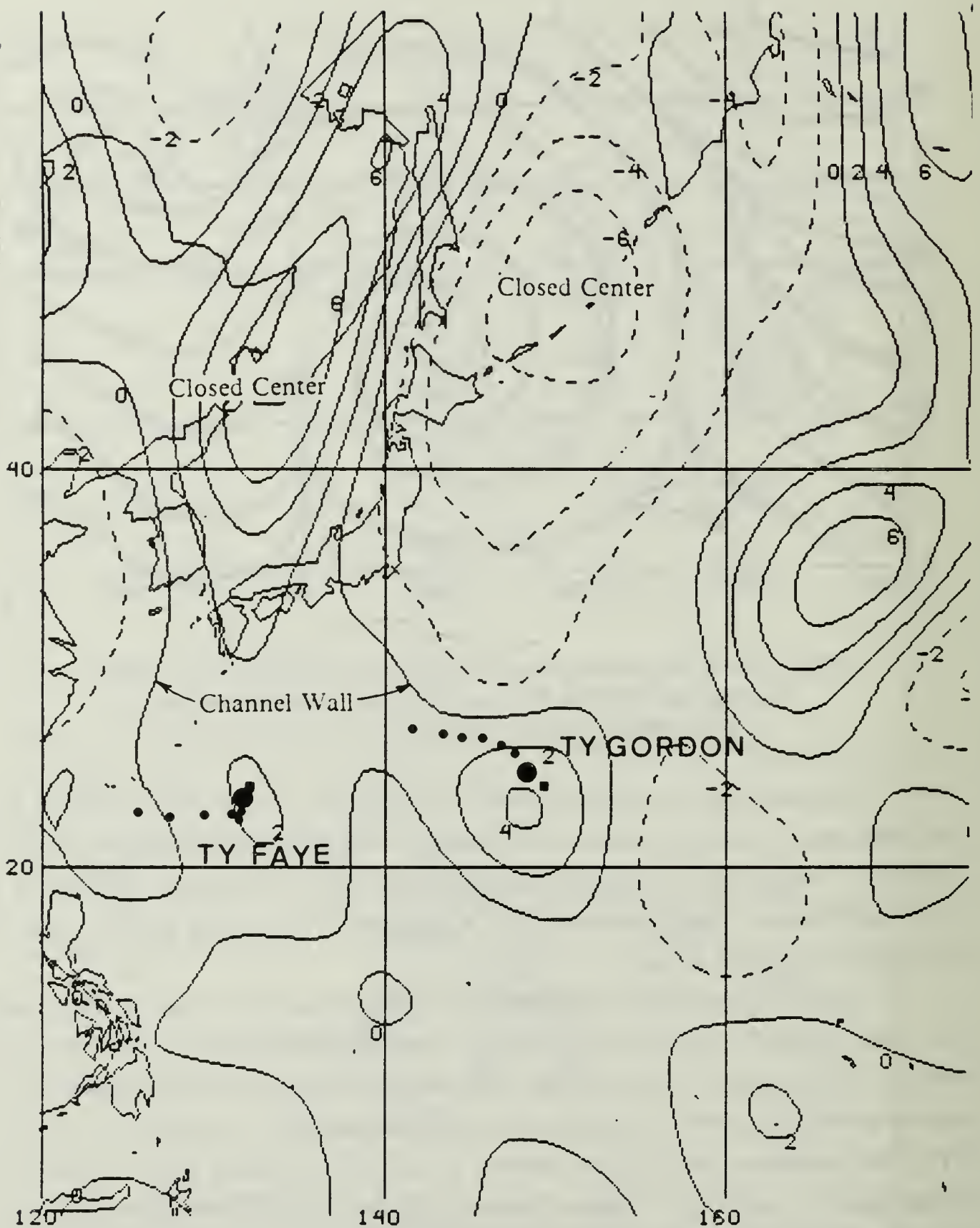


Fig. 3.21 Relative vorticity ( $\times 10^5 \text{s}^{-1}$ ) in LAV at 00 UTC 30 Aug 1982 illustrating Typhoon Gordon and Typhoon Faye interaction.

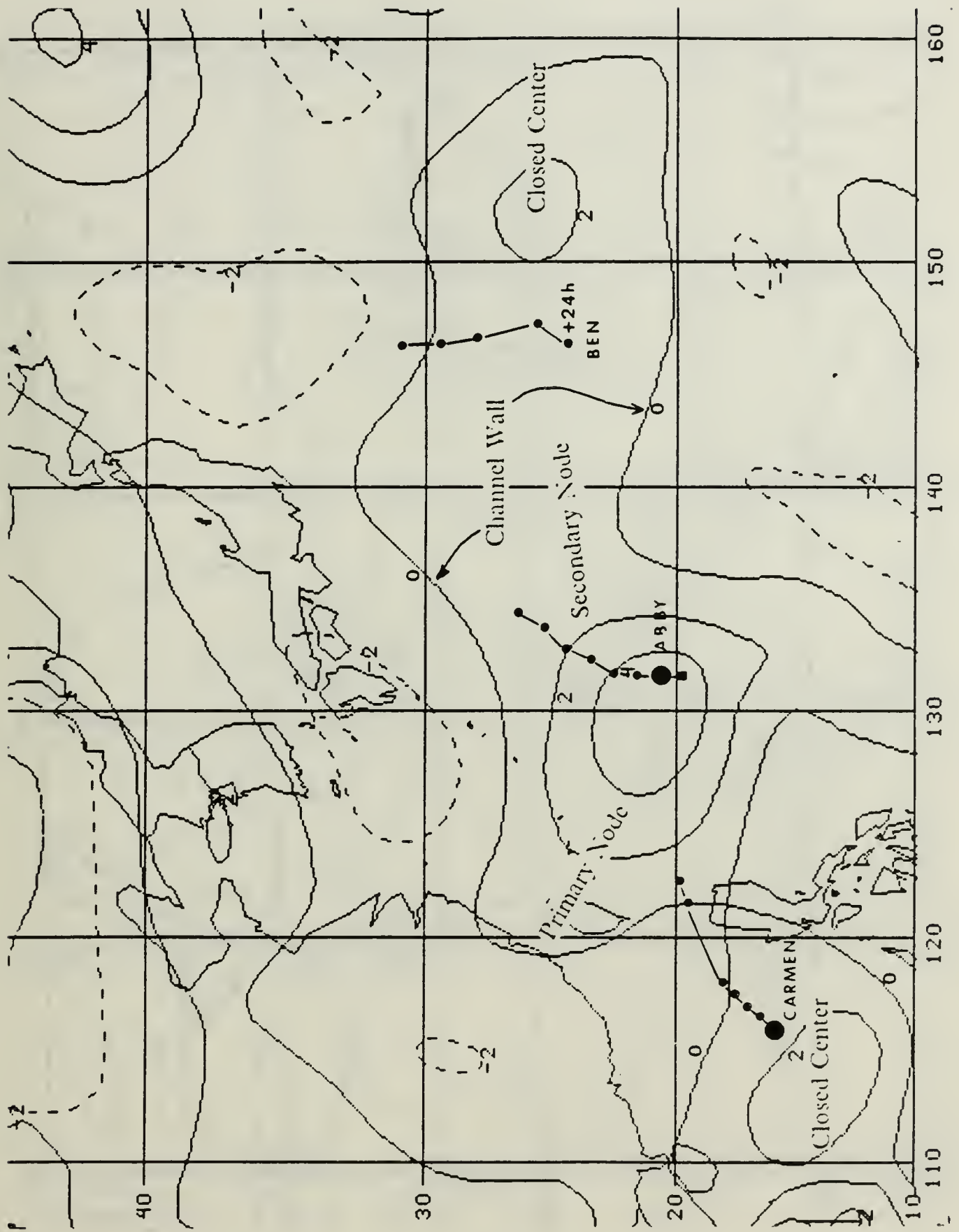


Fig. 3.22a Relative vorticity ( $\times 10^5 s^{-1}$ ) in LAV at 00 UTC 11 Aug 1983 illustrating Super Typhoon Abby - Typhoon Ben - Typhoon Carmen interaction.

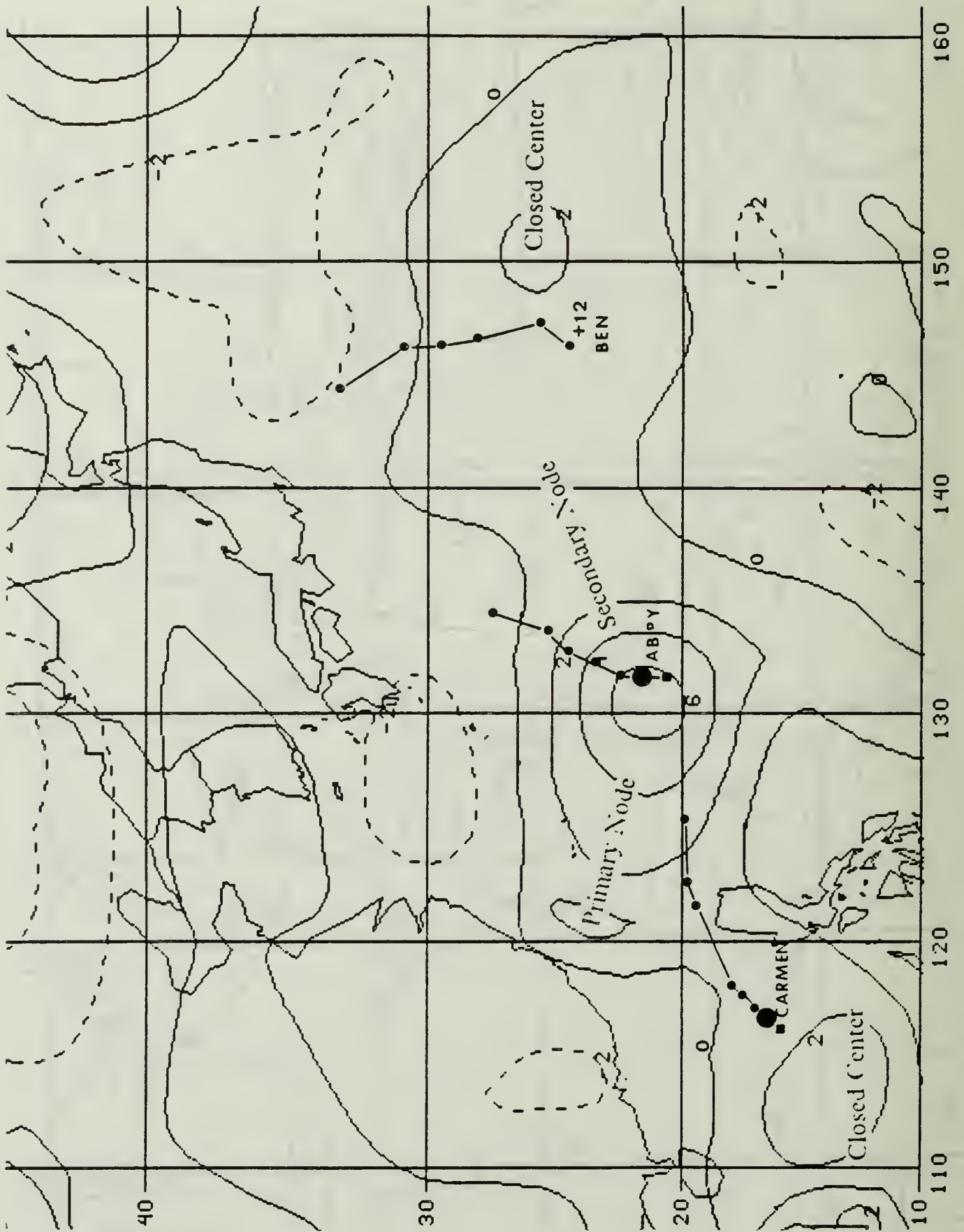


Fig. 3.22b Relative vorticity ( $\times 10^5 s^{-1}$ ) in LAV at 12 UTC 11 Aug 1983 illustrating Super Typhoon Abby - Typhoon Ben - Typhoon Carmen interaction.

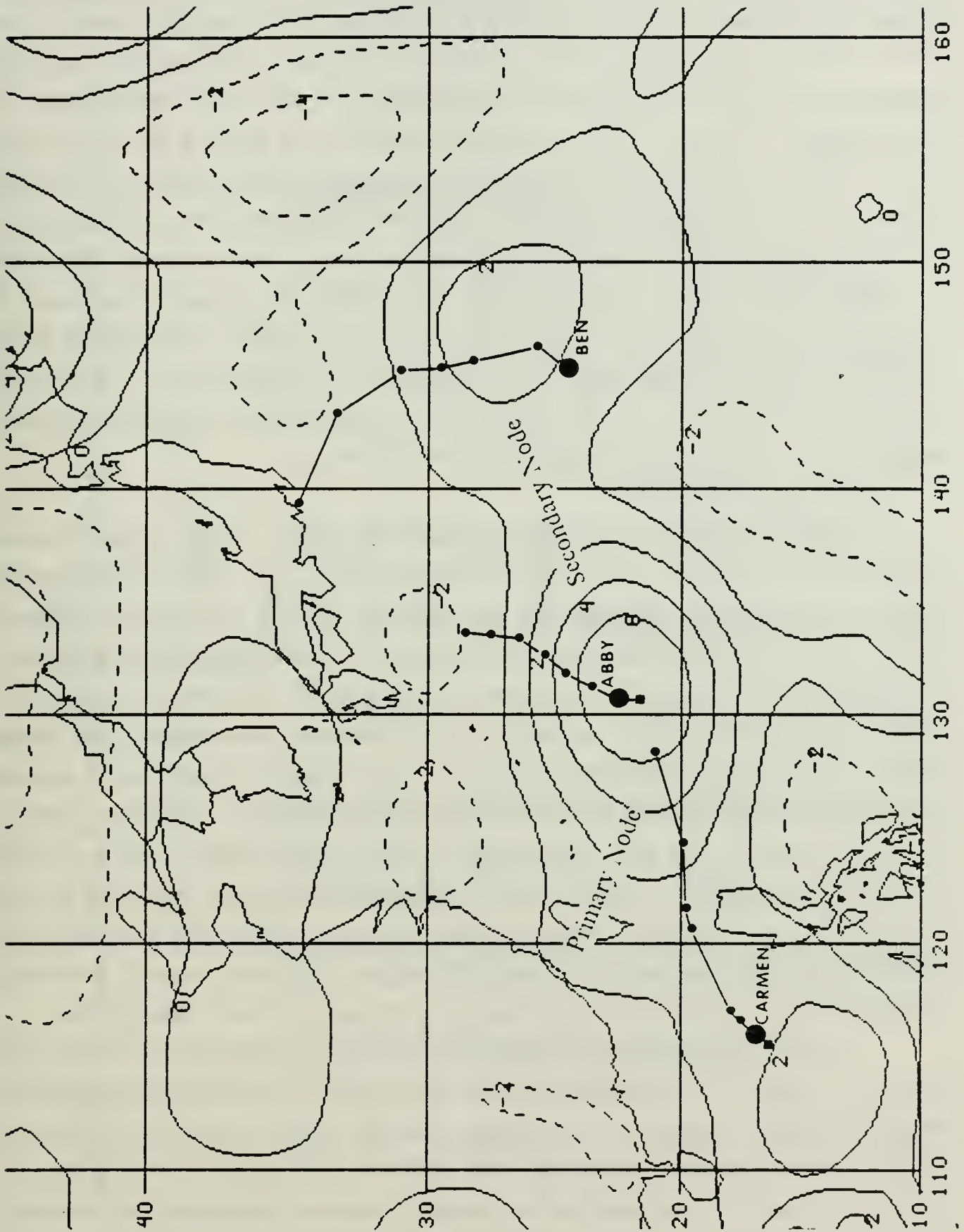


Fig. 3.22c Relative vorticity ( $\times 10^5 \text{ s}^{-1}$ ) in LAV at 00 UTC 12 Aug 1983 illustrating Super Typhoon Abby - Typhoon Ben - Typhoon Carmen interaction.

extends toward a +2 center in the South China Sea that will spawn Tropical Storm Carmen 3 days hence. The pattern is further complicated by the strong -2 center to the north of Abby. In the next 12 h (Fig. 3.22b), the interaction between Abby and the disturbance in the South China Sea becomes stronger at a distance of approximately 15 deg of latitude (900 n mi). The first available position for TS Ben is at 00 UTC 12 Aug (Fig. 3.22c) near 24.5°N, 145°E. In this field, interaction is taking place over a major portion of the western North Pacific basin and the South China Sea. The interaction may not just be multiple cyclone as large positive vorticity centers already exists that are adjacent (but separate from) both Ben and Carmen. The apparent interaction is taking place at a distance of 19 deg (1140 n mi) from the South China Sea to Abby and 16 deg (960 n mi) from Abby to the center to the northeast of Ben. Again, the strong ridge pattern north of STY Abby with the large negative (anticyclonic) center northeast of Ben further complicates the forecast situation.

### 3. Forecast Performance

Another consideration is which contours are giving the best overall forecast patterns and at what levels are the best forecast results found. Among the subjective aspects of the proposed technique are that different vorticity contours and different pressure levels may be involved as the storm evolves. The average rating values and time factors for the data set, by storm, are given in Table 8. Table 9 is a summary (by pressure level and by vorticity contour) of the occurrences, the average of the rating values and the average time factor (described above). Secondary node values are not given for the 700 mb level due to the small number of occurrences. Secondary nodes on the zero contour do not give high average ratings in this sample. The LAV field provides slightly better indications of track changes in this data set. This field may do even better if a mass weighted averaging scheme was used, as discussed previously. The -2 contour provides the most consistent information at all levels when it is present. Unfortunately, this contour is not as common as the zero contour in this data set.

A test of the technique performance is how well it predicts the observed storm track turns. Table 10 is a compilation of the turn indication performance (hindcasts in this developmental sample) of the relative vorticity pattern technique. With the exception of the period of recurvature and northwest movement for STY Abby, the technique appears very successful in this sample. Typhoon Gordon also had a vorticity pattern with a stationary negative vorticity center to the east of Japan that is larger than the one that caused some problems in the forecast of STY Abby. In the case of

TABLE 8  
AVERAGE RATING VALUES BY STORM, PRESSURE LEVEL AND VORTICITY CONTOUR

Storm	400 mb		700 mb			LAV					
	+2	0(pri)	-2	0(sec)	+2	0	-2	+2	0(pri)	-2	0(sec)
	xx/yy (n)	xx - avg. rating points yy - avg. time n - number of forecasts	yy - avg. time n - number of forecasts	yy - avg. time n - number of forecasts	yy - avg. time n - number of forecasts	yy - avg. time n - number of forecasts	yy - avg. time n - number of forecasts	yy - avg. time n - number of forecasts	yy - avg. time n - number of forecasts	yy - avg. time n - number of forecasts	yy - avg. time n - number of forecasts
Bess	4.1/20 (7)	4.2/44 (20)	4.6/58 (8)	1.4/71 (19)		4.7/50 (24)	5.3/64 (3)		4.7/52 (19)	5.3/63 (9)	2.1/38 (15)
Gordon	4.7/51 (16)	4.6/55 (14)	4.4/59 (12)	1.0/53 (8)	3.4/42 (16)	3.3/58 (17)	3.0/61 (11)	4.3/37 (15)	4.5/59 (17)	4.8/43 (5)	1.9/68 (13)
Wayne	4.5/32 (4)	3.4/38 (8)	4.0/72 (1)			4.1/39 (11)	5.3/44 (3)		3.7/39 (9)	4.4/67 (5)	0.5/54 (2)
Abby	4.9/51 (18)	4.4/60 (23)	5.0/64 (23)	2.6/41 (14)		4.0/51 (20)	4.0/52 (3)	3.7/52 (16)	4.2/66 (24)	5.0/64 (18)	1.5/70 (18)
Forrest	5.5/32 (8)	4.3/44 (13)	5.1/56 (12)	3.5/60 (8)	4.4/24 (10)	4/4/50 (14)	4.2/58 (6)	5.1/24 (8)	5.4/27 (14)	5.3/65 (10)	2.7/52 (7)
Ida	3.4/24 (2)	2.7/40 (6)	5.5/40 (4)	2.7/16 (3)		3.3/24 (8)	5.4/53 (5)	4.3/12 (3)	2.9/32 (7)	4.6/43 (7)	0.5/29 (4)
Lex	2.4/34 (5)	4.5/52 (8)		1.7/56 (3)	3.7/29 (6)	4.1/45 (8)		2.7/28 (6)	4.4/48 (8)		4.0/12 (1)
Marge	4.7/13 (3)	4.6/36 (14)	5.5/55 (14)	2.8/25 (12)	4.7/28 (7)	4.9/51 (14)	6.0/72 (3)	5.0/9 (4)	5.3/41 (14)	5.0/53 (5)	1.6/23 (9)
Ike	5.1/56 (14)	3.7/57 (22)	5.0/56 (9)	2.0/63 (4)		4.8/56 (19)	3.1/72 (15)	5.0/45 (4)	4.6/59 (22)	6.0/72 (3)	
Thad		5.3/58 (10)		2.0/72 (1)	5.0/72 (3)	5.4/62 (8)	5.0/72 (2)		5.4/52 (11)	5.0/72 (1)	
Vanessa		5.1/62 (16)	3.5/63 (4)	5.5/72 (4)	6.0/54 (4)	5.2/61 (15)	5.5/62 (10)	6.0/72 (1)	5.5/52 (15)	4.8/72 (6)	
Clara		5.9/49 (15)		6.0/68 (3)	6.0/68 (3)	4.3/51 (14)	4.3/39 (4)	4.8/63 (6)	5.2/60 (13)		

TABLE 9  
RELATIVE VORTICITY CONTOUR PERFORMANCE BY LEVEL

<u>Level</u> (mb)	<u>Contour</u>	<u># of Fcsts</u>	<u>Avg Rating</u> (points)	<u>Avg Time</u> (h)
400	2	77	4.5 (good)	35
	0(p)	169	4.4 (fair)	50
	0(s)	78	2.9 (poor)	55
	-2	87	4.8 (good)	58
700	2	42	4.7 (good)	48
	0	169	4.3 (fair)	49
	-2	62	4.5 (good)	58
LAV	2	60	4.7 (good)	38
	0(p)	172	4.6 (good)	49
	0(s)	67	1.9 (poor)	44
	-2	69	5.1 (good)	61

(p) primary, (s) secondary

TABLE 10  
TURN PREDICTION PERFORMANCE  
OF THE RELATIVE VORTICITY PATTERN TECHNIQUE

Turn type	Observed	Forecast	False Indicators
Right	8	7	0
Left	4	4	0
Recurvature	7	7	1 *
Loop	2	0	0

\* STY Abby - Resultant-vector pattern suggested recurvature while primary node indicated northwest movement.

Gordon, recurvature would be forecast based on this technique. However, the pattern was not as clear as in the other storms, and the time factor was reduced. A clear

recurvature pattern did not appear until 24 h before the event. The experience with this set suggests that a blocking high is a definite complicating factor in forecasting recurvature.

The one right turn that is not indicated by the synoptic pattern technique is a 30 deg change in the track of TY Ike as the system turned toward the west under the subtropical ridge after moving to the southwest for approximately two days. This occurred at low latitudes ( $9^{\circ}\text{N}$ ) under conditions where recurvature was not a consideration.

The loops in the the track of STY Abby and of TY Lex were short-term features (12 h or less), and were not evident in the 12 h time step of the fields. In any case, forecasting loops would probably cause the Typhoon Duty Officer's qualifications to be reevaluated and is not a high priority.

#### IV. CONCLUSIONS AND RECOMMENDATIONS

This study indicates that relative vorticity charts have the potential to be a useful tool in the recurvature forecast decision process. Following the poor performance in the official forecasts of Super Typhoon Marge during October-November 1983, the JTWC initiated an internal review of the forecast process. This review did not reveal anything that could have been done with the existing maps and resources to improve the performance! This study of Marge suggests that a different presentation of the data available in the JTWC during the forecast development might have contributed to better forecasts. Thus, the first recommendation is that software be made available to JTWC to allow presentation of the Global Band Analysis fields in terms of relative vorticity contours. These vorticity fields allow the relative strengths and weaknesses of the major troughs and ridges to be analyzed readily, and incorporate dynamical features that are not apparent in the streamline presentation. A systematic procedure of locating the strong or weak points in the ridge may refine the recurvature longitude selection process. A mass-weighted LAV is suggested based on the experience with Marge.

The developmental study had plotted best tracks on the relative vorticity contour charts to identify and locate the patterns described above. A true test of the operational importance and forecast capability of the technique should be carried out. The test should present an independent sample of storm sets in a manner similar to that found in the forecast center. The data presented should include only products and fields that would be available to the operational forecaster. Ideally, a first forecast should be developed for each 12 h period without having the relative vorticity fields available, followed at a later time by a second set of forecasts developed by the same forecaster having the relative vorticity fields. The skill level for each of the forecasts for a data set could be compared to a climatology-persistence forecast. The use of the same forecaster for each set would preclude individual inherent skills from biasing the results. To reduce any bias that would be introduced by the forecaster remembering tracks, a method of presentation that mixes the sequence of storms would be required. If the method helps eliminate from consideration forecast aids that are not likely to be correct, the translation speed may be better defined by the remaining aids. Further

study may also reveal a pattern in the relative vorticity fields that will help determine the translation speed. With the proper preparation and planning, the test could be carried out on a quasi real-time basis utilizing the data collection and display capabilities in the IDEA lab.

The storm-storm interaction analysis as currently practiced in the forecast center could be refined through the use of the relative vorticity fields. The pattern seen in STY Abby and in the TY Gordon-TY Faye cases suggest that interaction may be taking place at greater than expected ranges and that complex interactions patterns may be involved. The ability to detect these features in the analyzed fields may give the forecaster a basis for evaluating guidance from a numerical model that considers only a single vortex in the field. The early detection of vortex interactions might alert the forecaster to these complex interactions. Thus, a study focused on the storm-storm interaction cases using the relative vorticity fields is recommended.

The previous empirical orthogonal function (EOF) representations of storm-synoptic data by Wilson (1984), Schott (1985) and Weniger (1987) also might be applied to relative vorticity fields for eventual inclusion in the decision tree forecasting tool. A possible approach to stratification of the data set would be compositing of the data by the storm-synoptic parameters. The storm-synoptic approach could lead to improved forecast aid selection guidance. Another approach might be to composite the fields in a manner similar to the approach used by Allen (1984) in the COSMOS technique. Application of relative vorticity information to COSMOS type field categories could lead to the development of an improved COSMOS technique.

Future application and testing of this technique would be facilitated if the database in the IDEA lab included the best track data and the archived forecast aids. A study could then be undertaken to compare the relative vorticity patterns with the forecast aids for different categories of tropical cyclones. The objective is to select the "best" aid based on a set of rules developed from the past performance of the various aids under the conditions presented. The rules might be incorporated into an artificial intelligence shell on JTWC's computers for track aid selection. Even experienced forecasters could benefit from the detailed analysis of the new data required for inclusion in the rule base. Once the basic system is developed, the "experience" of the system could be continually updated as new information is available. This would provide a system for incorporating lessons learned in a particular forecast experience, which is now often lost when the forecaster leaves JTWC. Another advantage in the

development of an AI technique is that an interactive mode could be used in the training of new forecasters. Rules and decision points would be displayed to the trainee as a scenario develops. Appropriate and immediate feedback as decisions are made would develop the trainee's skills in a number of situations.

Even though new dynamical models or other track guidance tools may be developed, the typhoon forecaster still must evaluate this guidance in relation to existing techniques. This study suggests that the relative vorticity fields would be a useful tool in displaying and understanding the interaction of the typhoon with adjacent synoptic features. It is expected that availability of these vorticity fields could assist the forecaster and hopefully improve track forecasts in the future.

APPENDIX A  
PROGRAM--GLOBAL BAND FILE IDENTIFICATION

```
//SHGBID84 JOB (4697,9999),'SHERMAN 2200',CLASS = G
//*MAIN LINES = 40
//*
//* ** FILENAME FILETYPE **
//*   GBFID   NEDN
//*
// EXEC FORTVCLG,PARM.FORT = 'LANGLVL(66)'
//FORT.SYSIN DD *
C
C PGM TO IDENTIFY DATA FIELDS PRESENT IN GLOBAL BAND ANALS
C ON FNOC TAPE 144X49 MERCATOR GRID NEDN FORMAT
C
C ORIGINAL AUTHOR UNKNOWN, UPDATED AND MODIFIED BY
C   B. T. SHERMAN, APRIL 1987
C
C THE PROGRAM AS PRESENTED WILL GENERATE A LIST OF THE DATA
C FIELDS PRESENT ON A NEDN TAPE OF GBA FORMAT GRIDDED DATA.
C TWO CHANGES ARE REQUIRED TO RUN THE PROGRAM. THE JOB NAME
C AND USER ID INFO WILL NEED TO BE CHANGED TO GIVE A UNIQUE
C IDENTIFIER TO THE OUTPUT. THE TAPE TO BE READ MUST BE
C NAMED IN THE UNIT 10 SPECIFICATIONS AT THE END OF THE
C PROGRAM
      REAL*4 ID(4745),BCD(23)
      INTEGER*4 IDTG(8),NP(8),ISKP(33),ITITLE(42),NC(3)
      INTEGER*4 INI(23),ITAU(4),BCDTAU(4)
      INTEGER IDATA(7056)
      INTEGER*2 JDATA(14112)
C
      DATA ENDS/'AAAA'/
C
      EQUIVALENCE (IDATA(1),JDATA(1))
C
      NA = 14220
      NR = 7056
      NB = 0
      NCNT = 0
      NSK = 0
C
      CALL BUFFER(10,1,14220,ID)
C
C SKIP TO DESIRED DATA  NSKPRC = NO. OF RECORDS SKIPPED
```

```

C
  READ (5,1) NSKPRC
1  FORMAT (I5)
  WRITE (6,2) NSKPRC
2  FORMAT (' NO. OF RECORDS SKIPPED = ',I5)
  IF (NSKPRC.EQ.0) GO TO 55
  IF (NSKPRC.LE.1000) GO TO 5
  NSK = NSKPRC/1000
  DO 4 MSK = 1,NSK
  CALL SKPREC(10,1000,&99,&999)
4  CONTINUE
  NCNT = NSKPRC
  NSKPRC = NSKPRC - (NSK*1000)
5  CALL SKPREC(10,NSKPRC,&99,&999)

C
55  CONTINUE

C
  DO 926 L = 1,4745
926 ID(L) = ENDS

C
  CALL GETREC(10,&99,&9999)
  NCNT = NCNT + 1

C
  CALL GBYTES(ID(1),NC,0,6,0,3)
  DO 31 J = 1,3
31  IN1(J) = NC(J)
  CALL GBYTES(ID(1),ITAU,24,6,0,4)
  CALL XBCD(4,ITAU,BCDTAU)
  CALL GBYTES(ID(2),IDTG,16,6,0,8)
  I = 1
  DO 32 J = 4,11
  IN1(J) = IDTG(I)
  CALL XBCD(1,IN1(J),BCD(J))
32  I = I + 1
C  *** CONVERT BCD TO DECIMAL NUMBER *****
  CALL XINT(BCD,IYMDH,IER)
  CALL GBYTES(ID(4),NP,0,6,0,8)
  I = 1
  DO 33 J = 12,19
  IN1(J) = NP(I)
33  I = I + 1
  CALL GBYTES(ID(6),IUNIT,8,5,0,0)
  IN1(20) = IUNIT
  CALL GBYTES(ID(6),ISCLE,13,6,0,1)
  IN1(21) = ISCLE
  CALL GBYTES(ID(7),M,24,12,0,0)
  IN1(22) = M

```





APPENDIX B  
PROGRAM--GET GLOBAL BAND ANALYSIS

C THIS PROGRAM IS USED TO CREATE DATA TAPES FOR USE IN THE  
C IDEA LAB FROM NEDN FORMAT TAPES OF THE GLOBAL BAND ANAL.  
C THE PROGRAM READS THE TAPE, CONVERTS THE NEDN FORMAT TO  
C IBM EBCDIC FORMAT FOR PROCESSING AND THEN WRITES THE  
C SELECTED FIELD DATA TO TAPE IN ASCII FORMAT. THE OUTPUT  
C FROM THE GBFID PROGRAM IS USED TO SELECT THE NUMBER OF  
C RECORDS TO BE SKIPPED TO ARRIVE AT THE START OF THE FIELDS  
C THAT COMPRISE A STORM DATA SET AND IDENTIFY THE RECORDS  
C THAT MAKE UP THE DATA SET. IF RECORDS ARE MISSING FROM THE  
C GBA TAPES ENSURE THAT THE DATE/TIME INFOR FOR THE MISSING  
C FIELDS ARE NOT INCLUDED IN THE LIST OF DATA INPUT AT THE  
C END OF THE PROGRAM. SPECIFIC INFORMATION ON THE PARAMETERS  
C THAT WILL HAVE TO BE CHANGED FOR EACH DATA RUN IS SHOWN  
C AT THE END OF THE PROGRAM JCL STATEMENTS, NEAR THE LINES  
C TO BE CHANGED. REMOVE ALL COMMENT LINES THAT ARE NOT IN  
C THE PROGRAM OR SUBROUTINES BEFORE ATTEMPTING TO RUN THIS  
C PROGRAM.

C ORIGINAL AUTHOR UNKNOWN  
C UPDATED AND MODIFIED BY B. T. SHERMAN, MAY 1987

C  
//SG \_\_\_\_\_ JOB (\_\_\_\_,9999),'\_\_\_\_\_,2200',CLASS = G  
//\*MAIN LINES = 40,RINGCHK = NO  
//\*  
//\*  
// EXEC FORTVCLG,PARM.FORT = 'LANGLVL(66)'  
//FORT.SYSIN DD \*

C  
C PGM TO READ DATA FROM FNOC TAPE 144X49 MERCATOR GRID NEDN  
C FORMAT

C  
DIMENSION GLAT(49),GLON(144)  
REAL\*4 ID(4745),BCD(23)  
REAL\*4 DATA(7056)  
INTEGER\*4 IDTG(8),NP(8),ISKP(33),ITITLE(42),NC(3)  
INTEGER\*4 IN1(23),ITAU(4),BCDTAU(4),TSTTWO/'2/'  
INTEGER IDATA(7056)  
INTEGER\*2 JDATA(14112)

C\*\*NOTE\*\*

C DIMENSIONS OF OUT MUST MATCH THE GRID SIZE OF OUTPUT

C\*\*NOTE\*\*

REAL OUT(144,41),D(144,49)

```

C
    REAL XL(4)
C
    DATA ENDS/'AAAA'/
    DATA XL/'A','E','G','T'/
C A-SFC E-700 G-400 T-250 I-200
    DATA NLVL/4/
    DATA VRU/'1',VRV/'2'/
C
    DATA C/.0436610743/,DD/114.5915590262/
    NAMELIST/NGRID/ NWST,NEST,NSTH,NNTH
C
    EQUIVALENCE (IDATA(1),JDATA(1))
C
    NA = 28220
    NR = 7056
    NB = 0
    NNS = 0
    NCNT = 0
    INR = 0
    IOVER = 0
    IER = 0
    A = 100.
    B = -100.
CCC
C
C THESE ARE CURRENTLY FIXED, BUT CAN BE VARIABLE
C
    CLAT = .1
    CLON = 179.9
CCC
C
C DEFINE VALUES OF LAT,LON OF ALL GRID POINTS
C
C DO 2000 I = 1,49
C   GLON(I) = 60. + (I-1)*2.5
C2000 CONTINUE
C DO 2001 I = 50,144
C   GLON(I) = ((I-49.)*2.5)-180.
C2001 CONTINUE
C DO 2002 II = 1,49
C   I = 50-II
C   GLAT(I) = 90.-ATAN(EXP(-ABS(II-31.)*C))*DD
C   IF (II.GT.31) GLAT(I) = -GLAT(I)
C2002 CONTINUE
C
C

```

```

C** READ IN GRID SIZE
C
    READ (5,NGRID)
    WRITE (6,NGRID)
    NI = NWST + NEST + 1
    NJ = NSTH + NNTH + 1
C
    IUCOMP = 20
    IVCOMP = 20
    NRECU = 0
    NRECV = 0
C
C** READ IN NO. OF TAPES TO BE USED
C
    READ (5,78) NTAPE
    78 FORMAT (I2)
CC DO 1000 ITP = 1,7
    JUNIT = 10
    CALL BUFFER(JUNIT,1,14220,ID)
C
C** READ IN THE NO. OF TIME PERIODS TO BE INCLUDED IN THE
C STEP OF SKIPPING RECORDS AND SKIP TO DESIRED DATA
C
    READ (5,79) KTP
    79 FORMAT (I3)
    READ (5,7) NSKPRC
    7 FORMAT (I5)
    CALL SKIP (JUNIT,NSKPRC,IEND)
    MTP = 0
    IYMDH = 0
    224 MTP = MTP + 1
C
C***** ***** *****
C
    READ (5,225,END = 123) IY,MTH,JD,JH,IREW
    225 FORMAT (I2,2X,3I2,1X,I1)
    IF (IREW.EQ.1) CALL REWIND (JUNIT)
    KYMDH = IY*1000000 + MTH*10000 + JD*100 + JH
    IF (IYMDH.EQ.KYMDH) GO TO 75
C
    IF (MTP.LE.KTP) GO TO 751
    READ (5,79) LTP
    KTP = KTP + LTP
    READ (5,7) NSKPRC
    NSKPRC = NSKPRC - 2
    CALL SKIP (JUNIT,NSKPRC,IEND)
    IF (IEND.NE.0) GO TO 88

```

```

C
751 CONTINUE
927 DO 926 L = 1,4745
926 ID(L) = ENDS
C
      CALL GETREC(JUNIT,&88,&9999)
      GO TO 331
88 IF (NTAPE.EQ.1) GO TO 99
      CALL REWIND(JUNIT)
      JUNIT = JUNIT + 1
      CALL BUFFER (JUNIT,1,14220,ID)
      READ (5,79) LTP
      KTP = KTP + LTP
      READ (5,7) NSKPRC
      CALL SKIP (JUNIT,NSKPRC,IEND)
      GO TO 751
331 CONTINUE
C
C
      CALL GBYTES(ID(1),NC,0,6,0,3)
      DO 31 J = 1,3
31 IN1(J) = NC(J)
      CALL GBYTES(ID(1),ITAU,24,6,0,4)
      CALL XBCD(4,ITAU,BCDTAU)
C
C CHECK TO SEE IF IT IS A FCST FIELD IF SO IGNORE IT
      IF (BCDTAU(4) .EQ. TSTTWO) GO TO 751
      CALL GBYTES(ID(2),IDTG,16,6,0,8)
      I = 1
      DO 32 J = 4,11
      IN1(J) = IDTG(I)
      CALL XBCD(1,IN1(J),BCD(J))
32 I = I + 1
C *** CONVERT BCD TO DECIMAL NUMBER *****
      CALL XINT(BCD,IYMDH,IER)
      IF (IER.NE.0) GO TO 751
      CALL GBYTES(ID(4) ,NP,0,6,0,8)
      I = 1
      DO 33 J = 12,19
      IN1(J) = NP(I)
33 I = I + 1
      CALL GBYTES(ID(6),IUNIT,8,5,0,0)
      IN1(20) = IUNIT
      CALL GBYTES(ID(6),ISCLE,13,6,0,1)
      IN1(21) = ISCLE
      CALL GBYTES(ID(7),M,24,12,0,0)
      IN1(22) = M

```

```

CALL GBYTES(ID(8),N,4,12,0,0)
IN1(23) = N
CALL GBYTES(ID(27),IDATA,8,16,0,NR)
C
C CDC HAS ONE'S COMPLEMENT, IBM HAS TWO'S COMPLEMENT FOR
C NEGATIVE'S.
DO 30 I = 1,NR
30 IF (IDATA(I) .LT. 0) IDATA(I) = IDATA(I) + 1
C
C **** CHECK YYMMDDHH TO GET THE DATA WE NEED ****
CALL XBCD(20,IN1,BCD)
IF (IYMDH-KYMDH) 751,75,224
C *****
75 CONTINUE
IF(BCD(3).NE.VRV .AND. BCD(3).NE.VRU) GOTO 751
C
C SET UP TO UNPACK 16 BIT DATA POINTS. THUS JDATA WHICH IS
C *2 HAS ONE DATA POINT PER WORD. DATA IS IN THE RIGHTMOST
C 16 BITS OF IDATA WHICH IS *4. THE SCHEME BELOW DOES NOT
C WORK IF THE NBTSDP = 20 OR 08.
C
L=0
NR2=NR*2
IF (ISCLE .LT. 32) GO TO 40
ISL = 2**(ISCLE-32)
DO 17 I = 2,NR2,2
L=L+1
IDUM=JDATA(I)
17 DATA(L) = FLOAT(IDUM)/FLOAT(ISL)
GO TO 45
40 ISL = 2**(32-ISCLE)
DO 18 I = 2,NR2,2
L=L+1
IDUM=JDATA(I)
18 DATA(L)=FLOAT(IDUM)*FLOAT(ISL)
45 CONTINUE
C
C TEST FOR LEVEL
C
LVL=0
DO 500 K = 1,NLVL
LVL=K
500 IF(BCD(1).EQ.XL(K)) GOTO 505
501 GOTO 751
505 CONTINUE
C
510 CONTINUE

```

511 CONTINUE

C  
C  
C

DETERMINE GRID POINTS IS,IE,JS,JE FOR THE OUTPUT DATA

CALL FINDGR(GLAT,49,CLAT,1,NSTH,NNTH,JS,JE)  
CALL FINDGR(GLON,144,CLON,-1,NWST,NEST,IS,IE)  
IF (IS.LE.0) IS = IS + 144  
IF (IE.GT.144) IE = IE-144

C  
C  
C  
C  
C

CREATE THE OUTPUT VECTOR OUT  
IF JS.LE.0 OR JE.GT.49, DATA AT THAT GRID POINT OF  
VECTOR OUT WILL BE CONSIDERED MISSING

JD = JS-1  
DO 550 J = 1,NJ  
IDD = IS-1  
IFLAG = 0  
JD = JD + 1  
IF (JD.GT.JE) GO TO 551  
IF (JD.GT.0.AND.JD.LE.49) GO TO 539  
IFLAG = 1

539 DO 540 I = 1,NI  
IDD = IDD + 1  
IF (IDD.GT.144) IDD = IDD-144  
IF (IDD.GT.IE) GO TO 555  
IF (IFLAG.NE.0) GO TO 538  
OUT(I,J) = D(IDD,JD)  
IF (OUT(I,J).LT.B.OR.OUT(I,J).GT.A) IER = 1  
GO TO 540

538 OUT(I,J) = 99999.  
IOVER = 1

540 CONTINUE

550 CONTINUE

GO TO 570

551 WRITE (6,552) JS,JE,JD

552 FORMAT (' ERROR IN IDENTIFYING LAST LATITUDE LINE'  
1JS = ',I3,2X,'JE = ',I3,2X,'JD = ',I3)  
STOP

555 WRITE (6,556) IS,IE,IDD

556 FORMAT (' ERROR IN IDENTIFYING LAST LONGITUDE LINE'  
1IS = ',I3,2X,'IE = ',I3,2X,'IDD = ',I3)  
STOP

570 CONTINUE

C

IF(BCD(3).NE.VRU)GO TO 800  
NRECU = NRECU + 1  
WRITE(6,10) NRECU,IYMDH,(BCD(K),K = 1,20)

```

1      ,CLAT,CLON,IS,IE,JS,JE
1      ,D(IS,JS),D(IE,JE),OUT(1,1),OUT(NI,NJ)
2      ,IER,IOVER
10 FORMAT (1X,'NRECU = ',I4,I10,1X,3A1,1X,8A1
1,1X,9A1,2X,'CLAT = ',F5.1,' CLON = ',F6.1,2X,
2'IS = ',I3,' IE = ',I3,' JS = ',I3,' JE = ',I3,4F7.1,I3,I1)
CC WRITE (IUCOMP) NRECU,(BCD(K),K = 1,3),IYMDH,OUT
WRITE(IUCOMP,610)NRECU,(BCD(K),K = 1,3),IYMDH
610 FORMAT(I4,1X,(3(A1,1X)),I10)
WRITE(IUCOMP,620)OUT
620 FORMAT(10F8.2)
IOVER = 0
IER = 0
GO TO 751
800 IF(BCD(3).NE.VRV)GO TO 751
NRECV = NRECV + 1
WRITE(6,11) NRECV,IYMDH,(BCD(K),K = 1,20)
1      ,CLAT,CLON,IS,IE,JS,JE
1      ,D(IS,JS),D(IE,JE),OUT(1,1),OUT(NI,NJ)
2      ,IER,IOVER
11 FORMAT (1X,'NRECV = ',I4,I10,1X,3A1,1X,8A1
1,1X,9A1,2X,'CLAT = ',F5.1,' CLON = ',F6.1,2X,
2'IS = ',I3,' IE = ',I3,' JS = ',I3,' JE = ',I3,4F7.1,I3,I1)
CC WRITE (IVCOMP) NRECV,(BCD(K),K = 1,3),IYMDH,OUT
WRITE(IVCOMP,630)NRECV,(BCD(K),K = 1,3),IYMDH
630 FORMAT(I4,1X,(3(A1,1X)),I10)
WRITE(IVCOMP,640)OUT
640 FORMAT(10F8.2)
IOVER = 0
IER = 0
GO TO 751
CC STOP
C
775 WRITE (6,776) IYMDH,IX2,NCNT
776 FORMAT('ERROR IN RECORD ARRANGEMENT'/IYMDH = ',I10,2X,
1'IX2 = ',I10,'RECORD NO. = ',I5)
STOP
777 WRITE(6,150) IYMDH
150 FORMAT(1X,'PGM ENDED IYMDH = ',I10)
STOP
9999 WRITE(06,120)
120 FORMAT(1X,' PARITY ERROR GETREC ')
STOP
99 WRITE(06,121)
121 FORMAT(1X, ' EOF ENCOUNTERED IN GETREC ')
STOP
999 WRITE(06,122)

```

122 FORMAT(1X,' SKPREC FAILURE ')

123 STOP

END

C\*\*\*\*\* SUBROUTINE SKIP \*\*\*\*\*

C

    SUBROUTINE SKIP (JUNIT,NSKPRC,IEND)

C

C    THIS SUBROUTINE SKIPS NSKPRC RECORDS FROM JUNIT

C

    IEND = 0

C

    WRITE(06,2) NSKPRC

    2 FORMAT ('0','NO. OF RECORDS SKIPPED = ',I5)

    IF (NSKPRC.EQ.0) GO TO 6

    IF (NSKPRC.LE.1000) GO TO 5

    NSK = NSKPRC/1000

    DO 4 MSK = 1,NSK

    CALL SKPREC(JUNIT,1000,&99,&999)

    4 CONTINUE

    NSKPRC = NSKPRC - (NSK\*1000)

    5 CALL SKPREC(JUNIT,NSKPRC,&99,&999)

    6 CONTINUE

    GO TO 123

    99 IEND = 1

    RETURN

999 WRITE(06,122)

122 FORMAT(1X,' SKPREC FAILURE ')

    STOP

123 RETURN

END

C\*\*\*\*\* SUBROUTINE FINDGR \*\*\*\*\*

C

    SUBROUTINE FINDGR (A,N,P,IFLAG,NG1,NG2,MS,ME)

C

C    THIS SUBROUTINE DETERMINES THE GRID LINE CLOSEST TO

C    THE CYCLONE CENTER

C    AND RETURNS THE BOUNDARY GRID LINE NOS.

C

C    DEFINITION OF PARAMETERS

C    A = ARRAY OF N VALUES OF LAT/LON

C    P = POSITION (LAT/LON) OF CYCLONE CENTER

C    NG1 = NO. OF GRID POINTS ON WEST/SOUTH SIDE OF P

C    NG2 = NO. OF GRID POINTS ON EAST/NORTH SIDE OF P

C    MS = GRID LINE NO. ON WEST/SOUTH SIDE OF P

C    ME = GRID LINE NO. ON EAST/NORTH SIDE OF P

C    IN THE CASE THAT P IS EXACTLY IN BETWEEN TWO GRID LINES,

C    IFLAG DETERMINES WHICH GRID LINE WILL BE CONSIDERED THE





CCC WORK, THE PROGRAM ALSO CALLS A USER INACCESSIBLE ROUTINE  
CCC CALLED GETREC WHICH IS A PART OF THE TAPE UTILITIES  
CCC LIBRARY. \*REMOVE THESE FOUR LINES TO RUN\*

//LKED.SYSLIB DD

// DD

// DD

// DD

// DD

// DD DISP=SHR,DSN=SYS3.TAPE.LOAD,LABEL=(,,IN)

CCCC THESE NEXT TWO CONTROL STATEMENTS ARE THE READ AND  
CC WRITE FORMATS FOR THE TAPE UNITS.

CC THE FIRST IS THE READ FORMAT

CC FOLLOWING 'VOL=SER=' GIVE THE TAPE NAME(ON THE OUTSIDE)

CC FILL IN DATA FROM THE TAPE SCAN AT THE APPROPRIATE SPOT

CC LABEL=

CC BLKSIZE=

CC DEN=

CC \*\*\*\*\*REMOVE THESE 9 COMMENT LINES TO RUN \*\*\*\*\*

//GO.FT10F001 DD UNIT=3400-5,VOL=SER=GB1984,

// DISP=(OLD,KEEP),LABEL=(1,NL,,IN),

// DCB=(RECFM=F,BLKSIZE=14220,DEN=4)

CC THE NEXT CONTROL STATEMENT IS THE WRITE TO TAPE STATEMENT  
CC THAT PUTS THE DATA ON THE TAPE IN ASCII FORMAT.

CC FIRST CHANGE THE EXTERIOR LABEL LINE 'VOL=SER='XXXXXX

CC NEXT YOU WILL NEED TO ADJUST THE BLKSIZE OF THE OUTPUT

CC ONE FIELD SHOULD FILL ONE BLOCK FOR EFFICIENT MANAGEMENT

CC ON THE VAX, & BECAUSE THIS METHOD USES LESS TAPE/RECORD

CC RECSIZE = (HEADER) + (8\*GRIDSIZE)

CC HEADER = 1\*LRECL

CC GRIDSIZE = NPTS(N/S)\*NPTS(E/W)

CC BLKSIZE MUST BE AN INTEGER MULTIPLE OF LRECL.

CC IF RECSIZE IS NOT AN INTEGER MULTIPLE OF LRECL USE THE

CC NEXT INTEGER TO GET BLKSIZE

CC EX: IF RECSIZE = 63.4

CC BLKSIZE = (64 \* 80) = 5120

CC \*\*\*\*\*REMOVE THESE 15 COMMENT LINES TO RUN\*\*\*TCAD\*\*\*\*\*

//GO.FT20F001 DD UNIT=3400-5,VOL=SER=DSGB84,

// DISP=(OLD,KEEP),LABEL=(1,NL,,OUT),

// DCB=(OPTCD=Q,RECFM=FB,LRECL=80,BLKSIZE=28320,DEN=4)

//\*

//GO.SYSIN DD \*

&NGRID NWST=48, NEST=95, NSTH=10, NNTH=30&END

1 THIS IS THE NUMBER OF TAPES TO BE READ

1

3040 THIS THE NUMBER OF RECORDS TO SKIP

84 6 912 0 YEAR,MONTH,HOUR, REWIND CODE:0=NO, 1=YES

84 610 0 0

APPENDIX C  
PROGRAM--GLOBAL BAND TAPE TO DISK

```

program GBTTOD
c
c This program reads Global Band Analysis data from tape
c and writes it to a file on disk for further processing.
c The program uses QIO system services to read the data.
c The subroutine (mtread) which actually calls the QIO is
c located in disk$2:[metdept.tape]mt/lib.
c (GBTTOD means Global Band, Tape TO Disk)
c
c Brett Sherman & Jim Cowie 7/87 (NPS)
c
c
c*****
c
c      character data*28320
c      integer*2 data_len, real_len
c      integer*4 istat, status, channel, sys$assign, sys$deassign
c      parameter(data_len=28320)
c begin
c assign the QIO channel
c
c      istat = sys$assign( 'tape', channel,,)
c      write(*,*)'channel #',channel
c      if(.not. istat)then
c          write(*,*)' could""nt assign QIO channel number'
c          write(*,*)' istat=',istat
c          goto 999
c      endif
c
c open the disk output data file
c      open (unit=1,file='gbanal.dat',status='new')
c using QIO's, read the record from tape and write to disk
c
c      do 20 j=1,4
100      call mtread(channel,%ref(data),data_len,status,real_len)
c          write (*,*) 'real_len=',real_len
c          if (.not.status) then
c              call lib$signal(%val(status))
c              go to 999
c          end if
c          do 10 i=1,28320,80
c              write(1,200)data(i:i+79)

```

```
10     continue
20     continue
c  go back and read the next header and grid
    goto 100

c  deassign the QIO channel and exit the program
999   istat = sys$dassgn( channel )
200   format(a)
      stop
      end
```

APPENDIX D  
PROGRAM--FILE CONVERTER

```
program          FILE CONVERTER
cc This program converts the FNOC Global Band field data located in a
cc disk file created by GBTTOD.FOR, to a gempak grid file.  the program
cc uses gempak subroutines to create the navigation data, the grid file,
cc & write the data to the new file.  each file contains a complete
cc storm data set.
cc
cc Initial data relating to the grid size and lat/lon will have to be
cc adjusted to values corresponding to the grid being converted. Ngrid
cc will have to be changed to reflect the number of grids in the data
cc set. The file names for read file, header file and the gem file will
cc have to be changed for each different storm data set.
cc
cc In order for the grid conversion to run properly the LAT.DAT file
cc must be accessible by the program. The program converts the 2.5
cc degree longitude square GBA grid to a 2.5 deg latitude by 2.5 deg
cc longitude grid for use in the GEMPAK routines.
cc
cc          LCDR B.T. SHERMAN & JAMES COWIE    JUNE 1987
cc
cc-----
cc
cc
character file*80, rfile*80, setname*80, parm*4, lvl*1, hdrfil*80
integer level(2)
character time(2)*13, yymmdd*6, hh*2, mm*2, latfil*80
logical replace
integer fn, type, comp, grdno
dimension grid(80,40),rnvblk(256),ighdr(2),tgrid(7056),anblk(128)
real intlnt,igrd(144,49),mgrid(144,40),lat(49)
c
c define the file to be read & the name of the file created
c
  data rfile  //'THAD_1984.DAT'//
  data file   //'THAD_1984.GEM'//
  data hdrfil //'THAD_1984.HDR'//
  data latfil //'LAT.DAT'//
c
  open (unit=4,file=latfil,status='old')
  open (unit=5,file=rfile,status='old')
  open (unit=6,file=hdrfil,status='new')
c
  replace = .false.
```

```

c
c  read the latitude data
c
      j1 = 1
      do 4 i = 1,7
        read(4,5) (lat(j), j = j1 , j1 + 7)
5         format(8(f9.3))
      j1 = j1 + 8
4  continue
c  do 6 m = 1,49
c  write(6,*) lat(m)
c 6  continue
c
c
c  set initial parameters
c
c  ngrid is the number of grids in the data file to be converted, kx &
cc ky are dimensions of the grid, the lat/log limit designators are set
cc up as follows ex: rlatb = the real value of the latitude at the
cc bottom of the grid, mm = the minutes for the time designator, ivcord
cc = 1 designates pressure as the vertical coordinate, navsz,ihdrsz,
cc ianlsz are set by the subroutines in the gempak, level(2) = -1 is the
cc indicator that you are using only one level for the grid
c
  ngrid = 104
  kx = 80
  igx = kx
  ky = 40
  igy = ky
  npts = kx * ky
  rlatb = -40.000
  rlatt = 57.500
  rlonr = 257.500
  rlonl = 60.000
  navsz = 256
  ianlsz = 128
  ihdrsz = 2
  ivcord = 1
  data mm /'00'/
c
c  call the subroutine to create the nav data for the grid
c
  call gr_mllnv (kx,ky,rlatb,rlonl,rlatt,rlonr,rnvblk,iret)
c
c  if the return code indicates a problem print it and stop
c
  if (iret.ne.0) then
  write(*,*) 'gr_mllnv error - iret=',iret
  go to 999
  end if

```

```

c
c call the subroutine to create the new data file
c
  call gd_cret(file,navsz,rnvblk,ianlsz,anlblk,file,ihdrsz,iflno,iret)
  if (iret.ne.0) then
  write(*,*) 'gd_cret error - iret=',iret
  go to 999
  end if
c
  grdno = 0
c
  do 300 l = 1,ngrid
  read(5,10) fn,lv1,type,comp,yymmdd,hh
10      format(1X,i3,1x,a1,1x,i1,1x,i1,3x,a6,a2)
c
      WRITE(*,10)FN,LVL,TYPE,COMP,YMMDD,HH
  grdno = grdno + 1
      write(6,15)fn,lv1,type,comp,yymmdd,hh,grdno
15      format(1x,i3,1x,a1,1x,i1,1x,i1,3x,a6,a2,1x,i4)
  time(1) = yymmdd/'/'/'/'/hh//mm
  time(2) = ' '
c
c
  if (lv1.eq.'A') then
      level(1)=1000
  else if (lv1.eq.'E') then
      level(1)=700
  else if (lv1.eq.'G') then
      level(1)=400
  else if (lv1.eq.'T') then
      level(1)=250
c
  end if
c
      level(2)=-1
c
  if (comp.eq.1) then
      parm ='UWND'
  else if (comp.eq.2) then
      parm ='VWND'
  end if
c
  read (5,16)
16      format(80x)
  il=1
  do 400 m=1,706
  read (5,20) (tgrid(I), i =il,il+9)
20      format (10(f8.2))
  il=il+10
400      continue

```

```

c
write(6,*)'tgrid (1) =',tgrid(1)
c
kount = 0
do 100 j = 1,49
    do 200 k = 1,144
        kount = kount + 1
        igrd (k,50-j) = tgrid (kount)
200    continue
100    continue
c
c interpolate the GBA grid to NOGAPS format
c
do 510 i=1,144
    mgrd(i,17)=igrd(i,19)
    intl=2.5
    intj=18
c North of the Equator
do 520 j=20,48
    if(lat(j).lt.intl.and.lat(j+1).gt.intl)then
    mgrd(i,intj)=igrd(i,j)+(igrd(i,j+1)-igrd(i,j))*
*       (intl-lat(j))/(lat(j+1)-lat(j))
c
        intj = intj + 1
        intl = intl + 2.5
    endif
520    continue
c
c South of the Equator
c
intj = 16
intl = -2.5

do 530 j = 18,2,-1
    if (lat(j).gt.intl.and.lat(j-1).lt.intl)then
    mgrd(i,intj)=igrd(i,j)+(igrd(i,j-1)-igrd(i,j))*
*       (intl-lat(j))/(lat(j-1)-lat(j))
c
        intj = intj - 1
        intl = intl - 2.5
    endif
530    continue
510    continue
c
c make the grid to go to the GEM file
c
do 540 j = 1,40
    do 550 k = 1,80
        grid(k,j) = mgrd(k,j)
550    continue
540    continue
c

```

c

```
write(*,*)grdno,time,level,parm
```

```
call gd_writ (iflno,grid,igx,igy,ighdr,time,level,ivcord,parm,  
# nbsiz,replace,iret)
```

```
if (iret.ne.0) then
```

```
write(*,*) 'gd_writ error - iret=',iret
```

```
go to 999
```

```
end if
```

```
300 continue
```

```
999 stop
```

```
end
```

This latitude information is required by the grid conversion subroutine in the program FILE\_CONVERT (remove these three lines prior to processing data)

-40.956	-39.042	-37.076	-35.056	-32.986	-30.866	-28.698	-26.484
-24.226	-21.928	-19.593	-17.222	-14.821	-12.393	-09.943	-07.473
-04.990	-02.497	00.000	02.497	04.990	07.473	09.943	12.393
14.821	17.222	19.593	21.928	24.226	26.484	28.698	30.866
32.986	35.056	37.076	39.042	40.956	42.816	44.621	46.372
48.069	49.711	51.300	52.835	54.318	55.750	57.131	58.462
59.745	0.0	0.0	0.0	0.0	0.0	0.0	0.0

## LIST OF REFERENCES

- Allen, R. L., 1984: CYCLOPS objective steering model output statistics (COSMOS). Tech. Note 84-1, Naval Oceanography Command Center, Guam, 16 pp.
- Chan, J. C. L., 1984: An observational study of the physical processes responsible for tropical cyclone motion. *J. Atm. Sci.*, **41**, 1036-1048.
- Chan, J. C. L., 1985: Identification of the steering flow for tropical cyclone motion from objectively analyzed wind fields. *Mon. Wea. Rev.*, **113**, 106-116.
- Chan, J. C. L., and W. M. Gray, 1982: Tropical cyclone movement and surrounding flow relationships. *Mon. Wea. Rev.*, **110**, 1354-1374.
- Curry, W. T., 1985: An objective determination of tropical cyclone warning position. M.S. thesis, Naval Postgraduate School, Monterey, CA, 58 pp.
- DeMaria, M., 1985: Tropical cyclone motion in a nondivergent barotropic model. *Mon. Wea. Rev.*, **113**, 1199-1210.
- desJardin, M. L., H. M. Goodman and I. A. Graffman, 1986: GEMPAK User's Guide. NASA/Goddard Space Flight Center, Greenbelt, MD, 157 pp.
- Elsberry, R. L., and M. Fiorino, 1985: Design concerns for an advanced tropical cyclone model. TR 85-03, Naval Environmental Prediction Research Facility, Monterey, CA, 152 pp.
- Elsberry, R. L., and J. E. Peak, 1986: An evaluation of tropical cyclone forecast aids based on cross-track and along-track components. *Mon. Wea. Rev.*, **114**, 147-155.
- George, J. E., 1975: Tropical cyclone motion and surrounding parameter relationships. Atmospheric Science Paper No. 241, Colorado State University, Fort Collins, CO, 105pp.
- Joint Typhoon Warning Center, 1982: Annual Tropical Cyclone Report. U. S. Naval Oceanography Command Center, Joint Typhoon Warning Center, Guam, COMNAVMARIANAS, Box 17, FPO San Francisco, 96630, 241pp.
- Joint Typhoon Warning Center, 1983: Annual Tropical Cyclone Report. U. S. Naval Oceanography Command Center, Joint Typhoon Warning Center, Guam, COMNAVMARIANAS, Box 17, FPO San Francisco, 96630, 203pp.

- Joint Typhoon Warning Center, 1984: Annual Tropical Cyclone Report. U. S. Naval Oceanography Command Center, Joint Typhoon Warning Center, Guam, COMNAVMARIANAS, Box 17, FPO San Francisco, 96630, 227pp.
- Jones, H., 1986: Comparison of western North Pacific tropical cyclone aids using storm-related and synoptic parameters. M.S. thesis, Naval Postgraduate School, Monterey, CA, 140 pp.
- Matsumoto, C. R., 1984: A statistical method for one- to three-day tropical cyclone track prediction. Atmospheric Science Paper No. 379, Colorado State University, Fort Collins, CO, 201pp.
- McLawhorn, D. W., 1984: The tropical cyclone year 1983 - part II, The current philosophy of operations at JTWC. Proceedings Report, 1984 Tropical Cyclone Conference, Tokyo Japan, Environmental Group, Pacific Command, 17-27.
- Meanor, D., 1987: Vertical wind shear as a predictor of tropical cyclone motion. M.S. Thesis, Naval Postgraduate School, Monterey, CA, 74 pp.
- Neumann, C. J., and J. M. Pelissier, 1981: Models for the prediction of tropical cyclone motion over the North Atlantic: an operational evaluation. *Mon. Wea. Rev.*, **109**, 522-538.
- Peak, J. E., and R. L. Elsberry, 1987: Selection of optimal tropical cyclone motion guidance using an objective classification tree methodology. *Mon. Wea. Rev.*, **115**, 1851-1863.
- Renard, R. J., 1968: Forecasting the motion of tropical cyclones using a numerically derived steering current and its bias. *Mon. Wea. Rev.*, **96**, 453-469.
- Renard, R. J., and W. Levings, III, 1969: The Navy's numerical hurricane and typhoon forecast scheme: application to 1967 Atlantic storm data. *J. Appl. Meteor.*, **8**, 717-725.
- Renard, R. J., M. J. Daley and S. K. Rinard, 1970: A recent improvement in the Navy's numerical-statistical scheme for forecasting the motion of hurricanes and typhoons. NPS-51RD0011A, U.S. Naval Postgraduate School, Monterey, CA, 25 pp.
- Renard, R. J., S. G. Colgan, M. J. Daley and S. K. Rinard, 1972: Numerical statistical forecasts of tropical cyclone tracks by the MOHATT scheme with application to the North Atlantic area. Technical Note 72-4, Fleet Numerical Weather Center, Monterey, California, 41 pp.
- Renard, R. J., S. G. Colgan, M. J. Daley and S. K. Rinard, 1973: Forecasting the motion of North Atlantic tropical cyclones by the objective MOHATT scheme. *Mon. Wea. Rev.*, **101**, 206-214.

- Sandgathe, S. A., 1987: Opportunities for tropical motion research in the Northwest Pacific region. Tech. Rep. NPS-63-87-006, Naval Postgraduate School, Monterey, CA, 36 pp.
- Schott, T. B., 1985: Application of wind empirical orthogonal functions in tropical cyclone motion studies. M.S. Thesis, Naval Postgraduate School, Monterey, CA, 99 pp.
- Tsui, T. L., 1984: A selection technique for tropical cyclone objective forecast aids. Postprints, 15th Conf. on Hurricanes and Tropical Meteorology, Amer. Meteor. Soc., Boston, 40-44
- United States Naval Weather Service, 1975: Numerical Environmental Products Manual, NAVAIR 50-1G-522, 155 pp.
- Wash, C. H., P. A. Durkee, L. C. Chou and J. Mueller, 1987: The Interactive Digital Environmental Analysis (IDEA) Laboratory at the Naval Postgraduate School. Paper presented at the Third International Conference on Interactive Information and Processing Systems for Meteorology, Oceanography and Hydrology, Amer. Meteor. Soc., Boston, 9 pp.
- Weir, R. C., 1982: Predicting the acceleration of northward-moving tropical cyclones using upper-tropospheric winds. Tech Note 82-2, Naval Oceanography Command Center/Joint Typhoon Warning Center, Guam, 40 pp.
- Weniger, E. L., 1987: Tropical cyclone intensity prediction based on empirical orthogonal function representation of the wind and shear fields. M.S. thesis, Naval Postgraduate School, Monterey, CA, 55 pp.
- Williams, B. J., 1986: Effects of storm related parameters on the accuracy of the nested tropical cyclone model. M.S. thesis, Naval Postgraduate School, Monterey, CA, 107 pp.
- Wilson, W. E., 1984: Forecasting of tropical cyclone motion using an EOF representation of wind forcing. M.S. thesis, Naval Postgraduate School, Monterey, CA, 88 pp.

## INITIAL DISTRIBUTION LIST

		No. Copies
1.	Defense Technical Information Center Cameron Station Alexandria, VA 22304-6145	2
2.	Library, Code 0142 Naval Postgraduate School Monterey, CA 93943-5002	2
3.	Chairman, Code 63Rd Department of Meteorology Naval Postgraduate School Monterey, CA 93943-5000	1
4.	Chairman, Code 68Co Department of Oceanography Naval Postgraduate School Monterey, CA 93943-5000	1
5.	Professor Russell L. Elsberry, Code 63Es Department of Meteorology Naval Postgraduate School Monterey, CA 93943-5000	5
6.	LCDR Brett T. Sherman, USN Commander Second Fleet FPO New York, NY 09501-6000	3
7.	Director Naval Oceanography Division Naval Observatory 34 <sup>th</sup> and Massachusetts Avenue NW Washington, DC 20390	1
8.	Commander Naval Oceanography Command NSTL Station Bay St. Louis, MS 39522	1
9.	Commanding Officer Naval Oceanographic Office NSTL Station Bay St. Louis, MS 39522	1
10.	Commanding Officer Fleet Numerical Oceanography Center Monterey, CA 93943-5000	1

11. Commanding Officer 1  
 Naval Ocean Research and Development Activity  
 NSTL Station  
 Bay St. Louis, MS 39522
12. Commanding Officer 1  
 Naval Environmental Prediction Research Facility  
 Monterey, CA 93943-5000
13. Chairman, Oceanography Department 1  
 U. S. Naval Academy  
 Annapolis, MD 21402
14. Chief of Naval Research 1  
 800 North Quincy Street  
 Arlington, VA 22217
15. Dr. Ted Tsui 1  
 Naval Environmental Prediction Research Facility  
 Monterey, CA 93943-5000
16. Commanding Officer 1  
 Naval Oceanography Command Center  
 Box 17  
 COMNAVMARIANAS  
 San Francisco, CA 96630
17. Director 1  
 Joint Typhoon Warning Center  
 Box 17  
 COMNAVMARIANAS  
 FPO San Francisco, CA 96630
18. Commanding Officer 1  
 Naval Western Oceanography Center  
 Box 113  
 Pearl Harbor, HI 96818
19. Dr. J.C.-L. Chan 1  
 Royal Observatory  
 Nathan Road  
 Kowloon, Hong Kong
20. Professor William M. Gray 1  
 Department of Atmospheric Sciences  
 Colorado State University  
 Fort Collins, CO 80523
21. Dr. Michael Fiorino 1  
 Fleet Numerical Oceanography Center  
 Monterey, CA 93943-5000

22. Professor Melinda Peng, Code 63Pg 1  
Department of Meteorology  
Naval Postgraduate School  
Monterey, CA 93943-5000
23. Professor Greg Holland, Code 63Ho 1  
Department of Meteorology  
Naval Postgraduate School  
Monterey, CA 93943-5000
24. Commander Scott A. Sandgathe 1  
3823 Eagan Dr.  
Fairfax, VA 22030
25. Lieutenant Colonel Charles P. Guard 1  
Aerospace Services Directorate  
Headquarters Air Weather Service  
Scott Air Force Base, IL 62225-5008 1  
3823 Eagan Dr.  
Fairfax, VA 22030
26. Dr. Mark DeMaria 1  
HRD/AOML/NOAA  
4301 Rickenbacker Causeway  
Miami, FL 33149

Synoptic patterns related to tropical cy



3 2768 000 78641 2

DUDLEY KNOX LIBRARY C.1